Study on the role of zona pellucida in pre- and post-implantation development of mouse embryos

(マウス胚の着床前後の発生における透明帯の役割に関する研究)

北海道大学　　大学院農学研究院

生命フロンティアコース　博士後期課程

范 威宏

Contents

Abbreviations

ART	Assisted reproductive technology
AT	Assisted technology
BSA	Bovine serum albumin
CARM1	Coactivator-associated arginine methyltransferase 1
CO_2	Carbon dioxide
COCs	Cumulus oocyte complexes
cWOW	Customized well-of-well
cDNA	Complementary DNA
DEG	Differentially expressed gene
DMR	Differentially methylated regions
DNMT	DNA methyltransferase
DNA	Deoxyribonucleic acid
EPC	Ectoplacental cone
EPI	Epiblast
ESCs	Embryonic stem cells
ET	Embryo transfer
ExE	Embryonic ectoderm
EZP	Empty zona pellucida
FBS	Fetal bovine serum
GO	Gene ontology
GO system	Glass oviducts system
hCG	Human chronic gonadotropin
HTF	Human tubal fluid
H3R26me2	Histone H3 arginine 26 methylation
ICSI	Intracytoplasmic sperm injection
ICM	Inner cell mass
IVC	*In vitro* culture
IVF	*In vitro* fertilization
IVP	*In vitro* production
mRNA	Messenger RNA
MZT	Maternal-zygotic transition
NT	Nuclear transfer
PBS	Phosphate buffered saline

PE	Primitive endoderm
PFA	Paraformaldehyde
PMSG	Pregnant mare serum gonadotropin
PVA	Polyvinyl alcohol
RNA-seq	RNA sequencing
RT-qPCR	Real time quantitative polymerase chain reaction
SEM	Standard error of the mean
2D	Two-dimensional
3D	Three-dimensional
TCN	Total cell number
TE	Trophectoderm
TGC	Trophoblast giant cell
TUNEL	Terminal deoxynucleotidyl transferase biotin-dUTP nick end Labeling
UHRF1	Ubiquitin-like, containing PHD and RING finger domains, 1
VE	Visceral endoderm
WOW	Well of the Well
ZF	Zona free
ZI	Zona intact
ZP	Zona pellucida
ZPR	Zona pellucida removal

Unit measures abbreviations

%	Percentage
× g	Times gravity
°C	Degree Celsius
h	Hour
IU	International unit
mg	Microgram
min	Minute
mL	Milliliter
g	Gram
V/V	Volume by volume
µl	Microliter
µm	Micrometer
s	Second

Abstract

The zona pellucida (ZP) is a specialized extracellular elastic coat that surrounds the mammalian ovarian oocyte, and preimplantation embryo. ZP is composed of four typical glycoproteins (ZP1, ZP2, ZP3, ZP4) in humans which are composed of three typical glycoproteins (ZP1, ZP2, and ZP3) in mice. ZP play key roles in preventing heterogeneous sperm from entering the egg, ensuring genetic purity and genetic stability between species, protecting the embryo and maintaining its integrity, preventing premature attachment to the oviduct and endometrial surface, and preventing bacterial and fungal infections in the reproductive tract during the mammalian embryonic development.

The ZP plays various roles in preimplantation embryonic development both *in vivo* and *in vitro*. Previous studies have shown that excessive thickness and hardening of the ZP impair the hatching ability of human embryos produced *in vitro*, thus zona pellucida removal (ZPR) of the early blastocyst is effective in improving implantation rates, which is thought to be the result of successful contact and communication between the trophectoderm (TE) and the endometrium. Therefore, the use of assisted zona hatching (AZH) in *in vitro* production (IVP) procedures as well as in human *in vitro* fertilization (IVF) procedures is widely used.

In addition, the current ZPR procedure is also applied to remove ZP at the embryonic cleavage stage and is widely used for producing hand-made somatic cell nuclear transfer embryos, production of identical twins or quadruplets, gene transfer,

and chimeric embryos. Although the preimplantation development of zona free (ZF) embryos has been studied, the role of ZP in the differentiation, gene expression, as well as post-implantation development of ZF embryos is not fully understood. Therefore, I investigated the role of ZP in the pre- and post-implantation development of mouse embryos.

In Chapter II, I first investigated the *in vitro* development of ZF embryos treated with acid Tyrode's solution and cultured using the different culture systems. Under the ordinary microdroplet culture condition, ZPR significantly decreased the blastocyst rate compared with the ZI embryos. Due to the low developmental capacity of ZF embryos cultured *in vitro*, the commercial Well of Well (WOW) culture system specified for single embryo culture was evaluated for performing to improve the development of ZI embryos. Although the commercial WOW system could improve blastocyst rates of ZF embryos compared to the microdroplets system, irregular embryos were still observed during compaction when ZF embryos developed to the morula stage because of a potential collapse of blastomere structure in the large and flat bottom of WOW well for mouse ZF embryos. Therefore, the customized WOW (cWOW) system made with a smaller microwell size was newly developed and evaluated the development of ZF embryos. Subsequently, I compared the microwell sizes of commercial WOW and cWOW by three-dimensional (3D) surface scanning and found that the average diameter of microwells in the cWOW system was significantly smaller than that of commercial WOW wells. However, the depth of microwells did not differ significantly between these two culture systems. Thus, the cWOW culture system provided a suitable

size for mouse ZF embryos and could improve the developmental ability *in vitro*.

In Chapter III, I investigated the effect of ZPR on pre-implantation embryonic development and cell lineage-specific gene expression. The results showed that ZPR induced earlier compaction compared with ZI embryos. Furthermore, the expression of inner cell mass (ICM) (*Oct4, Sox21*) -related genes was significantly increased, and the expression of TE (*Cdx2, Eomes,* and *Tfap2c*) -related genes was significantly decreased in the ZF embryos compared with ZI embryos at the morula stage. In the blastocyst stage, the expression of these genes was similar to the morula stage, in which the significantly increased expression of ICM-related genes (*Nanog*, *Oct4, Sox2,* and *Sox21*) and decreased expression of the TE-related genes (*Cdx2, Eomes,* and *Tfap2c*) in the ZF embryos compared with ZI embryos. In addition, the differentiation-specific protein expression of both ICM (OCT4) and the TE (CDX2) was significantly altered and the expression pattern was consistent with the results of gene expression (*Oct4*/*Cdx2*) in the blastocyst. These findings suggest that ZPR disrupts the expression of ICM/TE-related genes.

In Chapter IV, I investigated the effects of ZPR on the post-implantation development of mouse embryos. After embryo transfer (ET), ZF embryos had a lower rate of implantation and lower number of live fetuses than ZI embryos, whereas there was no significant difference in fetal weight at E17.5. In contrast, the placental weight of ZF embryos was significantly increased compared with ZI embryos. Then, RNA-seq analysis of the placenta was performed. The RNA-seq analysis showed a total of 473 differentially expressed genes (DEGs) that significantly influenced the biological

processes (BP). These results showed that the ZPR affected the post-implantation development of mouse embryos after ET.

In Chapter V, I investigated the effect of blastomere structure at the 4-cell stage due to the loss of the ZP protection and the morphological changes from a 3D structure to a two-dimensional (2D) structure on the subsequent development and gene expression. The blastomere allocation of ZF 4-cell stage embryos was significantly different compared with that of ZI embryos, which were classified into four types (3P, 4P, 5P, 6P) based on the number of blastomere attachment surface sites. In contrast, most ZI embryos showed two types (5P and 6P), and 3P and 4P types were not observed. There was no significant difference in the blastocyst rates of ZF embryos showing 3P, 4P, 5P, and 6P types compared with ZI embryos. The total cell number (TCN) of the blastocyst developed from the 3P type was significantly lower than that of the ZI and other types, whereas the TCN of the 4P, 5P, and 6P types was not significantly different compared with the ZI blastocysts. In addition, the expression of *Carm1* mRNA and protein, which has been recently discovered as a transcriptional regulator for differentiation, was significantly higher in ZF 4-cell embryos than in ZI embryos. At the blastocyst stage, the expression of DNA methylation-related genes (*Dnmt1, Uhrf1, Dnmt3a,* and *Dnmt3b*) was also significantly decreased in the ZF embryos compared with ZI embryos. These results suggest that the ZPR at the 2-cell stage affects the morphological changes of blastomere allocation in 4-cell embryos associated with TCN of the blastocyst and the expression of DNA methylation-related genes.

In Chapter VI, I developed a new ZPR protocol by combining acid Tyrode's

solution and proteinase K treatment and subsequent culture in the cWOW system. Although acid Tyrode's solution treatment is commonly used for ZPR and reduces ZPR time, I found that the acid Tyrode's solution has detrimental effects on blastomere morphology such as wrinkled surface and on developmental competence with induction of apoptosis in the blastocyst. Besides, proteinase K treatment, which is also used for ZPR, increased ZPR time and significantly decreased the blastocyst rate, but did not increase apoptotic cell numbers or induce the expression of apoptosis-related genes. In contrast, a serial combined treatment (two-step method) significantly reduced ZPR time and improved blastocyst rate by increasing the TCN and reducing the apoptotic cell numbers. These results suggest that a new ZPR protocol is beneficial for reducing the toxicity of ZF embryo development and its quality.

In conclusion, I elucidated the role of ZP not only keeps the blastomere structure for embryonic development, but also affects the gene expression and differentiation of pre- and post- implantation development. The new method for quick and harmless ZPR and culture systems suitable for mouse ZF embryos will contribute to the development of assisted reproductive technology (ART).

Chapter I

General Introduction

Mammalian eggs are surrounded by an outer layer called the zona pellucida (ZP). All mammalian eggs have ZP, but the thickness (~1-25 μm), protein content (~1-30 ng) of eggs, and glycoproteins composition are highly varied greatly depending on the species of animal [1, 2]. In humans, the ZP is composed of four glycoproteins (ZP1, ZP2, ZP3, ZP4) [2], but in mice, ZP is only composed of three glycoproteins (ZP1, ZP2, ZP3) [2], all encoding a relatively conserved recognition domain which contributes to oocyte/sperm interactions during the initial phases of fertilization [3].

The ZP surrounds the mammalian oocyte, ovulated egg, and preimplantation embryo until the early blastocyst stage of development. The ZP plays important role in fertilization and preimplantation development. For example, during fertilization, ZP regulates the binding of sperm to the ovulated egg and inducing the acrosomal reaction and preventing polyspermy [4]. The ZP also ensures the integrity of the preimplantation embryo for its successfully transported through the reproductive tract [5] and prevents premature attachment to the oviduct and endometrial surfaces [6].

After fertilization, the zygotes undergo a series of changes, including zygotic genome activation (ZGA) and cell lineage specification, all of which are essential for the development of the blastocyst. The blastocyst consists of the inner cell mass (ICM) and the trophectoderm (TE), the ICM forms the epiblast (EPI), and the primitive

endoderm (PE) [7, 8], and the ICM forms the fetus in the future. TE is subdivided into a polar TE covering the EPI at the embryonic pole to form the ectoplacental cone (EPC) and a mural TE covering the blastocyst cavity and forming the giant cells in the future [9, 10]. After implantation, TE differentiates to the EPC, the EPI, embryonic ectoderm (ExE), visceral endoderm (VE), the parietal yolk sac, and the trophoblast giant cell (TGC) layer, which together surrounds the entire conceptus [11-14]. By the end of gastrulation, three major germ layers have formed, and all fetal tissues will develop from the ectoderm, mesoderm, and definitive endoderm. Therefore, for achieving successful implantation, placental and fetal growth, embryos should be escaped from ZP when the embryo reached the uterus.

A previous report has mentioned that the thickness and hardening of the ZP affect the hatchability of embryos produced *in vitro*, resulting in relatively low implantation rates [15]. In humans, normal hatching at the blastocyst stage occurs in good quality embryos, while poor quality embryos do not successfully complete the hatching when they are transferred to the uterus [16]. However, another research has demonstrated the potential improvement of implantation of embryos that have difficulty in hatching ability by ZP before ET. This report took the opposite view to Urman et. al (2002) showing that the success of *in vitro* hatching is independent of blastocyst quality [17]. Several studies have shown that partial or complete ZPR in human blastocysts can improve implantation rates. For example, partial or complete ZPR prior to ET may improve implantation rates, mainly in patients with poor fertility prognosis [15, 16, 18]. For improving the hatching ability of embryos, several methods of ZPR are available

including physical methods (mechanical dissection, laser drilling) and chemical methods (acid Tyrode's solution and enzyme with pronase) [19-23]. However, at present, the effects of ZPR at the blastocyst stage on ICM and TE are still not clear [16]. In assisted reproductive technology (ART), intracytoplasmic sperm injection (ICSI) has become the most widely used method of assisted fertilization treatment [24]. In most cases, ICSI is highly efficient in achieving high fertilization rates, independent of oocyte and sperm factors [25-27]. However, a previous study reported that ZP loss occurs in human IVF using the ICSI due to mechanical damage during oocyte retrieval [28]. At present, it is not clear whether ZPR at the early stages affects subsequent embryonic development.

In vitro production (IVP) of mammalian embryos has been rapidly improved and is now widely used in reproductive technologies, such as ART, including humans in medicine and animals designed to facilitate breeding and development, production of transgenic animals, and cloning [29]. The ZP is often manipulated during IVP procedures with changes including thinned ZP and complete or partial ZPR. ZPR is used for several applications for basic research and production of chimera [30], transgenic animals [31], identical multiplets by blastomere separation [32], handmade cloning [33], and RNA interference [34].

A previous study has reported that blastomere association in ZF 4-cell stage embryos has important effects on further differentiation into ICM and TE when using a multi-plate system, affecting subsequent embryonic development in mice [35]. The ZP plays diverse roles in embryonic development both *in vivo* and *in vitro*. During early

embryonic development, one of the key roles of ZP is to maintain the structure between blastomeres [36]. Without the ZP, the contact between each blastomere becomes loose, resulting in the arrest of embryonic development or loss of embryonic integrity [37]. Therefore, several culture systems for ZF embryos have been developed, including the glass oviduct, Well of the Well (WOW), and empty ZP [38], all with the aim of improving outcomes [39, 40]. Collectively, ZPR at the early stage of embryos may affect embryonic development during the cleavage stage and subsequent implantation.

In this study, I first developed the customized WOW system (cWOW) suitable for mouse ZF embryo culture which can improve the developmental ability *in vitro*, and then I investigated the effect of ZPR at the 2-cell stage on the pre-implantation and post-implantation development and gene expression. This culture system suitable for mouse ZF embryos using the quick and harmless ZPR method will contribute to the development of ART.

Chapter II

Establishment of the optimized *in vitro* culture system for zona free mouse embryos

Introduction

The zona pellucida (ZP) is a mixed structure of glycoproteins produced both by the oocyte and the ovarian follicles and surrounds follicular oocytes, ovulated eggs, and preimplantation embryos [41]. ZP has multiple roles in oocyte growth, fertilization, and early development of blastocyst before implantation in the uterus [42]. In humans, ZP is constructed of four glycosylated proteins, called hZP1-4, that are also encoded by single-copy genes located on different chromosomes [43]. The mouse ZP is composed of several glycoproteins (ZP1, ZP2, ZP3), called mZP1-3, mouse ZP4 is a pseudogene, encoded by single-copy genes located on different chromosomes [2, 44, 45], and all encoding a relatively conserved recognition domain which contributes to oocyte/sperm interactions during the initial phases of fertilization [3].

In order to develop a new individual after fertilization, the initial stages of embryonic development require a rapid transformation of the germ cells into a totipotent state [46]. The totipotent state is reprogrammed among differentiated germ cells, eggs, and sperm during the first hours after fertilization. A newly fused and formed zygotic genome can subsequently start differentiation to form different cell

types in the adult animal during this process [47]. This efficient reprogramming relies on maternally supplied RNA and proteins stored in the oocyte [46]. When reprogramming occurs, the zygotic genome continues its development after the initial reprogramming stage. Transcriptional control is passed to the zygote through a process called maternal-zygotic transition (MZT), in which degradation of the maternal product is coordinated with zygotic genome activation (ZGA) [48]. As with ZGA, maternal mRNA clearance is a gradual process [49]. Some transcripts are eliminated soon after fertilization, while others are degraded only after the major wave of transcription [48]. Depending on the species, overall, up to 60% of maternal mRNA levels are significantly reduced [50]. Of these, 30-40% of maternally deposited mRNA is eliminated by degradation. The mechanisms regulating genomic activation are different between species models. For example, in humans, the main period of ZGA occurrence is the 8-cell stage [51]. In mice, the zygotic genome is mainly activated at the 2-cell stage [51, 52].

A previous study has shown that in human embryos, removal of the ZP and culturing in the WOW system for ZF embryos could reduce the cytoplasmic fragmentation, which may provide the major breakthrough needed for those patients who have difficulty obtaining quality embryos [53]. However, a previous study reported cellular association at the ZF 4-cell stage embryos importantly affects the further differentiation of ICM and TE when using multiple systems influencing subsequent embryonic development in mice [35]. To date, several culture systems for ZF embryos have been developed including glass oviducts, and WOW, all designed to

improve outcomes [39, 40]. In humans, although *in vitro* culture of embryos is an important step in assisted reproduction, only 1.2% of studies published in five major journals in the field of human reproduction since 2019 focused on *in vitro* culture conditions. The more culture system currently used in the research or commercial is Well of the Well (WOW). Despite the size and shape of the original WOW providing a practical and useful solution to improve the overall quality of cultured embryos [54], three-dimensional (3D) surfaces are currently used instead of the large flat bottom and microdroplets. Also, these microwells are designed for optical clarity rather than for the needs of ZI embryos [54], especially not for ZF embryos. Therefore, a culture system is required for supporting the development of mouse ZF embryos.

In this chapter, I developed a customized WOW system designed to accommodate the smaller microwell size and investigated the optimal environment for mouse ZF embryo development *in vitro*.

Materials & Methods

Animals

ICR male and female mice (8 weeks, Sankyo, Tokyo, Japan) were used for all experiments with feeding a standard diet and housed in a controlled environment with a 12 h day: night cycle. All animal experiments were performed with the approval of

the Institutional Animal Care and Use Committee at Hokkaido University (approval number 19 (77)-2).

Oocyte collection and in vitro fertilization

Oocytes were collected using standard methods and superovulation was induced by injecting 5 IU pregnant mare serum gonadotropin (PMSG) (ASKA Pharmaceutical, Tokyo, Japan) and then 5 IU human chorionic gonadotropin (hCG) (ASKA Pharmaceutical, Tokyo, Japan) 48 h later.

Spermatozoa were collected from cauda epididymis of male mice and preincubated in the droplets of human tubal fluid (HTF) medium at 5% CO_2 and 37 °C for 1.5 h. Cumulus oocyte complexes (COCs) were collected from the oviduct 15 h after hCG injection and then transferred to preprepared HTF droplets. These HTF droplets were then mixed with the preincubated spermatozoa to facilitate IVF. After 6 h of insemination, putative zygotes were transferred into droplets of M16 medium for *in vitro* culture. All culture droplets were covered with paraffin oil (Nacalai Tesque Inc, Kyoto, Japan). Zygotes that reached the 2-cell stage after 24 h were used for the experiments.

Establishment of a culture system for ZF 2-cell embryos

ZF 2-cell embryos were obtained by incubating the zona intact (ZI) embryos in

acid Tyrode's solution (Sigma-Aldrich, Gillingham, UK) for 60 s. ZF embryos were then cultured in a (1) conventional microdroplet culture system using a flat bottom Petri dish (60 × 15 mm, Corning, NY), (2) a commercial WOW dish (DNP, Japan), or (3) a customized WOW (cWOW) dish by making wells manually in a 60 mm × 15 mm Petri dish (Corning, NY, USA). The cWOW system was performed as described previously with some modifications, in which the microwell size was designed for the size of mouse embryos rather than for optical clarity [40, 54]. The microwell size of commercial WOW and cWOW was measured using color 3D laser microscopy (VK-9710, KEYENCE, Osaka, Japan). The cWOW dish containing 16 microwells was covered with 88 μl of a droplet of the M16 medium under paraffin oil. Individual ZF embryo was put into the bottom of each microwell and cultured for 2.5 days under 5% CO_2 in air at 37 °C. After 2.5 days, the blastocyst rate was evaluated.

Statistical analysis

Data are representative of at least three independent experiments. All data are shown as the mean ± standard error of the mean (SEM). Statistically significant differences were assessed by student's *t*-test and one-way analysis of variance (ANOVA)-Tukey's Multiple Range Test implemented in Graphpad Prism® 7 Software (La Jolla, CA, USA). Statistical significance was set at $p < 0.05$.

Results

Effect of culture systems on the development ability of ZF embryos in vitro

In the initial study, I used acid Tyrode's solution treatment at the 2-cell stage to produce ZF embryos to evaluate the effects of different culture systems including flat microdroplets (Figure. 1-①), WOW (Figure. 1-②), and cWOW (Figure. 1-③). First, I compared the developmental ability of ZF embryos in the different culture systems *in vitro*. The blastocyst rate of ZF embryos cultured in cWOW was significantly higher than that of those cultured in flat microdroplets and commercial WOW system (Table 1). Next, to provide conditions to keep the 3D blastomere structure, I used the cWOW culture system (Figure. 1-③), which was designed to reduce the microwell size and to provide a better condition for embryos to keep communication between each blastomere. The blastocyst rate was significantly increased compared with the flat microdroplets and WOW systems.

Effect of different culture systems on the morphology of ZF embryos

To investigate the reasons for the low blastocyst rate of ZF embryos in different culture systems, I observed the morphology in different culture systems from 2-cell to blastocyst stages. In the flat microdroplets, the morphology in the blastomere allocation at the 4-cell stage was obviously different, appearing as a linear arrangement of

blastomere, which showed an irregular shape rather than a compacted status when developing to the morula stage (Figure. 2-A). In the WOW system, although the morphology of the 4-cell stage remained different from that of the ZI embryos, the morphology of the morula stage was improved, approaching the round compacted morula (Figure. 2-B). Compared to the flat microdroplet and WOW systems, the shape of the morula embryos in cWOW (Figure.2-C) significantly improved the compaction process, showing a more rounded compacted embryo shape.

Comparison of microwell sizes between the commercial WOW and cWOW

I compared the microwell sizes of the WOW and cWOW by 3D surface scanning and revealed that the average diameter of the microwells in the cWOW system was significantly smaller than those of the commercial WOW (Figure. 3C). The diameter of commercial WOW plates was approximately 280 μm, whereas, this cWOW microwell had a diameter of approximately 170 μm. However, the depth of these wells was not significantly different in these two systems (Figure. 3D).

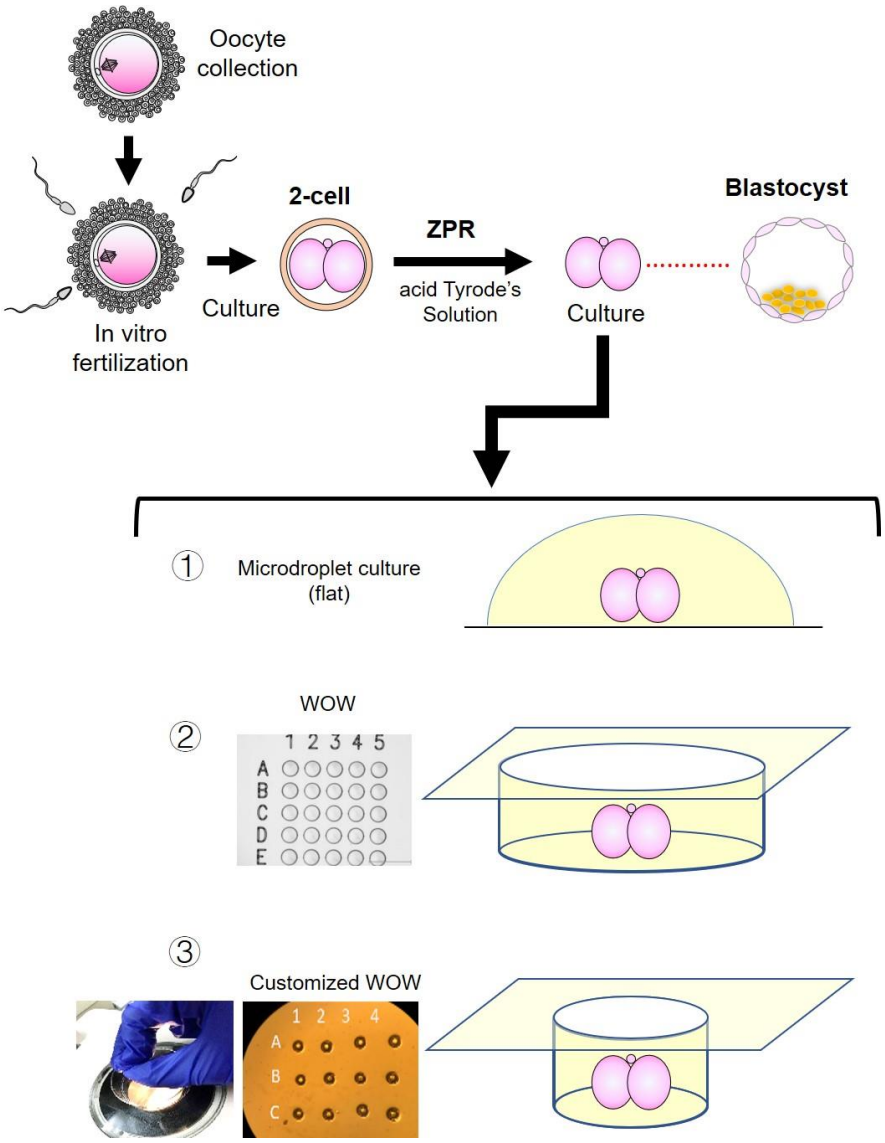

Figure 1. Workflow describing the method of ZPR and ZF embryo culture.

The 2-cell embryos were treated with acid Tyrode's solution until the ZP was completely removed. Two-cell stage of ZI embryos was used as the control and ZF embryos were cultured using the following systems of microdroplet ①, WOW ②, or cWOW ③. These microwells were manually produced using an aggregation needle and paraffin oil and each microwell contained a single ZF embryo at the bottom of the dish. ZF: Zona Free.

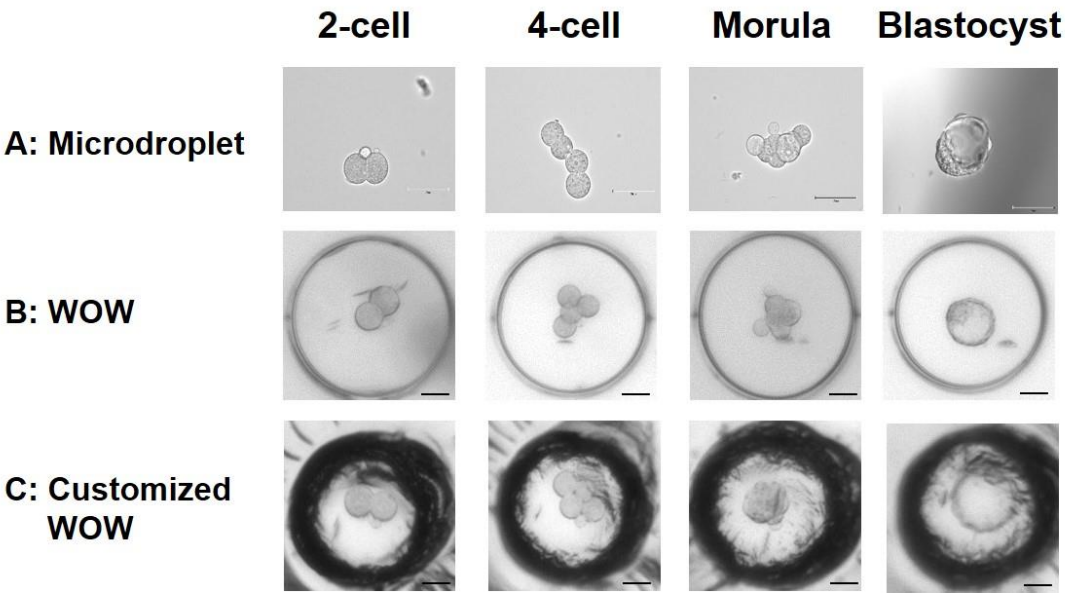

Figure 2. Morphological differences in the ZF embryos cultured in each culture system.

Enlarged image of the morphological differences during the various development stage in the ZF embryos cultured in each culture system. A: Microdroplet system. B: Commercial WOW system C: Customized WOW system. Scale bar: 50 μm.

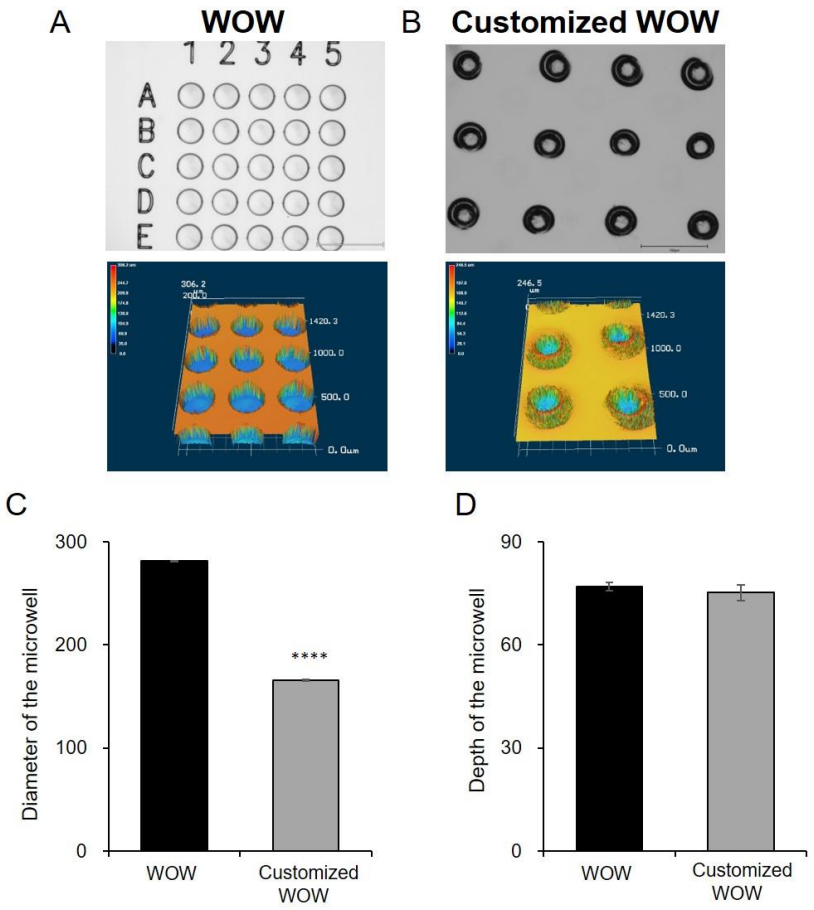

Figure 3. Comparison of microwell sizes in the WOW and cWOW systems.

The microwell size in each culture system was determined using color 3D laser microscopy. A: Commercial WOW system. B: Customized WOW system. Scale bar: 750 μm. C: The diameter of each of the microwells in each culture system. D: Depth of the microwells in each culture system. The results are reported as the mean ± S. E. M., and the Student's *t*-test was used for all statistical analyses. Asterisks indicate significant differences (**** $p < 0.0001$).

Table 1. Effect of different culture systems on the development of ZF mouse embryos

Culture system	No. of replication	No. of embryos cultured (Started from 2-cell)	No. of blastocyst developed (Mean ± SEM)
Microdroplets	4	85	31 (36.5 ± 1.4^{a})
WOW	4	70	41 (59.0 ± 2.5^{b})
cWOW	4	88	61 (69.3 ± 0.79^{c})

ZF embryos were cultured in the following systems (1) a flat microdroplet, (2) WOW, and (3) cWOW.

Flat microdroplets: ZF embryos were cultured in a normal flat microdroplet. WOW: ZF embryos were cultured in the commercial WOW containing 25 microwells. Customized WOW: ZF embryos were cultured in a cWOW system containing 16 microwells. The data are expressed as the mean ± SEM, and one-way ANOVA was used to analyze the data. Different letters indicate statistical differences (a *vs.* b: $p < 0.0001$, a *vs.* c: $p < 0.0001$, b *vs.* c: $p < 0.05$).

Discussion

Establishing a more suitable culture system for ZF embryos is essential for improving quality and broadening their application in ART and embryology. Here, I developed and evaluated an *in vitro* culture system suitable for ZF embryos by applying the cWOW system with a smaller microwell size, which can be suitable for the culture of ZF embryos.

In humans, *in vitro* culture of embryos is an important step in ART, however, only 1.2% of research papers published in five representative journals in the field of human reproduction focused on *in vitro* culture conditions in 2019, giving the impression that the optimization process is nearing its limits [54]. In addition, in recent decades, ART has been developed in several mammalian species. It has been reported the beneficial effect of microwell culture on the development of bovine embryos by customized WOW [40, 55] and commercially available WOW (25 microwells) [56].

In addition, a previous study has demonstrated that the rate of cleavage and blastocyst was higher in the WOW system than in the droplet culture system [57]. The size of microwells and the shape of the bottom of these WOW microwells provide a practical and straightforward solution to combine the advantages of communal and individual incubation and improve the overall embryonic quality *in vitro* culture.

One of the most important roles of the ZP during early embryonic development is the maintenance of the 3D structure of blastomeres to keep in contact with each other. Without ZP, cleaved blastomeres often adopt 2D forms (Figure. 2) and retain this

structure until compacted in a flat bottom dish. This indicates that the weakening of 3D contacts between the blastomeres affects further development, differentiation, and embryonic developmental ability. A previous study revealed that WOW improves the development of bovine ZI and ZF embryos [40]. The possible reason for the beneficial effect of WOW for individual embryos is that the better 3D structure can provide the culture condition by the effective usage of the embryo-secreted factors, and prevent the movement of ZF embryos in the culture medium. Besides, the smaller microwell structure also keeps the attachment and 3D structure of blastomeres for ZF embryos followed by the improvement of development. Although commercial WOW has shown positive effects on mouse single blastomere culture *in vitro* [32] as well as the cytoplasmic fragmentation of ZF embryos in humans [53], the effectiveness of commercial WOW on the culture of the mouse embryos and its impact on their developmental competence has not yet been reported. In the present study, these results show that the blastocyst rate for ZF embryos in the flat microdroplet system was significantly low (Table 1).

In contrast, the use of a commercially available WOW system improved the blastocyst rate in ZF embryos, However, the diameter of the commercially available WOW microwell is large and flat to support the development of ZF embryos in mice. Therefore, cWOW with a smaller microwell bottom area was shown to be the more efficient system for ZF culture compared with commercial WOW. In addition, this cWOW produced a significant increase in the blastocyst rate compared to commercial WOW which microwell size affects the subsequent development. In general, when

comparing the size of the ZF mouse embryos (approximately 100 μm) with the diameter of commercial WOW plates (approximately 280 μm), we can see that these microwells are likely to be too wide (Figure. 2, 3). In contrast, this cWOW microwell had a diameter of approximately 170 μm which may provide more suitable conditions for cell division and the maintenance of the 3D blastomere structures, allowing for improved development and differentiation.

In the present study, cWOW was a handmade culture system, thus the uniformity of microwell size was not precise. Therefore, the production of cWOW by the 3D printer or by other methods to make a large number of cWOW will contribute to the improvement of embryos customized for the species-dependent culture system. In summary, in this thesis of Chapter II, I propose a WOW culture system in which these microwells are designed for the own needs of the mouse ZF embryos to improve their development *in vitro*.

Chapter III

Effect of ZPR on the pre-implantation development and gene expression of mouse embryos

Introduction

As mentioned in Chapter II, zona pellucida (ZP) is the extracellular elastic coat that encapsulates mammalian ovarian oocytes, ovulated oocytes, and preimplantation embryos [41, 58]. When embryos start to cleave after fertilization, the contact among the blastomeres is very vulnerable. Thus, the role of the ZP is important to protect the embryos, maintain their integrity, and prevent the premature attachment of embryonic cells to the oviductal and endometrial cells before implantation [6].

In addition to the physiological role of the ZP for keeping the 3D structure of blastomeres, differentiation is also dynamically altered during the blastomere cleavage and differentiation. After fertilization, maternal mRNAs and proteins are gradually degraded, and the zygotic genome begins to be activated at the 2-cell stage, known as zygotic genome activation (ZGA) [52]. The 2-cell stage embryos have totipotency and exhibit cellular plasticity at the 4-cell stage [59]. Subsequently, the embryos undergo multiple cleavages to initiate compaction. After compaction, the first cell lineage segregation occurs at the time of blastocyst formation. Most of the outer cells form the trophectoderm (TE), whereas the inner cells become the inner-cell mass (ICM) in

blastocysts, which is referred to as the first cell fate decision [60-62]. When mouse embryos develop to d4.5, the cells located in the inner layer of the ICM become epiblast (EPI), and the cells located in the blastocoel become primitive endoderm (PE) [63, 64]. ICM develops into the entire fetus, whereas TE forms the fetal portion of the placenta [62, 64]. During embryonic development, all transcription factors act as a network that influences and interact with each other, which is essential for the specification of distinct cell types. It is well known that the key regulators, *Oct4, Sox2*, and *Nanog* are essential for the formation and maintenance of ICM during mouse embryonic development as well as pluripotent embryonic stem cells (ESCs) self-renewal [65-67]. *Sox17* is an important marker of the PE and its derivatives, which are involved in developmental processes [68]. In addition, the regulatory region of *Sox21* is the target of OCT4 binding, and its expression is regulated by SOX2. SOX21 is involved in ESCs differentiation and the inhibition of *Cdx2* expression [69-71]. Moreover, *Cdx2* is a well-known transcription factor expressed specifically in TE, which represses the expression of the pluripotency regulator *Oct4* and vice versa [72].

The ZP plays diverse roles in embryonic development, both *in vivo* and *in vitro*. During early embryonic development in mice, one of the key roles of ZP is to maintain the structure of blastomeres [36]. Without the ZP, the contact between blastomeres becomes loose, resulting in growth retardation, affecting compaction, and the potential loss of embryonic integrity [37]. In contrast, a previous study has shown that the excessive thickness and hardening of the ZP also impair the hatching ability of *in vitro*-produced human embryos [15]. Nowadays, assisted zona hatching (AZH) is used in *in*

vitro production (IVP) procedures. A previous study demonstrated that ZPR before ET does not reduce the implantation rates of human embryos, which is thought to result from the successful contact and communication of the TE with the endometrium; thus it is effective for improving the implantation rate [17]. To date, ZPR procedures have been broadly used for nuclear transfer (hand-made cloning), production of identical twins or quadruplets by blastomere separation, gene transfer [36], or preparation of chimeric mice by blastomere aggregation [59]. Although preimplantation development of ZF embryos has been investigated, little is known about the role of the ZP in early embryonic development and gene expression. Thus, the aim of this Chapter III was to assess the effect of ZPR on the pre-implantation development and ICM- and TE-related gene expression of mouse embryos.

Materials & Methods

Animals

ICR male and female mice (8 weeks, Sankyo, Tokyo, Japan) were prepared as described in Chapter II.

Preparation of mouse embryos

The mouse ZF embryos were prepared as described in Chapter III.

In vitro culture of ZF embryos

Mouse ZF embryos were produced by acid Tyrode's solution (Sigma-Aldrich) for 1 min. After the treatment, ZF embryos were washed in the M2 medium and then cultured in a cWOW system as described in chapter II. Embryos were cultured at 5% CO_2 and 37 °C. Well-developed embryos were used for the experiments of qPCR, TUNEL assay, and immunostaining.

RNA extraction and quantitative PCR

RNA extraction and qPCR were performed as previously described [36]. According to the manufacturer's guidelines, five embryos were used for RNA collection and cDNA synthesis by applying the Super Prep Cell Lysis & RT Kit for qPCR (TOYOBO). qPCR was performed using the THUNDERBIRD SYBR qPCR Mix (TOYOBO, Osaka, Japan) to evaluate the expression of ICM- and TE-related genes and the primers used for qPCR in this study were listed in Supplementary Table 1. The thermal cycling for the qPCR program was carried out (1 cycle of 95 °C for 30 s; 45 cycles of 95 °C for 10 s, 55 °C for 15 s, and 72 °C for 30 s) with Light Cycler Nano (Roche Diagnostics, Basel, Switzerland). The mRNA levels of all genes were calculated using the ΔΔCt method [73], and *Gapdh* was considered as a reference gene [74]. All gene expression data were applied to all analyses and repeated at least three

times.

Immunostaining

Relatively well-developed blastocysts were fixed with 4% (v/v) paraformaldehyde (Fujifilm Wako Pure Chemical Corporation, Osaka, Japan) in phosphate-buffered saline (PBS) for 60 min and then permeabilized using 0.2% (v/v) Triton X-100 in PBS (T-PBS) solution for 60 min at room temperature. Subsequently, embryos were washed three times for 10 min each in 0.2% PVA-PBS and then incubated with anti-CDX2 antibody (1:400; ab76541, Abcam, UK) and anti-OCT4 antibody (1:100; Sc-5279, Santa Cruz Biotechnology, Texas, USA) diluted with blocking solution overnight at 4 °C. After five times washing for 10 min each in 0.1% (v/v) Triton X-100 and 0.3% (w/v) bovine serum albumin (Sigma-Aldrich, St. Louis, USA) in PBS, the embryos were incubated with a secondary antibody with Alexa Fluor 568 donkey anti-rabbit IgG (1:400; Invitrogen, MA, USA) or Alexa Fluor 488 goat anti-mouse IgG antibody (1:400; Invitrogen, MA, USA) diluted in the blocking solution for 60 min at room temperature. Finally, blastocysts were mounted onto a glass slide using VECTASHIELD with DAPI (Vector Laboratories, Burlingame, CA, USA) for nuclear staining. Fluorescence was detected using a scanning confocal microscope (TCS SP5, Leica Microsystems, Mannheim, Germany). The obtained images were analyzed with ImageJ software [75].

Terminal deoxynucleotidyl transferase biotin-dUTP nick end labeling (TUNEL) assay

of blastocyst

Early blastocysts were assessed for apoptosis by the TUNEL method with MEBSTAIN Apoptosis Kit Direct (MBL, Life science, Tokyo, Japan) according to the manufacturer's instructions. After blastocysts were fixed with 4% (w/v) paraformaldehyde solution (FUJIFILM Wako Pure Chemical Corporation, Osaka, Japan) diluted in PBS for 60 min at room temperature, embryos were rinsed three times in 0.2% PVA-PBS for 10 min each. Then embryos were permeabilized by 60 min of incubation in 0.2% T-PBS dilution. Then blastocysts were then rinsed three times in 0.2% PVA-PBS for 10 min each and the fragmented DNA ends of the cells were labeled with fluorescein-dUTP for 60 min at 37 °C. Early blastocysts were incubated in 1 μg/mL of Hoechst 33342 solution (Sigma-Aldrich, Darmstadt, Germany) for nuclear staining. The fluorescence of the fragmented DNA ends was detected by a Leica confocal microscope (TCS SP5, Germany), and the apoptotic index was calculated for each blastocyst as follows: (number of TUNEL-positive cells/TCN) × 100.

Statistical analysis

All data are representative of at least three replicates and statistically significant differences were identified using one-way analysis of variance (ANOVA)-Tukey's multiple range test implemented in GraphPad Prism 7 software (LA Jolla, CA, USA). Statistical significance was set at $p < 0.05$.

Results

Effect of ZPR on the developmental status at the 8-cell stage

During preimplantation development of mice, zygotes undergo cleavage three times to generate 8-cell stage embryos and start compaction. To explore the effects of ZPR on the timing of compaction, morphological changes were observed and the developmental status was estimated at the 8-cell stage. ZF embryos started compaction faster than ZI embryos (Figure. 4A). In addition, there were distinct differences in the morphology was observed in ZF embryos at the 8-cell which varied form from the compacted morula stage (Figure. 4A), and even some ZF embryos started cavitation (Figure. 4A-3, 4). The rate of compaction (E2.5-E2.75) was significantly faster in ZF embryos than in ZI embryos at the 8-cell stage (Figure. 4B).

Effect of ZPR on the expression of ICM- and TE-specific genes in morula stage

Since ZI and ZF embryos had different developmental speeds and morphologies at the 8-cell stage, I next investigated the effect of ZPR on the expression of differentiation-specific genes both in the morula and blastocyst stages.

Expression levels of ICM-related genes (*Nanog, Oct4, Sox2, Sox21*) and TE-related genes (*Cdx2, Eomes, Tfap2c*) are shown in Figure. 5 and Figure. 6, respectively.

The expression of *Oct4* and *Sox21* was significantly higher in ZF than in ZI embryos, whereas *Nanog* and *Sox2* indicated high expression levels, but, a significant difference was not observed between ZI and ZF embryos. The gene expression of *Cdx2*, *Eomes*, and *Tfap2c* was significantly lower ($p < 0.05$) in ZF embryos than in ZI embryos.

Effect of ZPR on the expression of ICM- and TE-specific genes in blastocysts

ICM- (*Nanog, Oct4, Sox2, Sox17,* and *Sox21*) and TE (*Cdx2, Eomes,* and *Tfap2c*) related genes were detected at the blastocyst stage as shown in Figure. 7 and Figure. 8, respectively. The mRNA expression levels of *Oct4, Nanog, Sox2,* and *Sox21* were significantly higher ($p < 0.05$) in ZF blastocysts than in ZI blastocysts. In contrast, the mRNA expression of *Sox17,* a PE marker, was significantly lower ($p < 0.05$) in ZF blastocysts. In addition, the expression of TE-related genes (*Cdx2, Eomes,* and *Tfap2c*) was significantly lower ($p < 0.05$) in ZF blastocysts than in ZI blastocysts.

By comparing the expression pattern of morula and blastocyst stages, a similar pattern was observed in the expression of specific ICM and TE genes by ZPR. To investigate whether the ZPR treatment of acid Tyrode's solution disturbs the expression of ICM/TE differentiation-related genes, ZPR was performed with proteinase K (pH 7) solution followed by culture in the cWOW system until development to the blastocyst stage. The mRNA expression levels of ICM/TE marker genes (*Oct4/Cdx2*) were examined by qPCR (Figure. 9). *Oct4* mRNA expression level was significantly higher ($p < 0.05$) in ZF blastocysts than in ZI blastocysts. The *Cdx2* mRNA expression level

was significantly lower ($p < 0.05$) in ZF embryos than in ZI embryos. Gene expression patterns of *Oct4* and *Cdx2* were similar in blastocysts obtained both by acid Tyrode's solution (pH 2.5) and proteinase K (pH 7) treatment. These results suggest that the change of gene expression in ZF embryos was caused by ZPR itself, rather than by a different treatment.

To examine the expression of marker proteins (OCT4 and CDX2) and cell numbers in the ICM and TE of blastocysts, immunostaining of OCT4 (Figure. 10), and CDX2 (Figure. 11) was performed. The fluorescent signal of OCT4 was clearly detected in ICM, and its intensity was significantly higher ($p < 0.05$) in ZF than in ZI embryos (Figure. 10C), whereas the cell number of ICM was not significantly different (Figure. 10B) between ZI and ZF embryos. However, the fluorescent signal of CDX2 was significantly lower ($p < 0.01$) in the TE of ZF blastocysts (Figure. 11C), and the TE cell number was lower in ZI blastocysts than in ZI blastocysts ($p < 0.0001$) (Figure. 11B).

Effect of ZPR on apoptosis and total cell number in the blastocyst stage embryos

Compared with ZI embryos, the total cell number (TCN) in early blastocysts was significantly lower ($p < 0.0001$) (Figure. 12B). Next, to investigate the effect of ZPR on apoptotic status, TUNEL assays were performed in the early blastocyst stage (Figure. 12A). In ZF embryos, the number of apoptotic cells was significantly increased ($p < 0.05$), as was the apoptotic index ($p < 0.01$) (Figure. 12C, D).

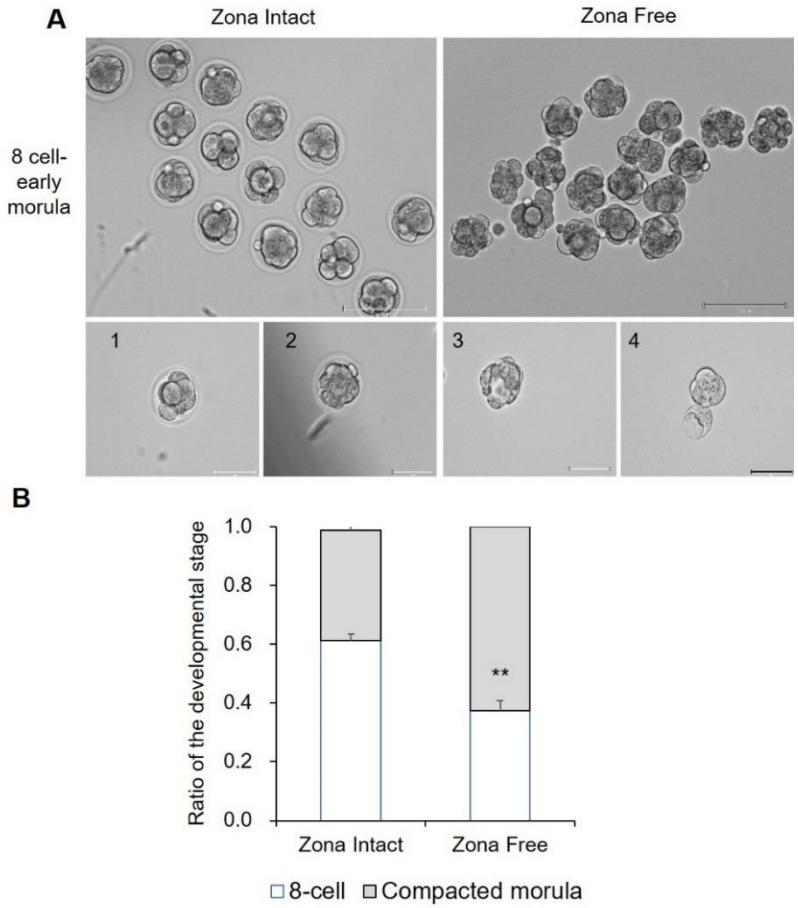

Figure 4. Representative microphotographs of embryos cultured with or without zona pellucida in the mouse 8-cell to morula stage.

A: Morphological change between ZI and ZF in mouse 8-cell to morula stage (approximately 62-66 h after fertilization). B: The ratio of the developmental stage at the 8-cell to the morula stage was statistically analyzed (ZI, n = 60; ZF, n = 68). n = the total number of embryos. Scale bar at the top of Figure A = 150 μm; Scale bar at the bottom of 1, 2, 3, and 4 = 75 μm. The data are expressed as mean ± standard error of the mean (SEM), and Student's *t*-test was used to analyze at least three replicated experiments. Value with asterisks indicates a significant difference, ** $p < 0.01$.

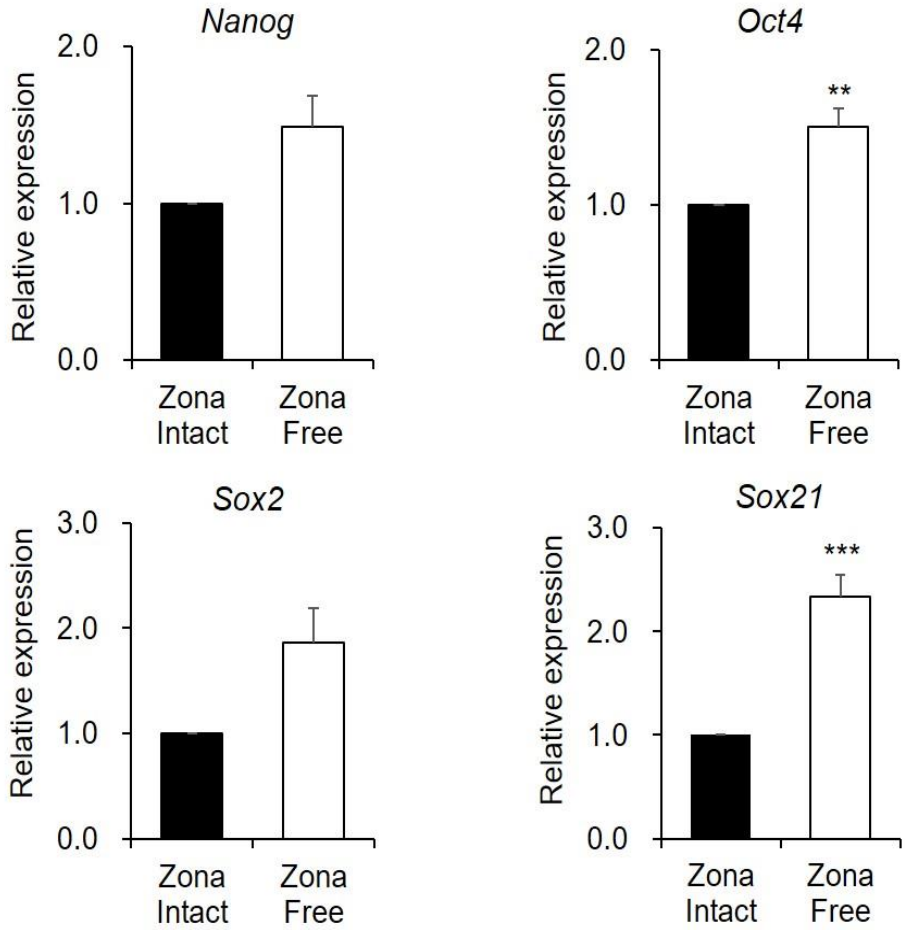

Figure 5. Effect of ZPR on the expression levels of ICM-specific genes in the morula stage.

Expression levels of *Nanog*, *Oct4*, *Sox2*, and *Sox 21* in the morula stage embryos were analyzed by qPCR. Data are expressed as mean ± standard error of the mean (SEM), and Student's *t*-test was used to analyze at least three replicated experiments. Value with asterisks indicates significant differences. ** $p < 0.01$, *** $p < 0.001$.

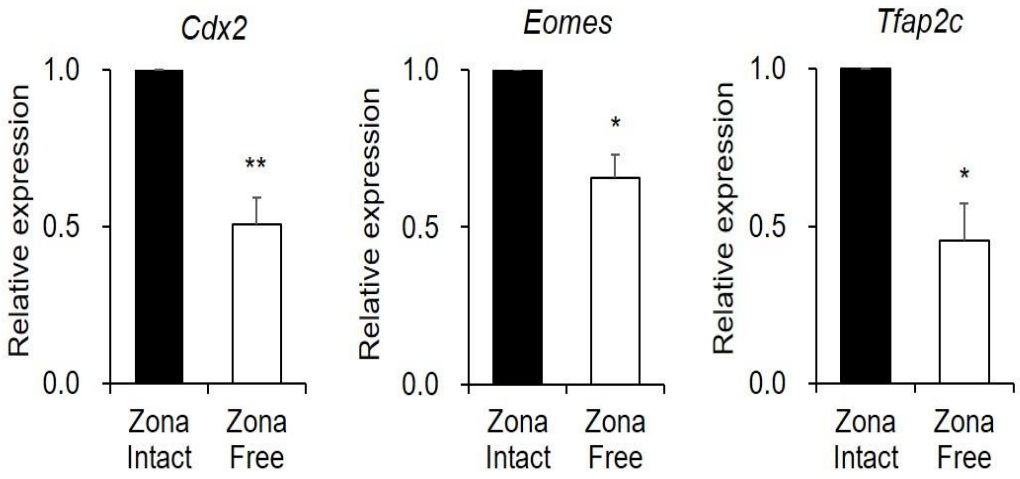

Figure 6. Effect of ZPR on the expression levels of TE -related genes in the morula stage.

Expression levels of *Cdx2, Eomes*, and *Tfap2c* in the morula stage embryos were analyzed by qPCR. Data are expressed as mean ± standard error of the mean (SEM), and Student's *t*-test was used to analyze at least three replicated experiments. Value with asterisks indicates significant differences. * $p < 0.05$, ** $p < 0.01$.

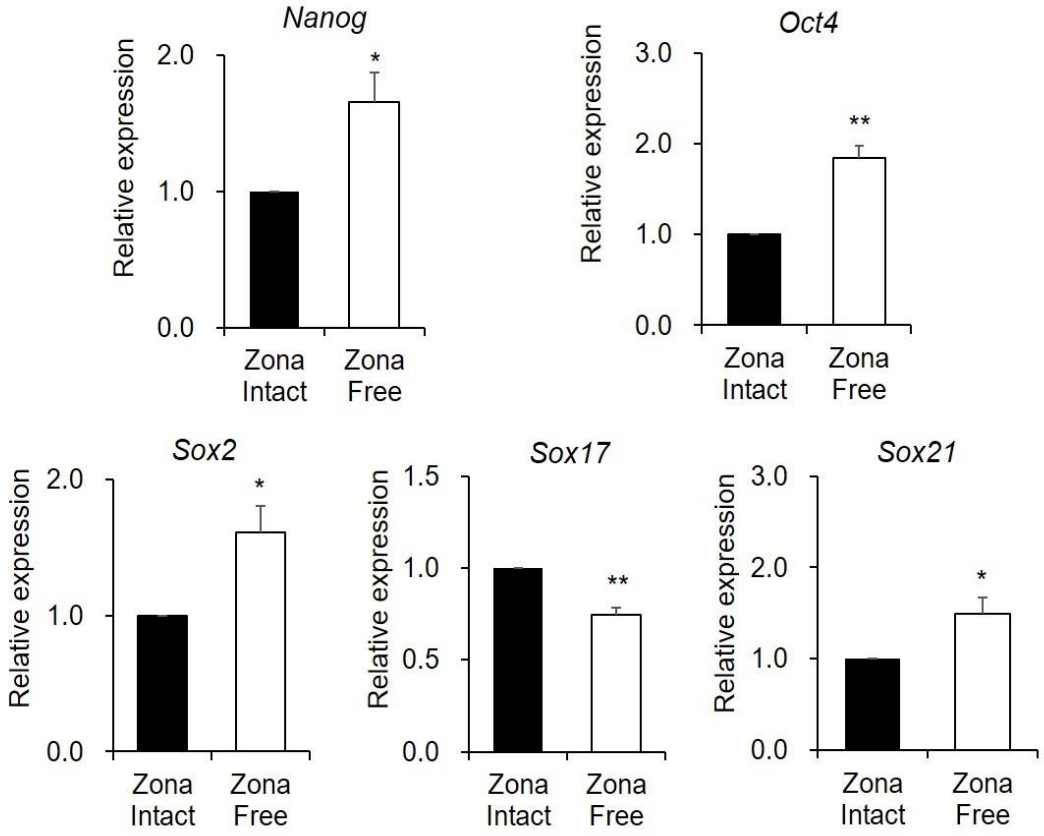

Figure 7. Effect of ZPR on the expression levels of ICM-specific genes in the blastocyst stage.

Expression levels of *Nanog, Oct4, Sox2, Sox17,* and *Sox 21* in the blastocyst were analyzed by qPCR. Data are expressed as mean ± standard error of the mean (SEM), and Student's *t*-test was used to analyze at least three replicated experiments. Value with asterisks indicates significant differences. * $p < 0.05$, ** $p < 0.01$.

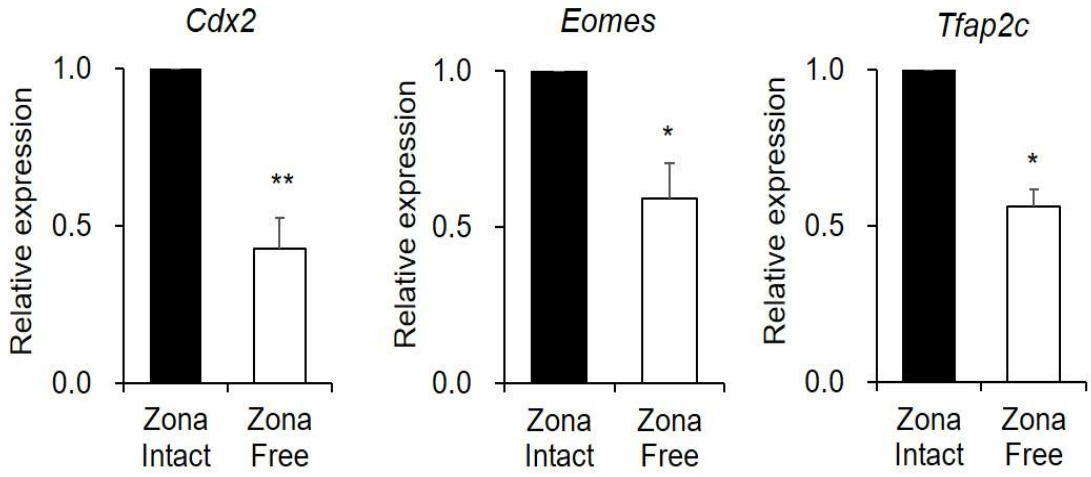

Figure 8. Effect of ZPR on the expression levels of TE -related genes in the blastocyst stage.

Expression levels of *Cdx2, Eomes,* and *Tfap2c* in the blastocyst stage embryos were analyzed by qPCR. Data are expressed as mean ± standard error of the mean (SEM), and Student's *t*-test was used to analyze at least three replicated experiments. Value with asterisks indicates significant differences. * $p < 0.05$, ** $p < 0.01$.

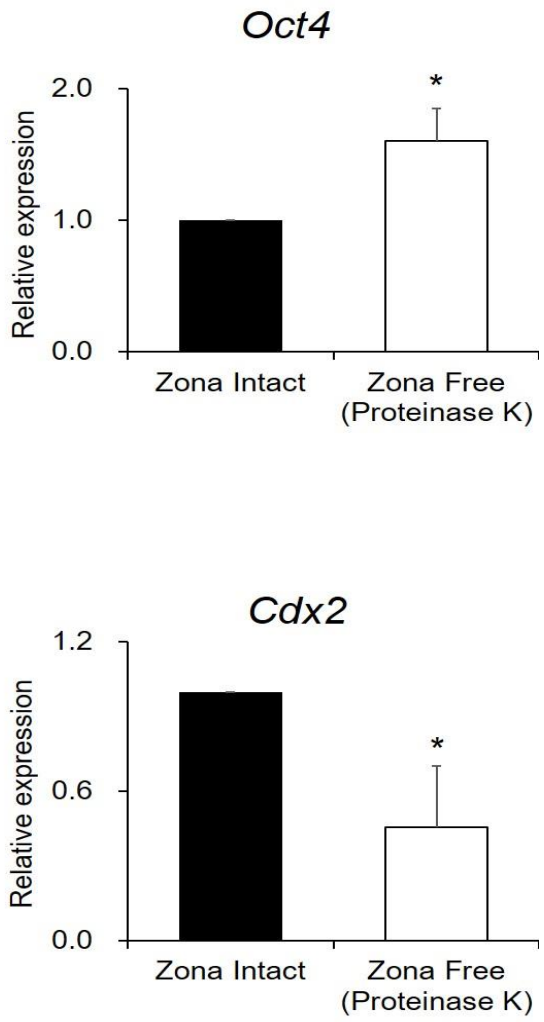

Figure 9. Effect of different methods for ZPR on the expression levels of ICM/TE -specific genes (*Oct4/Cdx2*) in the blastocyst stage.

Expression levels of ICM/TE-specific genes (*Oct4/Cdx2*) in the mouse blastocyst stage were analyzed by qPCR. Results are shown as mean ± standard error of the mean (SEM), and Student's *t*-test was used to analyze at least three replicated experiments. Values with asterisks vary significantly, * $p < 0.05$.

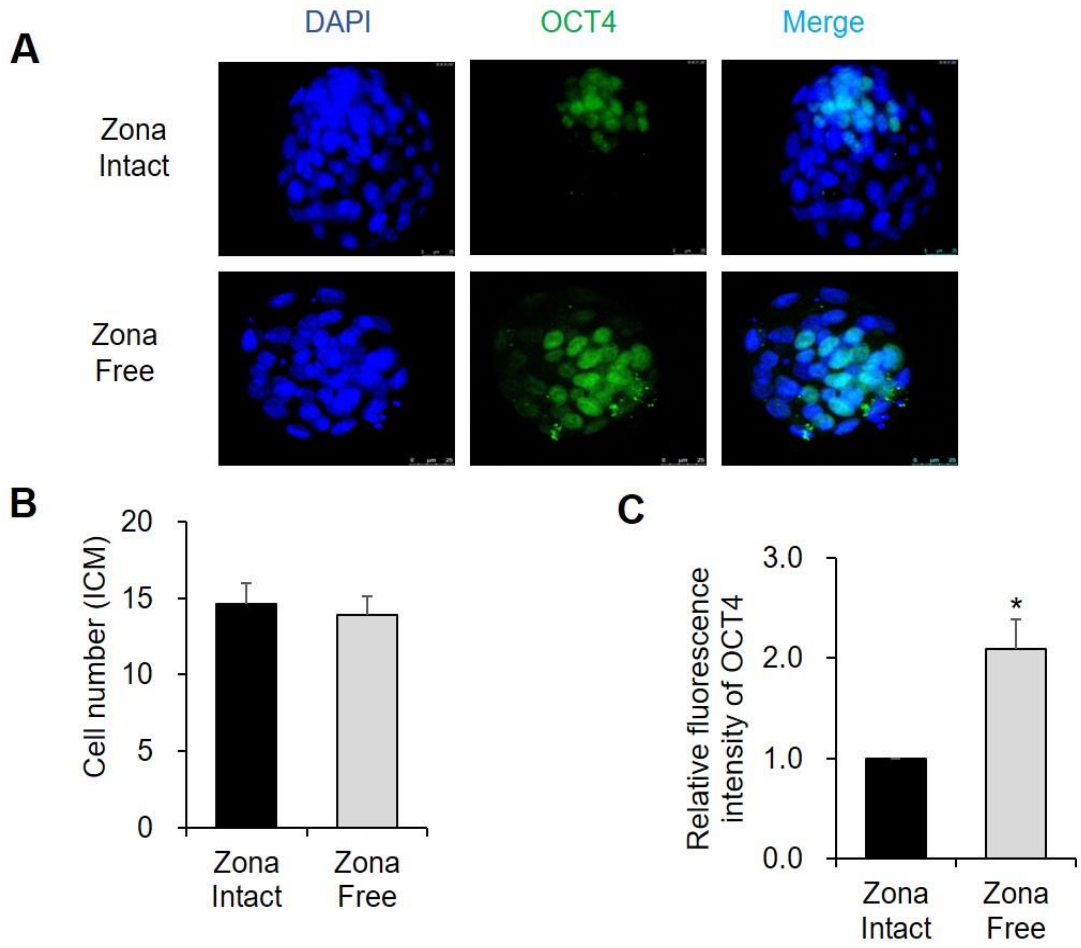

Figure 10. Effect of ZPR on the expression of OCT4 protein in the blastocyst stage.

A: Representative confocal images of ICM marker proteins (OCT4) in ZI and ZF blastocysts are shown (ZI, n = 19; ZF, n = 29). Green fluorescence: OCT4. Blue fluorescence: DAPI. Scale bar = 25 μm. (B, C) Immunofluorescence of OCT4 proteins in ZI and ZF blastocysts. B: The average number of positive-ICM cells. C: Relative fluorescence intensity of OCT4. Results are presented as mean ± standard error of the mean (SEM), and Student's *t*-test was used to analyze at least three replicated experiments. Value with asterisks indicates significant differences. * $p < 0.05$.

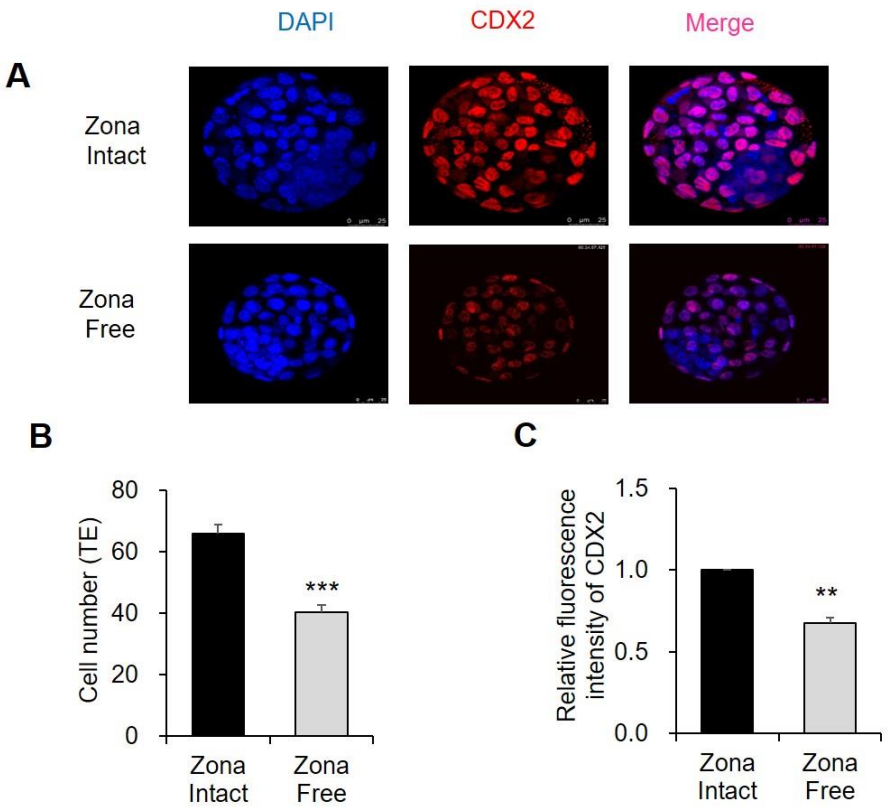

Figure 11. Effect of ZPR on the expression of CDX2 protein in the blastocyst stage.

A: Representative confocal images of TE marker proteins (CDX2) in ZI and ZF blastocysts are shown (ZI, n = 20; ZF, n = 25). Red fluorescence: CDX2. Blue fluorescence: DAPI. Scale bar = 25 μm. (B, C) Immunofluorescence of CDX2 proteins in ZI and ZF blastocysts. B: The average number of positive-TE cells. C: Relative fluorescence intensity of the CDX2. Results are presented as mean ± standard error of the mean (SEM), and Student's *t*-test was used to analyze at least three replicated experiments. Value with asterisks indicates significant differences. ** $p < 0.01$, *** $p < 0.001$.

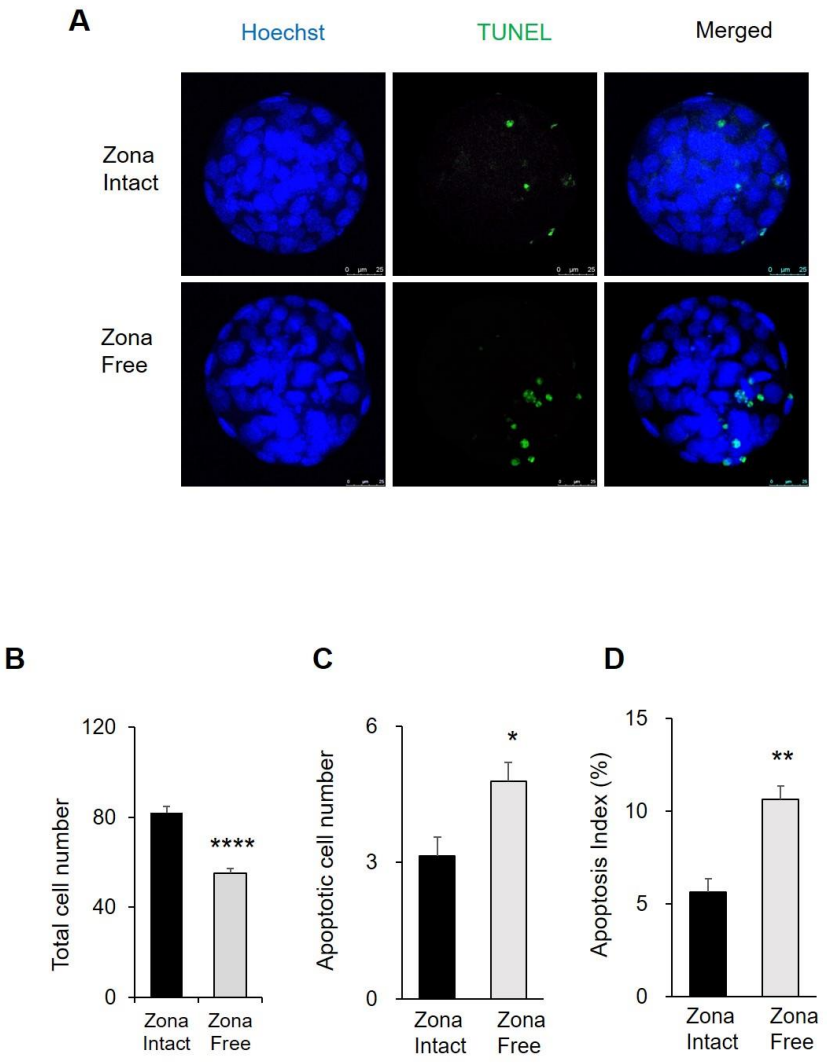

Figure 12. Effect of ZPR on the TCN and apoptosis status at the blastocyst stage.

A: Apoptotic blastomeres in blastocysts were detected by TUNEL (green) assays (ZI: n = 20; ZF: n = 19). Nuclei were stained with Hoechst (blue) to visualize all blastomeres. Scale bar = 25 μm. B: Total cell number. C: Apoptotic cell was determined in both ZI and ZF blastocysts. D: Apoptosis index. Data are presented as mean ± standard error of the mean (SEM), and Student's *t*-test was used to analyze at least three replicated experiments. Value with asterisks indicates significant differences. * $p < 0.05$, ** $p < 0.01$, **** $p < 0.0001$.

Discussion

It is well-known that the ZP plays a crucial role in the early development of mammalian embryos both *in vivo* and *in vitro* [76]. In human IVP procedures, ZPR has been used to improve the pregnancy rate with poor-quality embryos, producing identical twins or quadruplets. However, the effects of ZPR on embryonic development, gene expression, and post-implantation development remain unclear. Thus, in this study, ZPR was performed from the early 2-cell stage and its influence on the differentiation of ICM and TE in pre-implantation embryos was evaluated. Results of the present study show that ZPR at the 2-cell stage affects embryonic development by altering the expressions of differentiation-specific genes.

In this study, the 2-cell embryos were selected for treatment with acid Tyrode's solution to produce ZF embryos and cultured in the cWOW system *in vitro* until the blastocyst stage. The results show that ZPR disturbed the differentiation of ICM and TE during pre-implantation development. Previous studies have shown that ZPR from the zygote reduced the rate of blastocyst formation and viability in mice [35, 77]. In the present study, my findings are consistent with previous studies. Recent evidence has shown that cell fates are relatively flexible before the 8-cell stage, depending on the regulatory nature of mammalian embryonic development [7]. To date, zygotes and 2-cell blastomeres are known to have totipotency; however, some reports indicate that the ability of sister blastomeres in the 2-cell embryos generate epiblast and develop into a mouse was all unequal, and the asymmetric developmental state occurs when 2-cell

blastomeres are separated [78-80]. These data indicate that there is inequality in the potency of the 2-cell blastomere. Thus, in this study, the effects of ZPR on pre-implantation were evaluated.

I found that ZPR increased the speed of compaction compared with ZI embryos. In particular, a few of the compacted ZF embryos started to occur the cavitation early. Furthermore, the ICM-related genes (such as *Oct4* and *Sox21*) examined were upregulated at the morula stage, whereas TE-related genes were downregulated both in ZF-morula and blastocyst, such as *Cdx2*, *Eomes,* and *Tfap2c*. After E3.5, the ICM is specified in the PE and EPI lineages [7]. The EPI is exclusively characterized by *Nanog* and *Sox2* expression [67, 81, 82]. In addition, a previous study has shown that *Sox2* mRNA levels fluctuate more widely than *Oct4* during pre-implantation development [83]. Similarly, in this study, I also didn't find a significant expression of *Nanog* and *Sox2* in the ZF-morula embryos compared with ZI-morula embryos. Therefore, the effect of ZPR on the heterogeneity that leads to the ICM/TE cell fate decision should be investigated in further study.

For the faster compaction, one possible reason is that the cWOW system with the smaller microwells allows each blastomere to evolve toward easier intercellular binding and enhance cell-to-cell communication, thereby accelerating faster compaction. Another possible reason is the regulation of E-cadherin, which is a highly conserved calcium-dependent transmembrane adhesion molecule that plays a role in compaction, polarization, blastocyst cavity formation, and cell-fate specification [84-86]. The expression pattern of E-cadherin was not analyzed in this study. The effect of ZPR on

blastomere aggregation and E-cadherin expression should be investigated in further study. Overall, these results suggest that ZPR disrupts ICM and TE differentiation-related gene and protein expression. In contrast to my results, it was reported that ZPR at the zygote did not affect pluripotency-related genes (*Oct4* and *Sox2*) in bovine embryos [37]. The expression pattern of *Sox2* and *Nanog* in domestic cats is also opposite to the results of present my study and the report of Velásquez et. al (2013) [87].

There are several possible reasons for this inconsistency. (1) There are some differences between species. (2) There are differences in the term of development to the blastocyst stage i.e., 3.5-4.5 days (mouse), 7-8 days (bovine), and 8 days (domestic cats). Although the term of development of domestic cats and bovines are the same (d8), the expression of differentiation-related genes differs by species (3) the stage at which ZPR is performed may also affect ZF embryonic development. (4) Although ZF embryos have been successfully developed in *in vitro* culture systems including the commercial WOW system [34], cWOW system [36], glass oviducts (GO system) [39], and empty zona pellucida (EZP) [38], various culture systems may affect the arrangement and communication between blastomeres.

Next, I focused on ICM/TE differentiation at the early blastocyst stage by immunodetection of ICM and TE-specific proteins (OCT4 and CDX2). Compared with ZI embryos, immunolocalization of OCT4 embryos showed a clear fluorescence signal in ZF embryos, whereas CDX2 was weak in ZF embryos. This protein expression pattern is consistent with the expression patterns of both *Oct4* and *Cdx2* genes detected in blastocysts. In contrast, there was no significant difference in the number of ICM

cells between ZI and ZF embryos, whereas the number of TE cells showed a significant decrease in ZF blastocysts. Moreover, ZF embryos showed a significant increase in apoptotic cells and the apoptotic index compared with ZI embryos.

In summary, in Chapter III, I proved that ZPR affects the development and gene expression of pre-implantation embryos. Compaction occurred earlier due to the absence of ZP at the 2-cell stage. In addition, the expression of differentiation-related genes in the ICM/TE was significantly different in ZF embryos compared with ZI embryos. Specifically, at the blastocyst stage, compared with ZI embryos, due to the loss of ZP, the expression of ICM-related genes and proteins (except *Sox17*) was significantly increased, whereas the expression of TE-related genes and proteins was significantly decreased. Overall, in this chapter, these results suggest that ZPR disrupts the ICM/TE differentiation during the pre-implantation development.

Chapter IV

Effect of ZPR on the post-implantation development

Introduction

As mentioned in Chapter III, the zona pellucida (ZP) is a specialized extracellular elastic coat that surrounds the ovarian oocytes, the ovulated oocytes, and the preimplantation embryos [41, 58]. The ZP plays a role in fertilization, selection of morphologically normal sperm [11], induction of the acrosome reaction, and prevention of polyspermy [4] as well as influencing preimplantation development [88] and implantation [89].

In mammals, after fertilization, the zygotes undergo a series of changes, including zygote genome activation (ZGA) and lineage specification, all of which are essential for the generation of the blastocyst. The blastocyst consists of ICM and TE, the ICM forms the EPI and the PE [7, 8]. In the blastocyst, the TE is subdivided into a polar TE covering the epiblast at the embryonic pole to form the EPC and a mural TE covering the blastocyst cavity forms the giant cells in the future [9, 10]. When all three cell lineages are separated during the pre-implantation, the blastocyst enters the uterus and starts hatching from the ZP. The hatched blastocyst attaches and invades the maternal uterine endometrium and starts implantation.

The process of implantation includes three phases: apposition, attachment, and

penetration. During implantation embryonic development, the polar TE proliferates and differentiates into the ExE and the EPC, which will contribute to the part of the placental tissues [90]. On the other hand, a mural TE differentiates into primary trophoblast giant cell (TGC), which are necessary for embryonic implantation [91, 92].

After implantation, this cell lineage structure is modeled again, and the blastocyst undergoes a morphological transformation in which the original vesicle reorganizes into an elongated structure at E6.5. This elongated structure consists of (1) the EPC, (2) the EPI, (3) the ExE, (4) the endoderm (VE) that surrounds the EPI and ExE, and (5) the parietal yolk sac and TGC layer, which together surrounds the entire conceptus [8, 12-14]. After implantation, all transcription factors act as a network that influences the growth and development of fetal and placental tissues by interacting with each other, which is essential for the specification of distinct cell types. Self-renewing trophoblast stem cells (TSCs) are maintained in ExE that provide progenitors for EPC. ExE depends on the expression of *Elf5*, which is in a positive feedback loop with *Cdx2* and *Eomes*. TSCs can be obtained from polar TE or ExE up to E8.5 *in vitro* culture [90, 93]. The stem cell pool in ExE contributes to EPC, which subsequently produces spongiotrophoblasts and secondary TGCs [94, 95]. VE is a particularly important source of signals for embryonic pattern formation [13]. The precursor cells of the anterior VE (AVE) appear at the distal tip of the embryo (called distal VE) and then migrate to the anterior side of the embryo. By the end of gastrulation, three major germ layers have formed, and all fetal tissues will develop from the ectoderm (outer layer), mesoderm (middle layer), and definitive endoderm (inner layer).

The ZPR procedure is currently used more often in human ET, which is performed at the blastocyst stage, as an assisted technology (AT) to the abnormal or thickened ZP that affects the implantation. Other research on ZP thickness, as an important factor influencing the implantation and pregnancy rates, has been conducted in humans [89, 96, 97]. However, the effects of ZPR at the early stage are unclear. Based on the results in Chapter III, after ZPR at the 2-cell stage, there was a significant reduction in the TCN and a significant effect of ICM/TE differentiation at the blastocyst stage during early embryonic development, and now, it is unclear whether ZPR will continue to have subsequent effects on post-implantation development in mice, so I mainly performed ET experiments to explore the effects of ZPR during post-implantation development.

Materials & Methods

Animals

ICR male and female mice (8 weeks, Sankyo, Tokyo, Japan) were used as described in Chapter II.

Preparation of mouse embryos

The preparation of mouse embryos was prepared as described in Chapter III.

In vitro culture of ZF embryos

The mouse ZF embryos were performed as described in Chapter III. The relatively well-developed embryos were used for the ET experiments.

Embryo transfer

The relatively well-developed blastocysts were selected for ET. ET experiment was performed as described previously [98, 99] with slight modifications. Briefly, female mice were mated with vasectomized males, and females with vaginal plugs were selected as recipient mice. ZI and ZF blastocysts on day 3.5 were transferred to each uterine horn (left/right) of recipient female ICR mice at 2.5 days of pseudo-pregnancy. Ten blastocysts (equally distributed to the left/right uterine horns) were transferred to pseudo-pregnant mice in a single transfer. After ET was completed, the female mice were raised in a separate clean cage to avoid any negative conditions that might lead to the abortion of the fetuses. On 17.5 days after implantation, the female mice were sacrificed by cervical dislocation, the abdominal cavity was opened, and carefully collecting the fetuses and placenta from the left and right uterus of the female mice. Statistical analysis was performed on the implantation site, live fetus numbers, fetal weight, and placental weight.

RNA sequencing and bioinformatic analysis

After ET, samples were taken from the placenta of E17.5, and total RNA was extracted using ISOGEN II (Nippon Gene, Tokyo, Japan) and sent to Genome-Lead Co., Ltd (Kagawa, Japan) for RNA sequencing analysis. Before mapping, the clean reads were mapped to the mouse reference genome. Differentially expressed genes (DEGs) were analyzed based on gene counts using the processing tool DESeq2 [100] and visualized using R package ggplot2; transcripts with p-value < 0.05, log2 |fold change| > 1 were considered to be differentially expressed between samples. Gene ontology (GO) enrichment analysis of DEGs was performed using the topGO software [101].

Statistical analysis

All data are representative of at least three replicates and statistically significant differences were identified using one-way analysis of variance (ANOVA)-Tukey's multiple range test implemented in GraphPad Prism 7 software (LA Jolla, CA, USA). Statistical significance was set at $p < 0.05$.

Results

Effect of ZPR on the developmental ability of mice after embryo transfer

To determine the viability of ZF embryos, early blastocysts were transferred into the uterus of D2.5 pseudo-pregnant female mice. Representative morphological photographs of fetuses at E17.5 are shown in Figure. 13A. The rate of live fetuses was significantly lower in ZF embryos than that in ZI embryos. In particular, the live fetuses at E17.5 in the ZI group were also significantly higher than those in the ZF embryos ($p < 0.05$) (Figure. 13B and Table 2). The implantation rate in the ZI embryos was significantly larger than that in the ZF embryos ($p < 0.05$) (Figure. 13C and Table 2). However, the fetal weights in ZF embryos were not significantly different from that in ZI embryos (Figure. 13D and Table 2).

Effect of ZPR on the placental development of mice after embryo transfer

Figure. 14A shows representative morphological photos of live fetuses and placentas at E17.5. The placental weight at E17.5 of ZF embryos was significantly higher than that of ZI embryos ($p < 0.05$) (Figure. 14B and Table 2).

To further determine the molecular mechanisms affected by the increase in placental weight, I performed RNA-seq on the placentas between the ZI and ZF groups. Based on the RNA-seq data, compared to ZI groups, the results show a total of 473 DEGs, including 279 up-regulated and 194 down-regulated (Figure. 15). In addition, GO enrichment analysis revealed that the DEGs influenced cellular components, biological processes, and molecular functions, especially biological processes, such as embryonic organ development, mesenchyme development, blood vessel development,

regulation of cell communication, embryonic morphogenesis, and positive regulation of cell migration, etc. (Figure. 16). Therefore, these results suggest that ZPR affects placental development by regulating the expression of genes related to embryonic biological processes, and thus, placental weight.

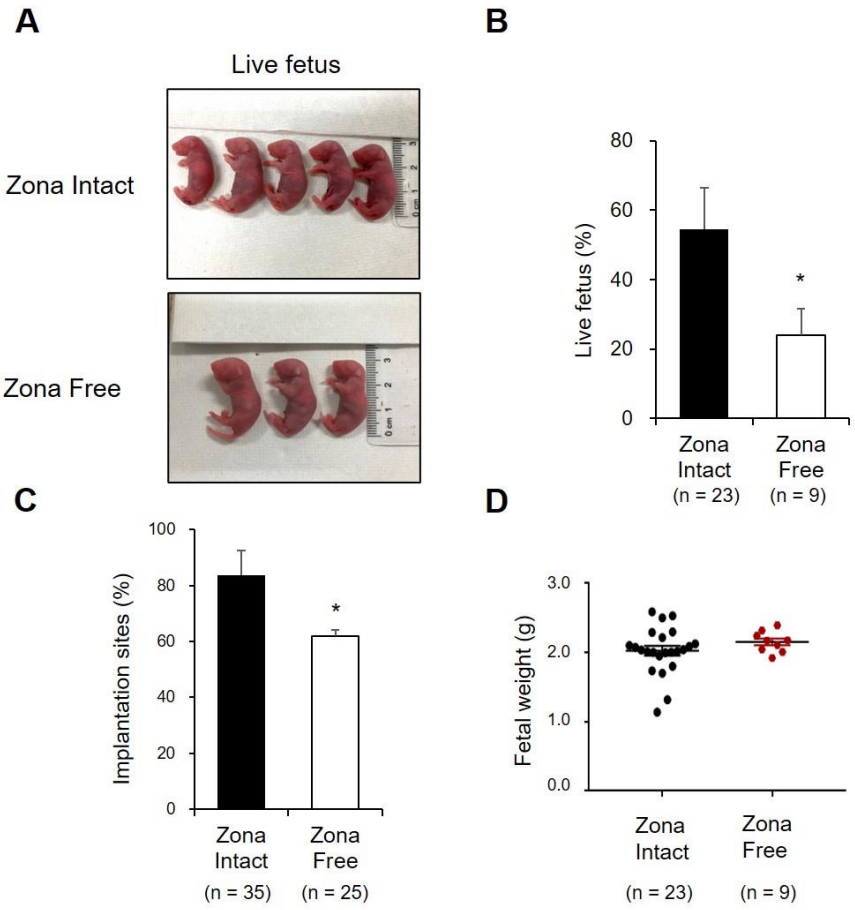

Figure 13. Post-implantation development of ZF embryos.

A: Representative images of live fetuses following the transfer of E3.5 blastocyst (Zona Intact and Zona Free) into the uterus of the recipient of D2.5 pseudo-pregnant female mice. B: The live fetal rate at E17.5; n: number of fetuses. C: The implantation rate at E17.5. The number of transferred blastocysts was 10 for each recipient. n: number of implantation sites. D: Fetal weight; n: number of fetuses. Results are presented as mean ± standard error of the mean (SEM), and Student's *t*-test was used to analyze four replicate experiments. Value with asterisks indicates significant differences, * $p < 0.05$.

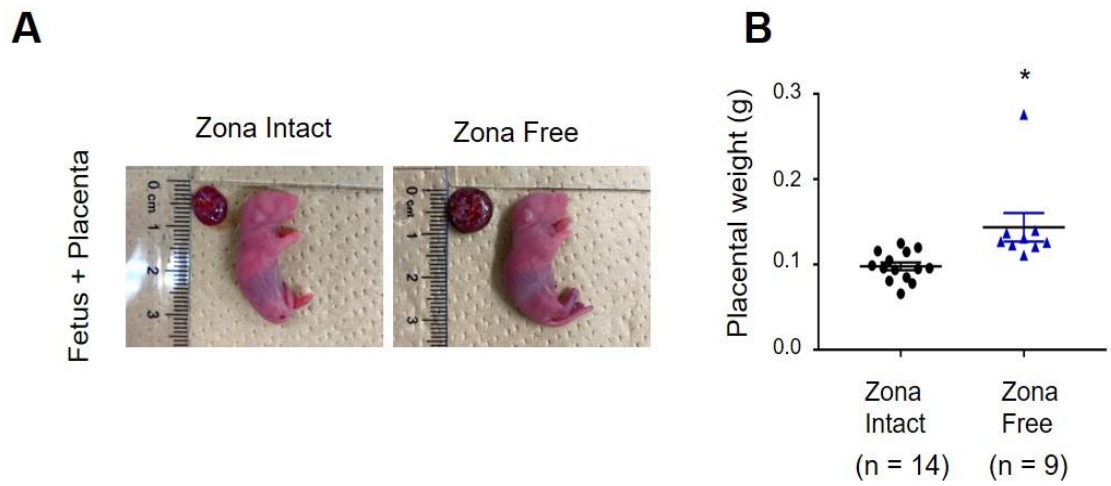

Figure 14. Effect of ZPR on placental weight after ET.

A: Representative pictures of live fetus and placenta (Zona Intact and Zona Free). B: Placental weight; n: number of placentas. Data are shown as mean ± standard error of the mean (SEM), and Student's *t*-test was used to analyze four replicate experiments. Value with asterisks indicates significant differences, * $p < 0.05$.

Table 2. Developmental ability after ZPR on post-implantation in each experiment

Group	Recipient ID No. in each experiment	No. of blastocyst transferred	No. of implantation sites	No. of retrieved fetuses	Average fetal weights (g)	Average placental weights (g)
Zona Intact	ID1	10	7	5	2.226	0.115
	ID2	10	10	9	2.109	None
	ID3	10	9	6	1.900	0.096
	ID4	10	9	3	2.114	0.075
Zona Free	ID5	10	6	2	2.282	0.127
	ID6	10	7	4	2.180	0.167
	ID7	10	6	1	2.008	0.137
	ID8	10	6	2	2.049	0.117

The rate of implantation and fetus following the transfer of E3.5 blastocyst (Zona Intact and Zona Free) into the uterus of a recipient of D2.5 pseudo-pregnant female mice. Four replicate experiments were listed in detail.

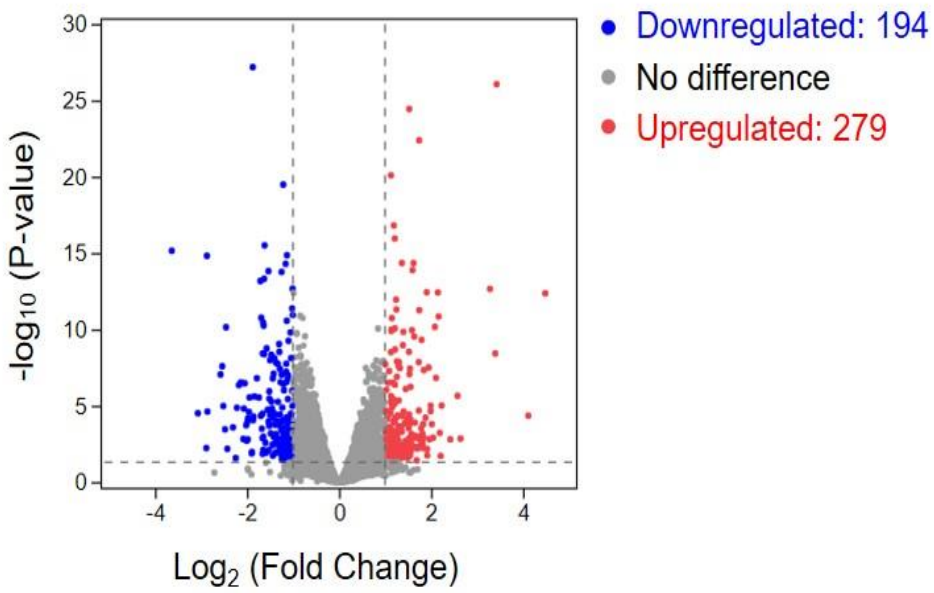

Figure 15. Effect of ZPR on differentially expressed genes in the placenta.

RNA extraction was performed from the placenta at E17.5 and subjected to RNA-seq analysis. Fold change was calculated from the averaged values in each group (n = 3). Volcano plot of upregulated (red) and downregulated (blue) DEGs, respectively.

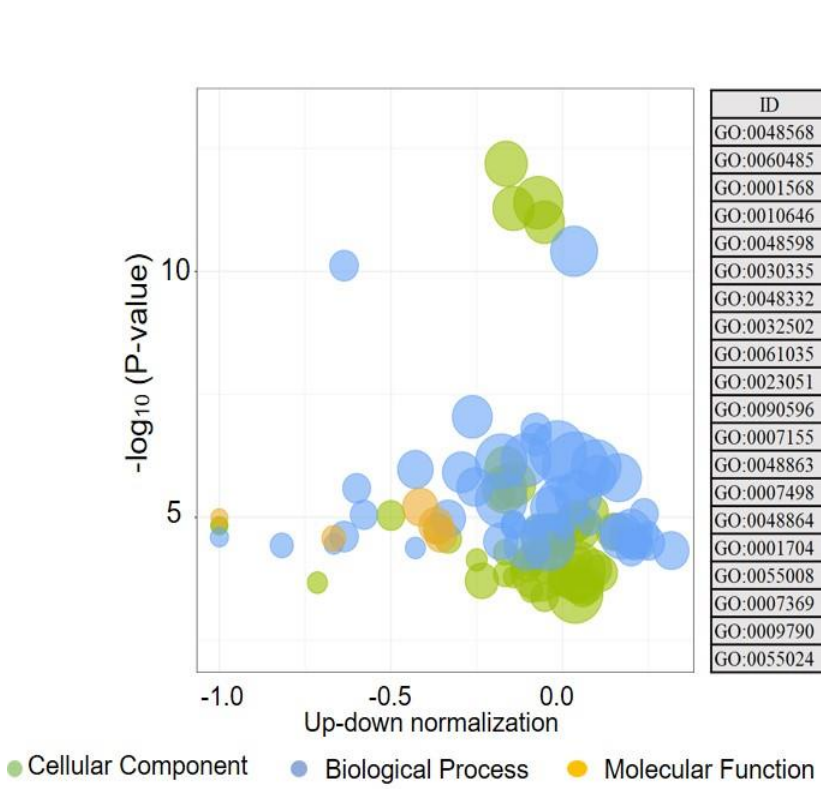

GO terms
(Biological Process)

ID	Descrption
GO:0048568	embryonic organ development
GO:0060485	mesenchyme development
GO:0001568	blood vessel development
GO:0010646	regulation of cell communication
GO:0048598	embryonic morphogenesis
GO:0030335	positive regulation of cell migration
GO:0048332	mesoderm morphogenesis
GO:0032502	developmental process
GO:0061035	regulation of cartilage development
GO:0023051	regulation of signaling
GO:0090596	sensory organ morphogenesis
GO:0007155	cell adhesion
GO:0048863	stem cell differentiation
GO:0007498	mesoderm development
GO:0048864	stem cell development
GO:0001704	formation of primary germ layer
GO:0055008	cardiac muscle tissue morphogenesis
GO:0007369	gastrulation
GO:0009790	embryo development
GO:0055024	regulation of cardiac muscle tissue development

Figure 16. GO enrichment analysis on the placenta.

RNA extraction was performed from the placenta at E17.5 and subjected to RNA-seq analysis. Left: Analysis of the GO bubble diagram by total DEGs. The three colors represent different GO categories, including cellular components, biological processes, and molecular functions. Right: Significant enrichment analysis of GO biological processes (BP) by DEGs.

Discussion

It is well-known that increasing the implantation rate is one of the main goals of ART. Excess embryos generated using ART can be cryopreserved for subsequent use [102]. In humans, failure to hatch due to ZP may be a major factor limiting the efficiency of assisted reproduction, and the effects of ZP hardening on embryo hatching may be one of the consequences of the embryo freezing and thawing process [103]. Therefore, manual thinning of the ZP, drilling, or ZPR may improve the implantation rate.

When all three embryonic cell lineages are separated, the blastocyst enters the uterus and hatches from the ZP. The hatched blastocyst starts to invade the maternal endometrial tissue and implantation. From the blastocyst implantation and the placenta formation and then to delivery, a rather complex process occurs within the maternal tissue, this has historically been difficult to study [8].

Although ZF embryos can form many seemingly normal blastocysts at the early stages of *in vitro* culture, it is not known whether these embryos affect the embryo implantation process and whether they could provide a more theoretical basis for future applications in *in vitro* production, such as cloned embryos, and the making of chimeric mice. In this thesis, considering the reduced number of TE-positive cells and the expression of TE-related genes and proteins, the development and differentiation of TE appear to have a greater impact on ZF blastocysts (Chapter III).

Next, I performed ET experiments, and the results show that the rate of survival

of fetuses at E17.5 and implantation on ZF embryos was lower than that of ZI embryos. This is consistent with the previous findings [77]. Overall, my results showed that the implantation rate and the number of live fetuses were lower in the ZF embryos than in ZI embryos. These results imply that ZPR at the early cleave stage prevents the implantation of conceptuses, thus decreasing the rate of fetuses (Figure. 13 and Table 2). Although the fetal weights in ZF embryos was not different from that of ZI embryos, placental weight was significantly increased in ZF embryos. It is well-known that the smaller litter size promotes both fetal and placental growth and development by supplying a consistent stream of nutrients and oxygen [104]. Therefore, we could not exclude the possibility of a decrease in litter size thus causing the higher placental weight of conceptuses derived from ZF embryos.

The placenta is an important extraembryonic organ that supplies the nutrition to support fetal development and growth in mammals [105]. To investigate the increasing placental weight in ZF embryos, subsequently, I performed RNA-seq to explore the comparative study of placental tissue after the transfer of ZI and ZF embryos. The RNA-seq analysis suggested that the DEGs influenced cellular components, biological processes, and molecular functions, especially biological processes. A total of 473 genes were significantly altered in the ZF placenta, including 279 upregulated and 194 downregulated DEGs. Therefore, the 279 upregulated DEGs may be one of the possibilities for increased placental weight in ZF embryos, thereby altering the placental development during the post-implantation process.

In summary, in Chapter IV, I demonstrated that after ET, the implantation rate and

the number of live fetuses were lower in ZF embryos than in ZI embryos, whereas the fetal weight at E17.5 was not different. However, placental weight was significantly increased in ZF embryos. RNA-seq analysis of the placenta showed a total of 473 DEGs that significantly influenced the biological process. It is necessary for the further study of the morphological and epigenetic analysis of the placenta and fetuses.

Chapter V

Effect of ZPR on the blastomere allocation at the early stage and subsequent development and gene expression

Introduction

As mentioned in Chapter II, ZP plays a key role in the fertilization and early embryonic development *in vivo*, as demonstrated by the difficulty of obtaining a newborn embryo in the ZF embryos when transferred into the recipient oviduct [106, 107]. The reason for this is that if embryos are deprived of protection, which may lead to adhesion of the ZF embryos to the oviductal wall [107] or to other cells [108]. In addition, without ZP may increase leukocyte infiltration [107] and infection by bacterial [109] in the reproductive tract.

A currently unresolved and critical study during mammalian development is when cells begin to differ from each other and whether these initial differences play any role in cell fate specification. In many experimental models, the initiation of cell-fate specification arises from heterogeneity between each blastomere, and the first cell-fate specification in the mammalian embryo leads to the separation of embryonic and extra-embryonic lineages. The embryonic lineage is pluripotent and will give rise to the fetus, whereas the extra-embryonic lineage will differentiate into the supporting structures, placenta, and yolk sac, which are essential for embryo implantation and fetal

development [110, 111]. How and when these lineages begin to segregate in morphologically homogeneous cells is difficult to address. From reports of the previous studies, it appeared that the embryo had the regulatory ability to compensate for changes in cellular arrangement, and thus cells of early mouse embryos were thought to be identical in their ability to produce embryonic or extra-embryonic lineages [112, 113]. However, recent research has suggested that the blastomeres at the 4-cell stage become heterogeneous, exhibiting differences in developmental fate and potential [59, 114, 115] and the activity of specific cell-fate regulators [116-118].

The ZP is also known to affect the entire development of mice. During early embryonic development and differentiation, epigenetic modifications are also important for embryonic genome activation, and gene expression is also highly dependent on the epigenetics of the genome [119]. The most described mammalian epigenetic modification is DNA methylation, and the most prominent form of its alteration is symmetric methylation of cytosines at the 5' position of CpG dinucleotides. DNA methylation can be considered to have dual biological significances which were namely gene regulation and structural fidelity [120, 121]. DNA methylation was firmly established as playing a key role in transcriptional repression, and allele-specific expression in many imprinted motifs had been determined by differential DNA methylation of parental alleles (i.e., differentially methylated regions, DMR) [122]. DNA methylation has other functions in X chromosome inactivation [123], genomic imprinting, retroviral sequence inactivation [119, 124], tumor formation [125], and aging processes [126]. In mice, DNA methylation undergoes extensive reprogramming

during the life cycle, including two erasures and two reconstructions [127]. In females, the oocyte genome remains hypomethylated until the primordial follicle is activated [128, 129]. Next, during oocyte development, specific *de novo* methylation occurs and genetic imprinting is re-established [130].

In mice, *de novo* DNA methylation is catalyzed by DNA methyltransferase 3a (*Dnmt3a*) and 3b (*Dnmt3b*), and maintained by DNA methyltransferase 1 (*Dnmt1*) [131, 132]. The deletion of *Dnmt1* in mice leads to global demethylation and embryonic death [131]. In addition, a recent study has revealed that *Uhrf1* (ubiquitin-like, containing PHD and RING finger domains 1) is a maternal effector gene that plays a crucial role in d*e novo* DNA methylation of oocytes and the maintenance of methylation in preimplantation embryos [133]. A previous study has found that UHRF1 is able to bind methylated CpG dinucleotide sequences while recruiting DNMT1 to maintain its methylation state during semi-replicative DNA replication [134]. Subsequently, UHRF1 can also bind to *Dnmt3a* and *Dnmt3b*, which are responsible for *de novo* methylation [135]. However, this pattern differs in different species [136]. Dynamic changes in DNA methylation are important because they have a crucial impact on the interactions between DNA and gene regulatory proteins.

Preimplantation embryonic development is regulated by epigenetic modifications such as DNA methylation, histone modifications, and chromatin reorganization associated with specific gene activation [137, 138]. These changes occur in the fertilized embryo necessary for the establishment of the blastocyst lineage: the ICM which will form the fetus in the future, and the TE, which will develop into other extra-

embryonic tissues of the placenta [139]. Previous studies have shown that differences in epigenetic modifications between early blastomeres are associated with their fate. Thus, cells with increased histone H3 arginine 26 methylation (H3R26me2), thought to be an activation marker, exhibit higher expression of a subset of pluripotency genes, including *Nanog* and *Sox2* destined to contribute to embryonic rather than extra-embryonic tissues [118, 140, 141]. Recent studies have shown that the differential levels of histone H3R26me2 are mediated by the heterogeneous activity of histone coactivator-associated arginine methyltransferase 1 (CARM1) in mouse blastomeres at 4-cell stage embryos [118, 142, 143]. CARM1 regulates various cellular functions, including mRNA modification, processing, transcription, and translation [144-146]. CARM1 is associated with pluripotency in embryonic stem (ES) cells and transactivates transcription factors associated with stem cells, including *Oct4* and *Sox2, Nanog* [147-149]. When *Carm1* is overexpressed, it contributes to high levels of H3R26me2 expression and directs its potency to the ICM [150]. Conversely, when *Carm1* is depleted, ES cells will differentiate into specific lineages [147]. The development from morula to blastocyst is associated with cell differentiation and cell fate decisions. In conclusion, CARM1 is important in regulating the developmental capacity of the blastomeres. However, it is not known whether CARM1 also plays a similar role in ZF embryos, thus ultimately altering the decisions of cell fate.

Previous studies have shown that the process of embryonic development may vary depending on the direction and sequence of cell division at the 4-cell stage [151, 152]. Also, previous studies have shown that the development of ZF embryos into blastocysts

and fetuses can differ in morphology depending on the 4-cell stage in mice [35]. Based on my results in Chapter III and Chapter IV, it has been shown that ZP embryos can develop to the blastocyst stage exclusively under *in vitro* culture and that the live fetuses can be obtained from ZF embryos after ET. This implies that the ZP is not necessary for pre- and post-implantation development. However, the rate of ZF embryos developing into live fetuses is significantly lower than ZI embryos. To date, the reasons for the low rates of pre- and post-implantation development remain unclear. Therefore, to explore whether ZPR has an impact on the morphological differences at the 4-cell stage and subsequent development of ZF embryos, and epigenetic modification patterns, thus the related experiments will be performed in terms of morphology and heterogeneity of the 4-cell stage as well as DNA methylation-related gene exploration in this chapter.

Materials & Methods

Animals

ICR male and female mice (8 weeks, Sankyo, Tokyo, Japan) were prepared as described in Chapter II.

Preparation of mouse embryos

The preparation of mouse embryos was performed as described in Chapter III.

In vitro culture of ZF embryos

The mouse ZF embryos were prepared as described in Chapter III.

RNA extraction and quantitative PCR

qPCR was performed as described in Chapter III.

Immunostaining

The embryos of different morphology at the 4-cell stage [153] were fixed with 4% paraformaldehyde (Fujifilm Wako Pure Chemical Corporation, Osaka, Japan) in PBS for 60 min and then permeabilized using 0.2% (v/v) T-PBS dilution for 60 min at room temperature. Subsequently, embryos were washed three times for 10 min each in 0.2% PVA-PBS and then incubated with anti-CARM1 antibody (1:100; Mouse mAb #12495, Cell Signaling) overnight at 4 °C. After washing five times for 10 min each in 0.1% (v/v) Triton X-100 and 0.3% (w/v) bovine serum albumin (Sigma-Aldrich, St. Louis, USA) in PBS, the embryos were incubated in secondary antibody with Alexa Fluor 488 goat anti-mouse IgG antibody (1:400; Invitrogen, USA) diluted in the blocking solution for 60 min at room temperature. Finally, blastocysts were then washed three times in PVA-PBS before being incubated in 1μg/mL Hoechst 33342 solution (Sigma-Aldrich,

Darmstadt, Germany) for nuclei staining. Fluorescence was detected using a scanning confocal microscope (TCS SP5, Leica Microsystems, Germany). The obtained images were analyzed with ImageJ software [75].

Nuclei staining

Blastocysts were fixed with 4% paraformaldehyde (Fujifilm Wako Pure Chemical Corporation, Osaka, Japan) in phosphate-buffered saline (PBS) for 30 min and then permeabilized using 0.2% (v/v) T-PBS dilution for 60 min at room temperature. Subsequently, blastocysts were then washed three times in PVA-PBS before being incubated in 1μg/mL Hoechst 33342 solution (Sigma-Aldrich, Darmstadt, Germany) for nuclei staining. Fluorescence DNA was detected using a scanning confocal microscope (TCS SP5, Leica Microsystems, Germany).

Statistical analysis

All data are representative of at least three replicates and statistically significant differences were identified using one-way analysis of variance (ANOVA)-Tukey's multiple range test implemented in GraphPad Prism 7 software (LA Jolla, CA, USA). Statistical significance was set at $p < 0.05$.

Results

Morphological classification of blastomere structure of 4-cell embryos and developmental competence of ZF embryos

The results of blastocyst rate according to Chapter II show that the rate of the blastocyst in ZF embryos is significantly lower ($p < 0.05$) than in ZI embryos. Next, I performed detailed morphological observation and analysis of ZF embryos at the 4-cell stage.

According to the observation of the bright field images, the ZF embryos at the 4-cell stage showed a different morphology compared with the control group of ZI embryos (Figure. 17). First, I made a detailed classification and definition of the different types of 4-cell embryos which are based on the number of contact points (P) between each blastomere. In general, after ZPR, ZF embryos at the 4-cell stage include 3 points (3P), 4 points (4P), 5 points (5P), and 6 points (6P) among each 4-cell blastomere (Figure. 18). However, control ZI embryos had two types including 5 points (5P), and 6 points (6P), but no types of 3P and 4P (Figure. 17). There was no significant difference in the rate of morula and blastocyst among the 3P, 4P, 5P, and 6P types (Figure. 19).

Next, the ZF embryos at the blastocyst stage of different 4-cell types were observed under a bright field (Figure. 18B), and it was found that there were size irregularities in the blastocysts of different 4-cell types. Next, I examined the total cell

number (TCN) of different types at the blastocysts by nuclei staining, and the results showed that the TCN of 3P types was significantly lower than that of control ZI embryos ($p < 0.05$), however, comparing the TCN of 4P, 5P, and 6P types, there were not significantly different among them (Figure. 20).

Expression levels of Carm1 mRNA and protein in ZI and ZF embryos at the 4-cell stage

To investigate the expression levels of *Carm1* mRNA and CARM1 protein in the ZI and ZF groups at the 4-cell stage, I performed qPCR and immunostaining, respectively. The results showed that *Carm1* mRNA expression level was significantly increased in the ZF embryos than in the ZI embryos after 24 h of ZPR (Figure. 21). Immunostaining data showed that the immunofluorescence intensity of CARM1 was also significantly increased in the ZF embryos compared with the ZI embryos, even in different types of the 4-cell stage (Figure. 22).

Effect of ZPR on DNA methylation-related genes in the blastocysts

Since ZPR affected the expression pattern of ICM/TE differentiation-related genes and proteins in Chapter III and differentiation regulatory factor gene, *Carm1* at the 4-cell stage, next I investigated the effect of ZPR on the expression of DNA methylation-related genes (*Dnmt1, Uhrf1, Dnmt3a,* and *Dnmt3b*) were performed by qPCR at the blastocyst stage (Figure. 23).

Expression levels of DNA methylation-related genes (*Dnmt1*, *Uhrf1*, *Dnmt3a*, and *Dnmt3b*) were significantly lower in ZF blastocysts than in ZI blastocysts. These results suggest that ZPR at the 2-cell may affect epigenetic modification during early embryonic development, such as DNA methylation patterns.

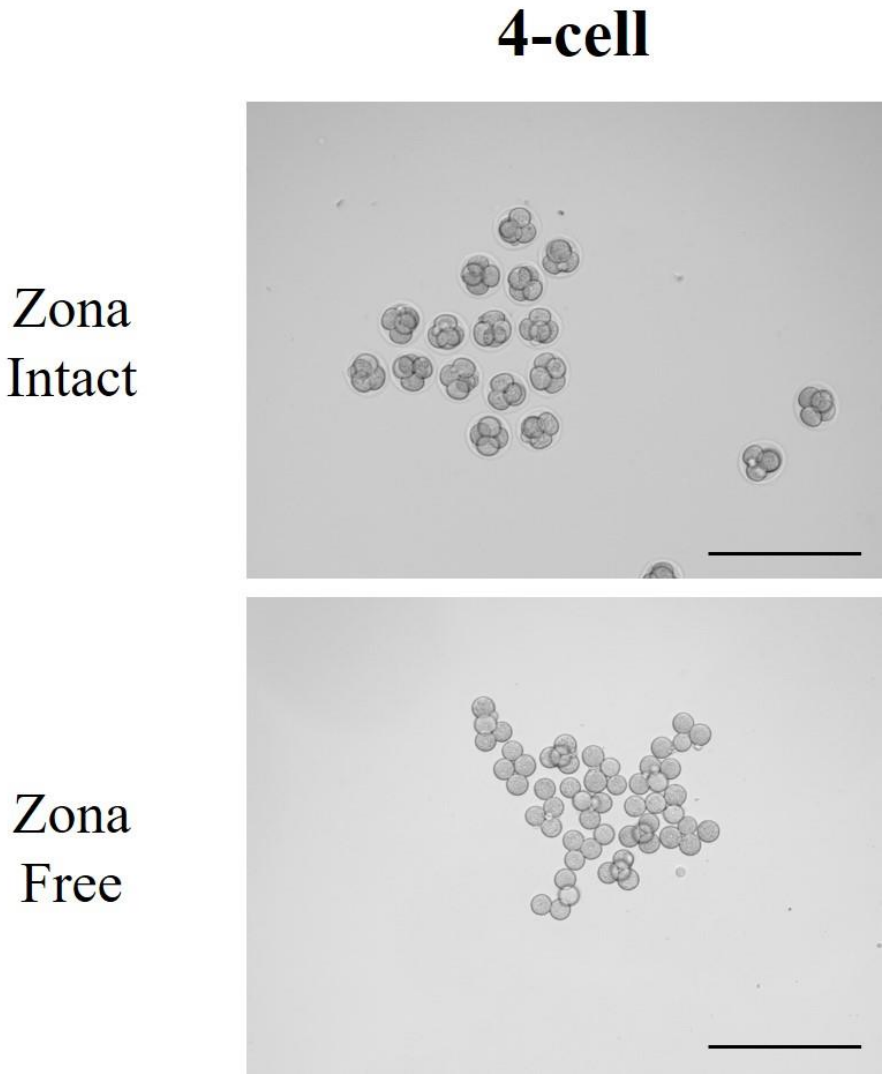

Figure 17. Representative microphotographs of embryos cultured with or without ZP in the mouse 4-cell stage.

A: Morphological difference between ZI and ZF in mouse 4-cell stage. Scale bar = 300 μm.

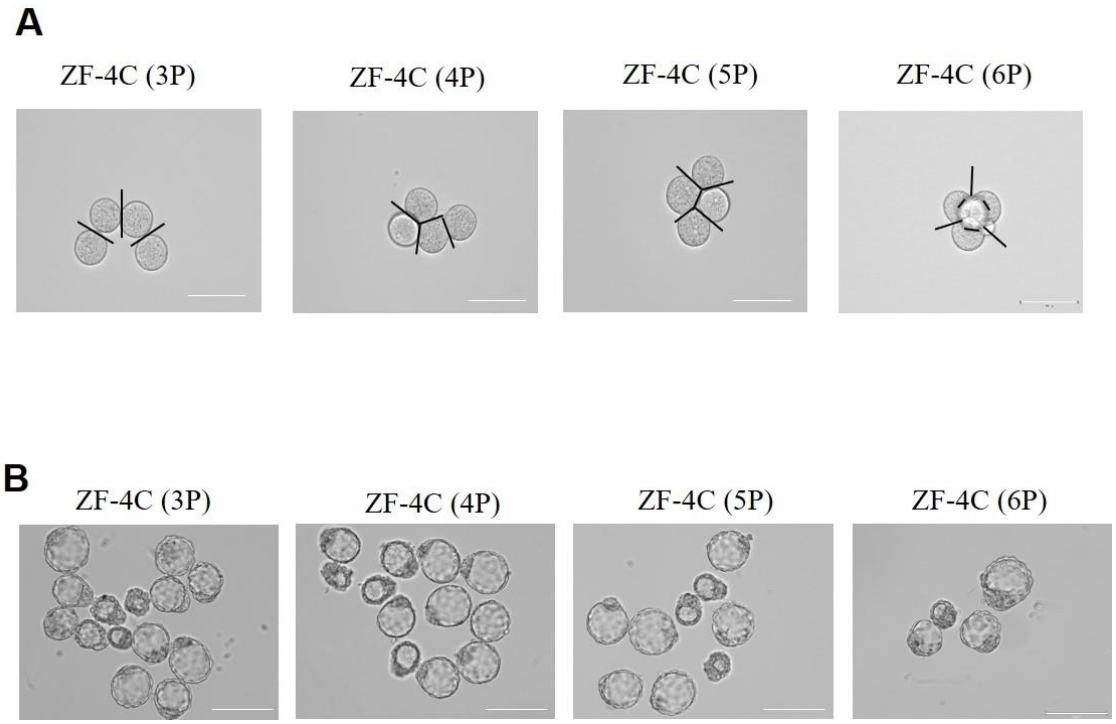

Figure 18. Representative microphotographs of different types of ZF embryos at the 4-cell stage and subsequent blastocyst stage.

A: Representative images of different types of ZF embryos at the 4-cell stage. Scale bar = 75 μm. The black straight line represents the position of contact with each blastomere. B: The blastocyst morphological changes corresponding to the different types of the 4-cell stage in ZF embryos. Scale bar = 150 μm.

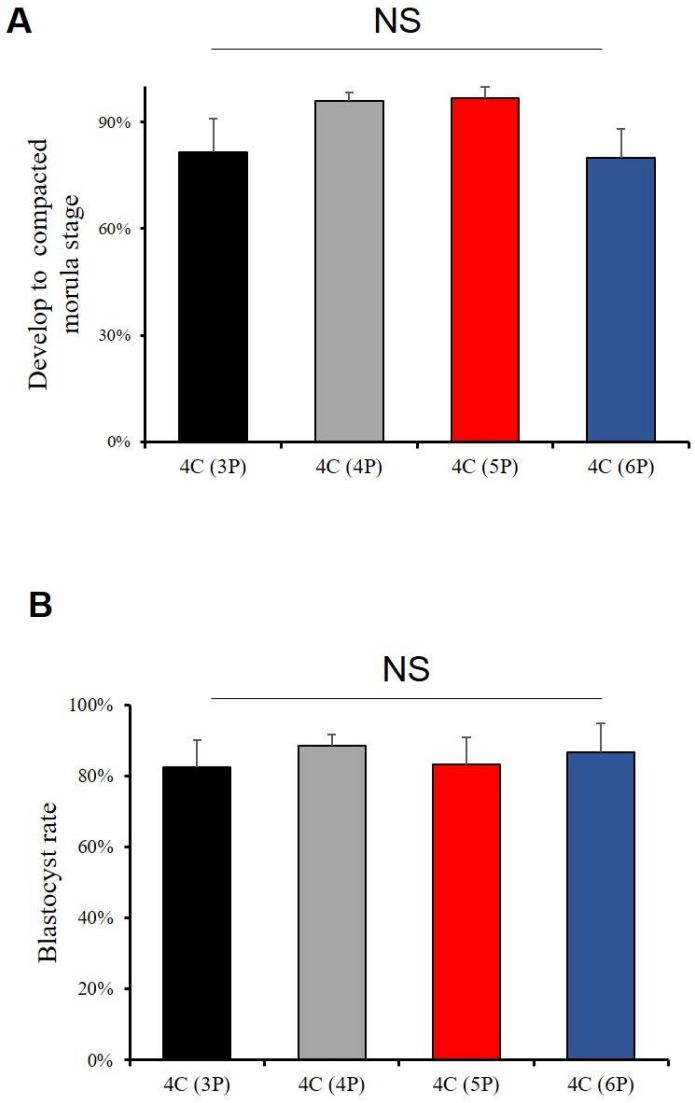

Figure 19. Effect of different morphological types at the 4-cell stage on the development of ZF mouse embryos.

A: The rate of morula of ZF embryos *in vitro* culture by cWOW system. B: The rate of blastocyst of ZF embryos *in vitro* culture by cWOW system. The data are expressed as the mean ± SEM, and one-way ANOVA was used to analyze the data. NS: Not significant difference.

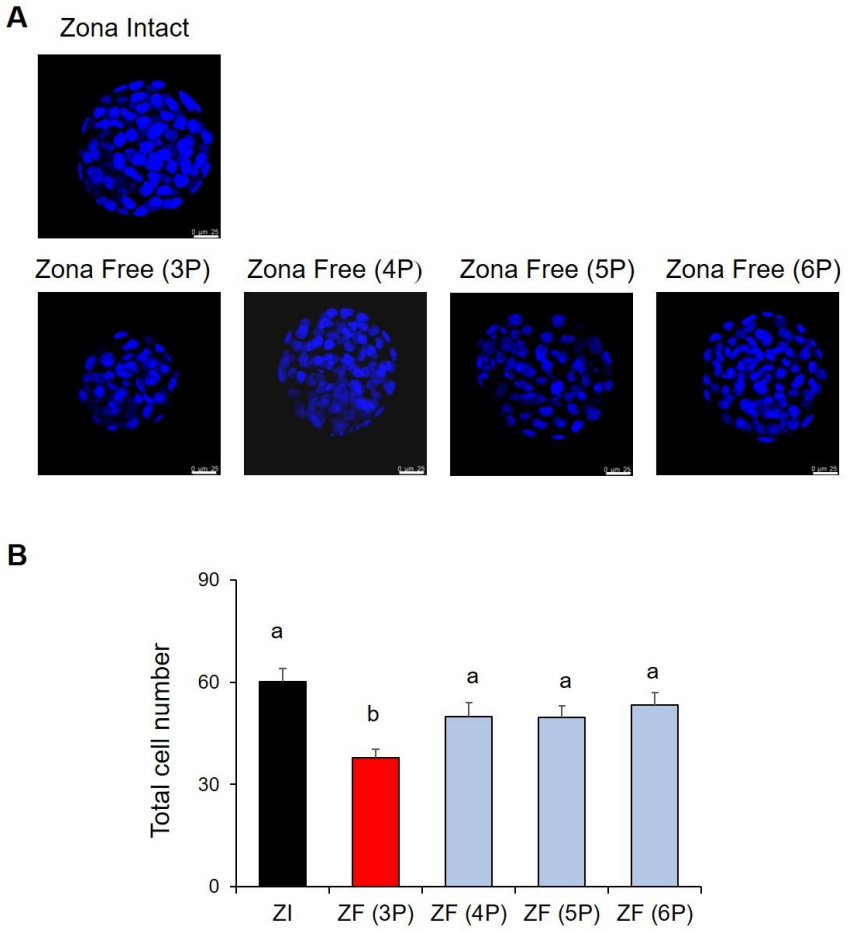

Figure 20. TCN of different 4-cell morphologies at the early blastocyst stage between ZI and ZF embryos.

A: Representative confocal images of DNA in ZI and ZF blastocysts are shown. Blue fluorescence: Nuclei were stained with Hoechst (blue). Scale bar = 25 μm. B: TCN in ZI and ZF blastocysts. Data are presented as mean ± standard error of the mean (SEM), and Student's *t*-test was used to analyze at least three replicate experiments. Different letters indicate statistical differences (a *vs.* b: $p < 0.01$).

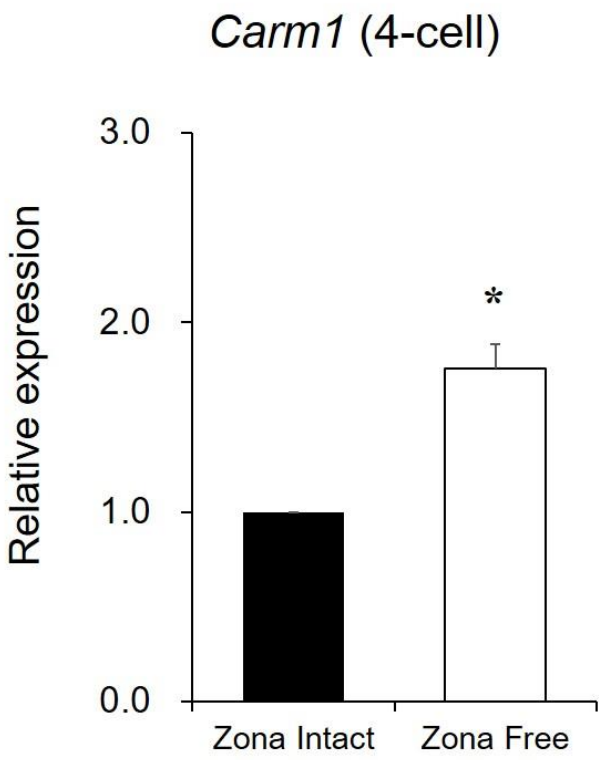

Figure 21. Effect of ZPR on the expression levels of *Carm1* at the 4-cell stage.

Carm1 gene expression in the mouse 4-cell stage. Data are expressed as mean ± standard error of the mean (SEM), and Student's *t*-test was used to analyze at least three replicate experiments. Value with asterisks indicates significant differences. * $p < 0.05$.

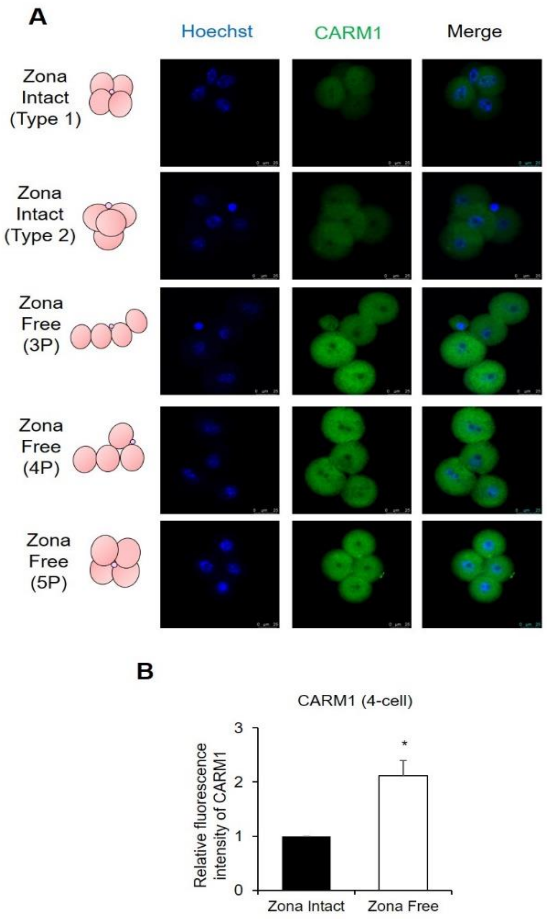

Figure 22. Effect of ZPR on the expression of CARM1 between ZI and ZF with different types at the 4-cell stage.

A: Representative confocal images of CARM1 in ZI and ZF blastocysts are shown. Green fluorescence: CARM1; Blue fluorescence: Hoechst. Scale bar = 25 μm. B: Immunofluorescence analysis of CARM1 protein in ZI and ZF blastocysts at the 4-cell stage (Total types). Results are presented as mean ± standard error of the mean (SEM), and Student's *t*-test was used to analyze at least three replicate experiments. Value with asterisks indicates significant differences. ZI: zona intact; ZF: zona free. * $p < 0.05$.

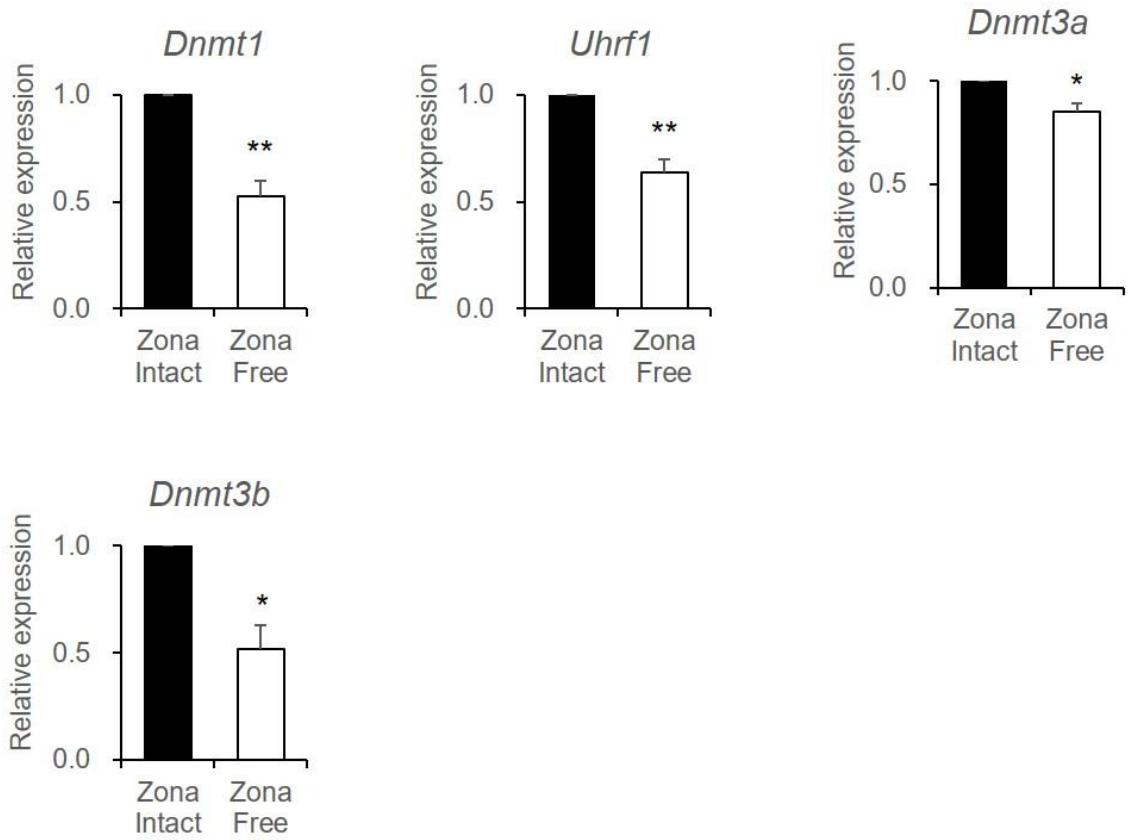

Figure 23. Effect of ZPR on the expression levels of DNA methylation-related genes in the blastocyst stage.

Expression levels of *Dnmt1, Uhrf1, Dnmt3a,* and *Dnmt3b* in the blastocyst stage were analyzed by qPCR. Data are expressed as mean ± standard error of the mean (SEM), and Student's *t*-test was used to analyze at least three replicated experiments. Value with asterisks indicates significant differences. * $p < 0.05$, ** $p < 0.01$.

Discussion

Some current research is disrupting the traditional ideas about mammalian development. The traditional view about mammals is that cell fate occurs randomly because early embryos are homogeneous and all blastomeres have the same expected cell fate each other [78]. However, some recent studies have raised the argument that cell fate is predictable because embryos are not completely homogeneous and therefore not all blastomeres are identical. Several studies have shown that there is inequality in the totipotency of blastomeres at the 2-cell and 4-cell stages in mice [79, 80, 154]. For example, a previous report suggested that when the blastomeres are separated at the 2-cell stage, only one blastomere can develop into a mouse. This full developmental potential can only be achieved when sufficient epiblast cells are produced at the blastocyst stage [78, 154, 155]. These findings support the view that 2-cell blastomeres do not have the same developmental potential. However, until now the decision of cell fate remains uncertain when the first cell specification event occurs during the second division of the embryo from the 2-cell stage to the 4-cell stage, i.e., how to allocate the cell fate between ICM and TE [156, 157].

In this study, when the ZP was removed at the 2-cell stage, the embryos developed to the 4-cell stage with different morphology due to the loss of the spatial restriction of the ZP. In the second division of the ZF embryo, mutual movement of the blastomeres occur even more during the division from the 2-cell stage to the 4-cell stage. Thus, at the completion of the second division, the cells present various morphologies of the 4-

cell stage. Next, I classified these different developmental patterns of ZF embryos according to the contact point between each blastomere at the 4-cell stage (Figure. 19A) and I also observed the blastocyst stage morphology according to the different 4-cell types (Figure. 19B). Figure. 17 showed that ZI embryos had more closely packed together than those of the ZF embryos at the 4-cell stage. Therefore, I think that the presence of the ZP may prevent the abnormal movement of each blastomere in the embryo during the second division. In addition, I compared the rate of morula stage and blastocyst state according to the different types of 4-cell stages. The results showed that the developmental ability of ZF embryos of four types *in vitro* does not differ, and they also did not differ from ZI embryos (Figure. 20), where the most likely reason is that the appropriate microwell size of the cWOW system mentioned in Chapter II enhances each blastomere communication and the cell junction during the process of compaction. Although the morphology of each type of 4-cell is the same as that of the morula and blastocyst, the blastocysts differ in the TCN (Figure. 20), especially the 3P type of 4-cell has a lower TCN than the other 4-cell types. Moreover, the morphology of the blastocyst also showed irregular size among the different types of the 4-cell stage (Figure. 19B).

Histone arginine methylation is a key regulator of cell fate determination in early mouse embryos [158], and coactivator-associated arginine methyltransferase 1 (CARM1) is an asymmetric arginine methylation enzyme. The timing of the first appearance of blastomere heterogeneity and how it occurs remained unclear until now. There are two contradictory views of CARM1 protein heterogeneity. Torres-Padilla et

al. (2007) reported that CARM1 heterogeneity in individual blastomere first appears at the 4-cell stage [158], but two emerging studies provide new evidence that heterogeneity is identified at the 2-cell to the 4-cell stage [159, 160]. It has been controversial the cell fate decision in the blastomeres of the 2-cell [161-163]. A previous study has reported that most cleaving embryos derived from the two first blastomeres had the potential to develop into blastocysts of a mixture between ICM and TE in mice [162]. Moreover, CARM1 is heterogeneous at the 2-cell stage and can promote ICM formation [158, 159]. I investigated the expression of CARM1 mRNA and protein in the 4-cell stage of mouse embryos. My results showed that *Carm1* mRNA was significantly increased in ZF embryos compared with ZI embryos (Figure. 21). Moreover, CARM1 expression was also significantly increased in ZF embryos compared with ZI embryos at the 4-cell stage (Figure. 22). A previous study revealed that CARM1 overexpression leads embryos to contribute mainly toward the ICM rather than the TE by epigenetic marker analysis [158]. This may be one of the reasons why ZF embryos in Chapter III lead to ICM/TE differentiation, especially, since more ICM-related genes are significantly expressed in ZF embryos than those in ZI embryos. This may be due to heterogeneity in the 4-cell and higher expression CARM1, thus directing the embryo toward a contribution to the ICM and reducing the contribution to the TE cell lineage.

In the early stages of embryonic development and differentiation, epigenetic regulation such as DNA demethylation starts in the embryonic genome and continues through the blastocyst stage. This process occurs firstly in the paternal genome in an

active way [164-166] and secondly, in a passive way from the 2-cell to the morula stage [164, 167]. Although the methylation levels at each developmental stage were not analyzed in this study, expression levels of DNA methylation regulatory genes in ZI and ZF embryos were examined at the blastocyst stage. These results showed that the expression pattern of the DNA methylation regulator has a significantly decreased at the blastocyst stage in the ZF embryos compared with ZI embryos.

The mechanisms underlying the epigenetic effects of the variability are currently unknown. However, there are several possible reasons that can be considered for the reduced DNA methylation regulator expression in this study. (1) The effect of ZPR and culture environment on embryonic development was shown in the previous study. Suzuki et al., (1995) reported that ZPR from mouse zygotes affected development at term and that this effect was each cell association formation of ICM at the 4-cell stage [35]. (2) Culturing under inappropriate conditions (e.g., use of serum in the medium) can impair the health of offspring of several species [168]. (3) In some species, the low efficiency of nuclear transfer (NT) and *in vitro* production (IVP) procedure is associated with altered expression of the imprinted genes as well as aberrant DNA methylation [169, 170]. Further studies are needed for the comparative DNA methylation analysis in the ZI and ZF embryos.

In summary, in Chapter V, I revealed that ZF embryos show 4 different types of morphological changes at the 4-cell stage and there is no difference between them in their *in vitro* developmental capacity. However, the TCN of blastocysts in the 3P type of 4-cell is significantly lower than the other 4-cell types as well as the ZI embryos.

Moreover, at the 4-cell stage, ZF embryos are also heterogeneous, with higher levels of CARM1 mRNA and protein expression than ZI embryos. However, the expression of DNA methylation-related genes was significantly decreased compared with ZI embryos. These results suggest ZPR affects the early 4-cell morphology and blastocyst development as well as epigenetic modification.

Chapter VI

Establishment and evaluation of a new ZPR method for the development of ZF embryos

Introduction

As mentioned in Chapter II of ZP roles, the IVP of mammalian embryos has been significantly improved over the last several decades and is now widely used in reproductive technologies in several different ways, including in ART, for both humans and animals designed to facilitate breeding and development, production of transgenic animals, and cloning [29]. The ZP is often manipulated during IVP procedures with these changes including ZP thinning and complete or partial ZPR and these changes are made to facilitate embryo applications such as chimera generation [30], transgenic procedures [31], blastomere separation [32], handmade cloning [171], and RNA interference experiments [34].

ZPR protocols are commonly performed as a single use of acid Tyrode's solution or pronase on their own [172, 173] with both options being reasonably popular due to their simplicity and relative cost-effectiveness [172]. Given this, several efficient ZPR protocols have been developed for a variety of species, including humans [172], cows [174], and pigs [175] with concentration or treatment time by considering the

suitable chemical composition of each ZP. However, some chemical (i.e., acid Tyrode's solution or pronase) treatments used for ZPR can reduce developmental competence due to their toxicity [176] with a long exposure time for complete ZPR to prevent insufficient digestion [172], or excessive digestion [17]. This means that there is still a need for a stable, high efficiency, and low toxic ZPR protocol to produce embryos suitable for ART and research into embryonic development and differentiation.

In humans, the ZP thinning application by acid Tyrode's solution treatment is commonly used to help blastocysts to hatch and thus improve the implantation rate. One of the reasons is the ZP is bilayered; the outer layer is thicker and easily digested by acid Tyrode's solution, while the inner ZP layer is denser and less easily digested [172]. Therefore, by considering the structure of ZP, chemical and enzymatical ZPR should be optimized. Considering these characteristics, I tried to perform ZP thinning by acid Tyrode's solution, then digested the inner layer with proteinase K.

Materials & Methods

Animals

ICR male and female mice (8 weeks, Sankyo, Tokyo, Japan) were prepared as described in Chapter II.

Oocyte collection and in vitro fertilization

Mouse oocyte collection and IVF procedures were performed as described in Chapter II.

Evaluation of the ZPR methods

After collection of 2-cell embryos, ZP was removed using one of the following methods until complete zona digestion: (1) incubation in acid Tyrode's solution for approximately 1 min (2) incubation in 0.5% proteinase K solution (Fujifilm Wako, Osaka, Japan) for approximately 6 min and (3) two-step combination in acid Tyrode's solution for approximately 40 s followed by several seconds in 0.5% proteinase K solution (Fujifilm Wako, Osaka, Japan). Precise ZPR time was recorded. After washing with M2 medium and M16 medium, ZF embryos were transferred into droplets of the M16 medium and cultured in the cWOW system for 2.5 days, then transferred into the droplets of the M16 medium until the late blastocyst at 5% CO_2 and 37 °C. The late blastocysts were used for gene expression analysis, TCN, and apoptotic cell detection.

RNA extraction and quantitative PCR

Most of qPCR procedures were performed as described in Chapter III. The late blastocysts were used for qPCR.

Terminal deoxynucleotidyl transferase biotin-dUTP nick end labeling (TUNEL) assay of late blastocyst

Most procedures of the TUNEL assay were performed as described in Chapter III. In this chapter, the fluorescence of the fragmented DNA was detected using LAS X on a DMi8 fluorescence microscope (Leica Microsystems, Germany) and the apoptotic index per late blastocyst was calculated as follows: (TUNEL-positive cells/TCN) × 100.

Statistical analysis

All data are representative of at least three replicates and statistically significant differences were identified using one-way analysis of variance (ANOVA)-Tukey's multiple range test implemented in GraphPad Prism 7 software (LA Jolla, CA, USA). Statistical significance was set at $p < 0.05$.

Results

Effect of ZPR methods on the morphology of blastomeres

There was no significant difference in treatment time between the acid Tyrode's solution and the two-step combined method (Table 3). In contrast, proteinase K required a significantly longer treatment time than the other two methods to

completely remove the ZP ($p < 0.0001$). In Figure. 24A of the control group, the 2-cell blastomere surface of the ZI embryos is shown to be smooth and the contact points between each blastomere are dense and not easily loosened. Just after ZPR by acid Tyrode's treatment, several blastomeres showing wrinkles on the surface were observed compared with ZI embryos (Figure. 24B, white arrows). In contrast, no obvious wrinkles were observed by proteinase K treatment, but loosening and detachment of blastomeres were clearly observed in other ZPR methods (Figure. 24C, black arrows) and ZI embryos (Figure. 24A). In contrast, ZF embryos obtained using the two-step method showed no morphological and attachment abnormalities of the blastomeres like ZI embryos (Figure. 24D).

Effect of ZPR methods on in vitro developmental capacity and quality

I compared the developmental ability and TCN of ZF blastocyst by three ZPR treatment methods. The rate of blastocyst was significantly decreased ($p < 0.05$) when embryos were treated with acid Tyrode's solution and proteinase K when compared with ZI embryos. In contrast, the blastocyst rate was significantly higher in the two-step combined method (Table 4).

I then assessed blastocyst quality by evaluating the TCN and apoptosis status in both the ZI and ZF blastocysts (Figure. 25A). The TCN of blastocyst was significantly higher in the two-step combined method than in acid Tyrode's solution and proteinase K ($p < 0.01$). In contrast, TCN was significantly higher in the two-step method

compared with both acid Tyrode's solution and proteinase K ($p < 0.05$), and not significantly different with ZI embryos (Figure. 25B).

Next, I assessed the apoptotic index of the ZF embryos produced by each of the ZPR methods using TUNEL staining (Figure. 25A). The apoptotic index significantly increased in response to treatment with acid Tyrode's solution ($p < 0.0001$), but there was no significant difference in the apoptotic indexes of the proteinase K or two-step combined method ZF embryos when compared with the ZI embryos (Figure. 26A). I also examined the effect of ZPR on the expression of apoptosis-related genes (*Bax* and *Caspase3*). This evaluation revealed no significant differences in the expression of *Bax* mRNA in acid Tyrode's solution-treated ZF embryos when compared with ZI embryos, however, expression of *Bax* was significantly increased in the acid Tyrode's solution group compared with either the proteinase K or two-step combined method group ($p < 0.001$) (Figure. 26B). Expression of *Caspase 3* was highest ($p < 0.0001$) in the blastocysts from the acid Tyrode's solution ZF embryos when compared with the other ZPR methods; however, there were no significant differences in *Caspase 3* expression in either the proteinase K or two-step combined method groups (Figure. 26C).

Table 3. Treatment time to complete ZPR

Treatment	No. of replicates	Time required for complete zona removal (min, Mean ± SEM)
Acid Tyrode's Solution	5	1.2 ± 0.2^{a}
Proteinase K	5	6.8 ± 0.6^{b}
Two-step	5	1.4 ± 0.2^{a}

A: Exposure time needed to complete ZPR. The results are shown as the mean ± SEM, and one-way ANOVA was used to analyze at least three replicates. Different letters indicate significant differences (a *vs.* b: $p < 0.0001$).

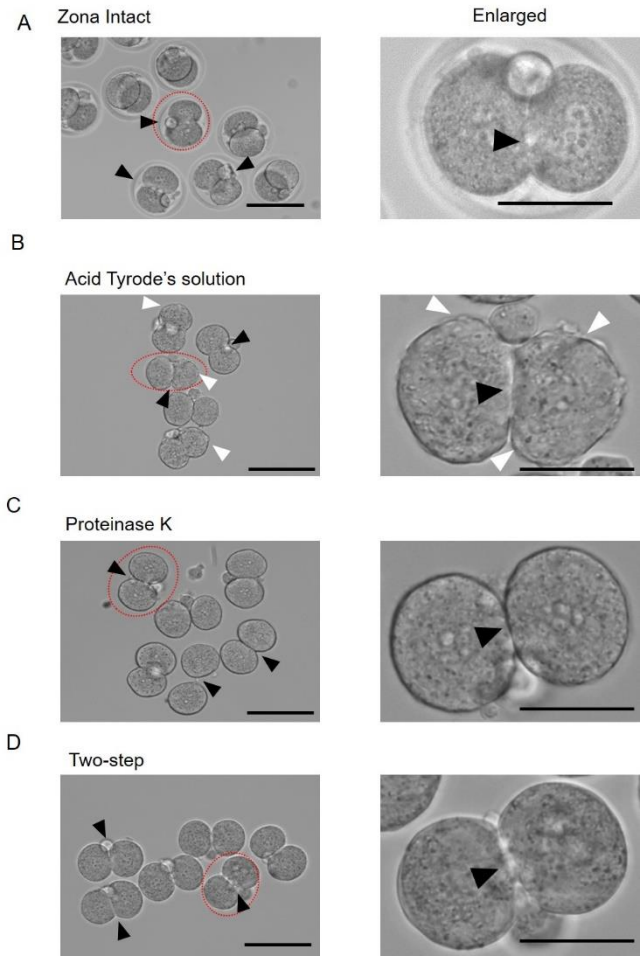

Figure 24. Effect of different ZPR methods on the morphology of the resultant blastomeres.

The blastomere membranes from ZI and ZF embryos were observed using a phase-contrast microscope. White arrows indicate wrinkles on the blastomere surface while black arrows indicate the blastomere attachment status. A: Zona intact (control group), B: Acid Tyrode's solution treatment, C: Proteinase K treatment, D: The two-step combined method of acid Tyrode's solution and proteinase K. Scale bar: 150 μm (left), 50 μm (right).

Table 4. Effect of different methods of ZPR on the development of ZF embryos

Treatment	No. of replicates	No. of embryos cultured	No. of Blastocysts (Mean ± SEM)
Zona intact	5	110	95 (86.3 ± 2.2)
Zona Free			
Acid Tyrode's Solution	5	148	103 (69.6 ± 2.3*)
Proteinase K	5	122	78 (63.9 ± 7.4*)
Two-step	5	90	69 (76.7 ± 2.2)

Zona Free (Acid Tyrode's Solution): Embryos where the ZP was removed at the 2-cell stage using acid Tyrode's solution. ZF (Proteinase K): Embryos where the ZP was removed at the 2-cell stage using proteinase K. ZF (two-step combined method): Embryos where the ZP were removed at the 2-cell stage using a combined two-step method. All ZF embryos were cultured in the cWOW. The data are expressed as the mean ± SEM, and one-way ANOVA was used to analyze the data. Value with asterisks indicates significant differences. * $p < 0.01$.

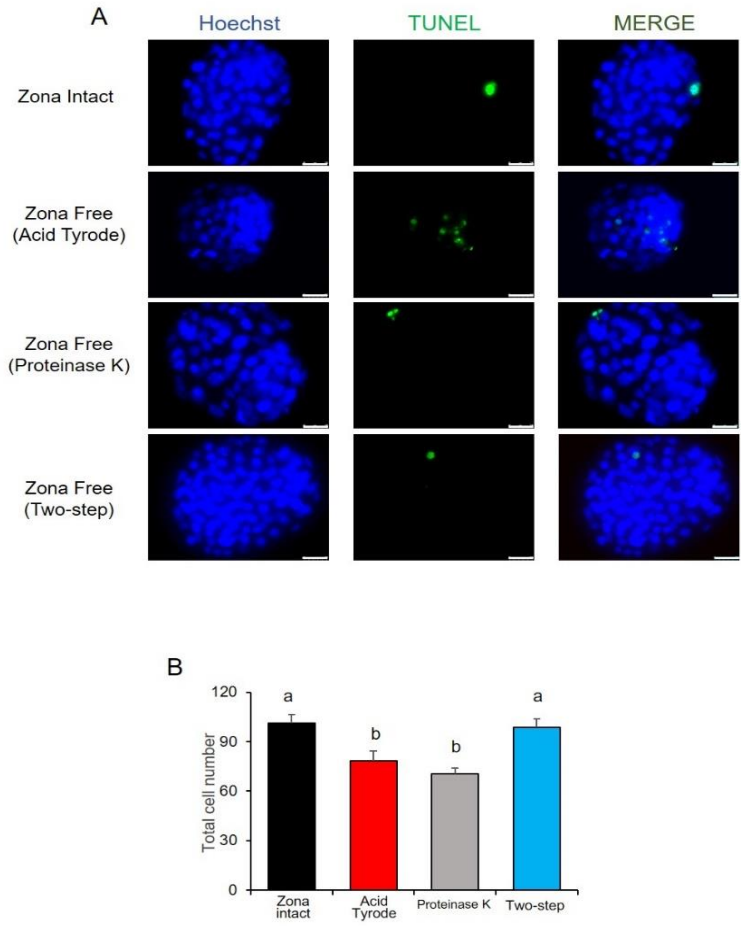

Figure 25. Effect of different ZPR methods on the TCN and their apoptotic status within the mouse blastocysts at the late blastocyst stage.

A: Apoptotic blastomeres within the murine blastocysts were detected using the TUNEL assay (green). Nuclei were stained with Hoechst (blue) to help visualize the individual blastomeres were counted in both the ZI and ZF blastocysts produced by different ZPR methods. Scale bar: 25 μm. B: Total cell number. The results are reported as the mean ± SEM, and one-way ANOVA was used to analyze at least three replicates for each experiment. Different letters indicate a significant difference, B: Total cell number (a *vs.* b: $p < 0.01$).

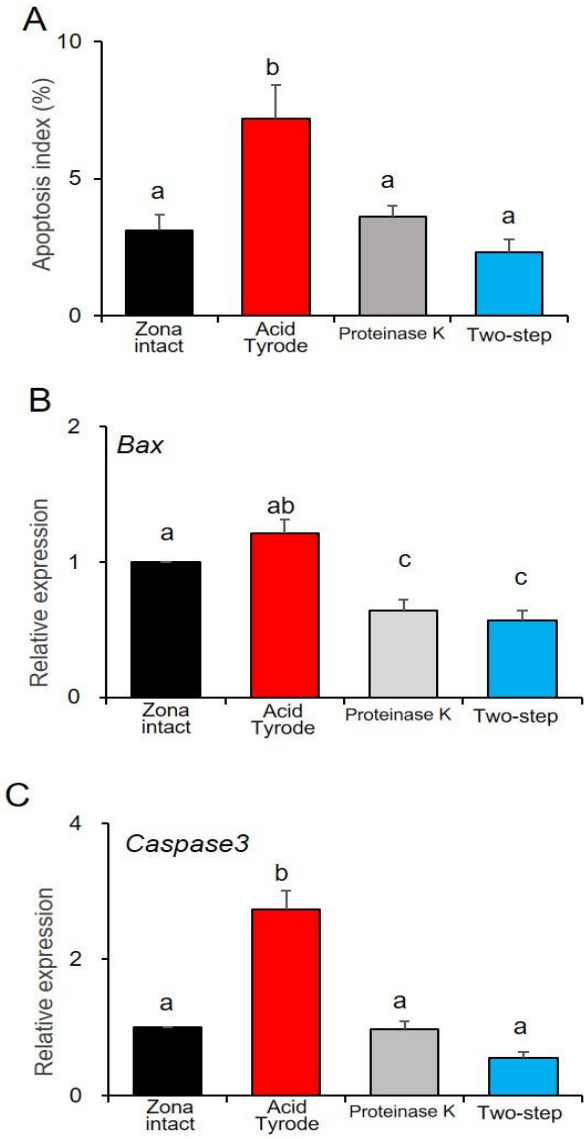

Figure 26. Effect of different ZPR methods on the expression of apoptosis-related genes and apoptosis index at the late blastocyst stage.

A: Apoptosis index. B, C: Differences in *Bax* (B) and *Caspase3* (C) transcription in blastocysts produced using different ZPR methods. The results are reported as the mean ± SEM, and one-way ANOVA was used to analyze at least three replicates for each experiment. A, C (apoptosis index and *Caspase 3* mRNA expression): a *vs.* b: $p < 0.0001$; B: a *vs.* c: $p < 0.05$, b *vs.* c: $p < 0.001$. Different letters indicate significant differences.

Discussion

Establishing a more robust method for ZPR is critical to improving the quality and broadening their application in ART and embryology. In this chapter, I established a novel method for optimizing ZPR by combination with Acid Tyrode's solution for thinning the outer of ZP, and Proteinase K for digesting the inner of ZP that reducing toxicity for embryos. This protocol uses a two-step combined method for complete ZPR and improves the development of ZF embryos by reducing the number of apoptotic cells in the blastocyst.

Acid Tyrode's solution is also commonly used in ART and has been applied to assisted hatching and blastomere separation in humans and mice. However, its toxicity is still remaining controversial. In humans, ZR of human blastocyst using acid Tyrode's solution has demonstrated the increased implantation rates, resulting in more successful pregnancies in patients with poor prognosis [177]. However, the toxicity of acid Tyrode's solution causes damage to the embryos and separation of the blastomeres during cleavage [176]. These facts have led to the development of several zona thinning techniques that rely on the partial digestion of the outer layer of the ZP. For example, partial and circumferential zona thinning has been described in several animal embryos [178]. According to my results in Chapter III, the number of apoptosis-positive cells increased in the TUNEL assay, while the TCN significantly decreased compared with the ZI embryos; According to the results in Chapter IV, the rate of live fetuses and the implantation site were significantly lower after ET than in ZI embryos. These results

might indicate that acid Tyrode's solution has potentially toxic. This is because when complete ZPR is performed, even though the transfer to the M2 medium is quick, there will inevitably be residues of the acid Tyrode's solution that are transferred to the M2 medium together, thus further exacerbating the damage to the blastomeres.

Previous studies have established that bovine ZP is most effectively achieved using 0.2% proteinase K for 5 min and that this process exhibited low toxicity [37]. In contrast, treatment with 0.5% proteinase K took approximately 6.8 min to completely remove the ZP in mouse embryos in the present study. This result suggests that proteinase K is not especially suitable for ZP in mouse embryos. However, despite the differences in digestion time between species this digestion did not induce any visible damage to the blastomere membranes. A previous report showed that the ZP is bilayered, the outer layer is thicker and easily digested by acid Tyrode's solution, while the inner ZP layer is denser and less easily digested [172]. Therefore, I considered whether using acid Tyrode's solution to digest the outer layer followed by proteinase K to digest the inner layer to minimize the damage of the residual fluid to the blastomeres. Then, I performed the two-step method to complete ZPR and compared the toxicity of three treatments.

However, I clarified that enzymatic treatment increased the loose of cell-to-cell contacts and blastomere detachment when compared with other ZPR methods. In addition, another study showed that prolonged exposure to proteinase K damages the ICM/TE structures and disturbs subsequent implantation in human blastocysts [17]. Therefore, enzymatical ZPR may digest the proteins on the blastomere surface needed

to maintain the cell-to-cell contacts necessary for cell growth and differentiation, thus inducing a decrease in blastocyst rate and TCN. In addition, blastocyst rate and TCN were significantly decreased following treatment with acid Tyrode's solution despite its shorter treatment time. Morphological changes including the development of wrinkles on the blastomere surface were clearly observed.

Acid Tyrode's solution-treated ZF blastocyst showed increased apoptotic cells and higher expression of *Caspase 3*, which is consistent with the previous study [179]. Given this, I evaluated the expression of *Bax*, which acts as a cell death inducer, and *Caspase3* as candidate genes to assess the apoptosis in response to each ZPR protocol. My results showed that exposure of ZF embryos to pH (2.5) increased the toxicity of acid Tyrode's solution. A previous study also showed that acid Tyrode's solution induced an increase in apoptosis, whereas the proteinase K-treated bovine embryos did not experience any increase in apoptosis [180]. This was similar to my results, which showed that proteinase K treatment did not affect *Caspase 3* or *Bax* expression and significantly reduced the apoptotic index of these embryos when compared with those of ZI embryos. In addition, there was also no significant difference in the apoptosis index of ZF embryos after combined two-step processing.

The two-step combined method used a 40s exposure to acid Tyrode's solution followed by several seconds of proteinase K treatment to remove the ZP from 2-cell embryos. This method was shown to reduce the toxicity of low pH to embryos, with a significantly increased blastocyst rate and TCN, and reduced cell apoptosis compared with the other ZPR treatments.

In summary, in Chapter VI, I propose a novel two-step combination method for complete ZPR to reduce toxicity and improve the development of ZF embryos in mice. This study may provide an efficient approach for IVP procedures in the near future.

Chapter VII

General Discussion

In the thesis, I demonstrated that ZP plays an important role in maintaining the three-dimensional (3D) structure and intracellular contacts of blastocysts during early embryonic development. In the absence of ZP, cleavage embryos tend to adopt a two-dimensional (2D) form and maintain this structure until compacted within a flat bottom dish. This suggests that the weakening of 3D contact between blastomeres affects further development, differentiation, and embryo quality *in vitro*. My results show that the blastocyst rate of ZF embryos is significantly low in the flat microdroplet system. This is consistent with a previous study [35].

In addition, in this thesis, I designed a cWOW system with a smaller microwell size (approximately 170 μm) to further improve the developmental ability of ZF embryos *in vitro* culture, which is more compatible with the size of mouse ZF embryos (approximately 100 μm). This may provide more suitable conditions for maintaining 3D embryonic structures, which could improve the developmental ability of ZF embryos *in vitro*. Therefore, in this study, I think that cWOW with a smaller microwell is a more efficient culture system for mouse ZF embryos *in vitro*.

A previous study has shown that the handmade WOW system improved the developmental ability *in vitro* culture in bovine ZF embryos compared with ZI embryos [40], but the effects of WOW and its various effects on their developmental capacity

have not been reported. In this thesis, 2-cell embryos were selected for treatment with acid Tyrode's solution to produce ZF embryos and cultured in the cWOW system until the blastocyst stage *in vitro*. The results of this study showed that before implantation, ZPR not only interfered with the differentiation of ICM and TE; after implantation, it also reduced the survival rate of fetuses. Previous studies have shown that ZPR from the zygote reduced the rate of blastocyst and viability in mice [35, 77]. The finding of the low rate of live fetuses after implantation in the present study is consistent with previous studies.

In this thesis, ZPR increased the speed of the compaction process and cavitation compared with ZI embryos. In addition, most of the examined ICM-related genes were upregulated (except *Sox17*), while TE-related genes were downregulated in both morula and blastocyst stages. qPCR results indicated that ZPR disrupted the differentiation-related gene expression of ICM and TE. The immunostaining results showed that the expression of ICM-specific protein OCT4 had a significant fluorescent signal in ZF embryos compared with ZI embryos, while the fluorescence intensity of TE-specific protein CDX2 was relatively weak in ZF embryos. This protein expression pattern was consistent with that of *Oct4* and *Cdx2* detected in blastocysts. Recent evidence has shown that cell fates are relatively flexible before the 8-cell stage, depending on the regulatory nature of mammalian embryonic development [7]. To date, zygotes and 2-cell blastomeres are generally considered totipotent; however, some reports indicate that only one of the 2-cell blastomeres develops into a mouse, and the asymmetric developmental state occurs when 2-cell blastomeres are separated [78-80]. These data

indicate that there is inequality in the potency of the two-cell blastomere. Since previous studies focused more on ZPR at the totipotent zygote stage, whereas the present study chose the main ZGA stage (2-cell) to start performing ZPR. In addition, because ZF embryos lose the protection of the ZP and thus the physical limitation of the close packing of blastomeres in the ZP is lost, the cell fate becomes relatively more flexible. *Carm1* plays an important role in the developmental process, which is associated with cell differentiation and cell-fate decisions. Therefore, these reasons may influence the developmental ability *in vitro* as well as ICM/TE differentiation in ZF embryos.

The TCN was significantly lower in ZF embryos compared with ZI embryos. In contrast, there was no significant difference in the number of ICM cells between ZI and ZF embryos, the number of TE cells showed a significant decrease in ZF embryos. In addition, the apoptotic cells and apoptotic index were significantly increased in ZF embryos compared with ZI embryos, therefore, this may be one of the reasons affecting the low implantation rate of ZF embryos. It is well known that acid Tyrode's solution can be toxic to embryos [181], therefore, for improving the quality of embryos, establishing a low toxicity ZPR method is essential to improve quality and expand its application in ART and embryology. In this study, a two-step combined method for ZPR (Acid Tyrode's solution for thinning the outer of ZP, Proteinase K for digesting the inner of ZP) was used to improve the development of ZF embryos by reducing the number of apoptotic cells in blastocysts.

It should be emphasized that, although correct cell association owing to the presence of the ZP is not a prerequisite for ZF embryos to develop into blastocysts *in*

vitro, post-implantation results show that the ZP plays a critical role in early embryonic development *in vivo*. A previous report showed that the mouse cell lineage is the result of continuous cell-to-cell interactions starting from the 2-cell stage [182]. Therefore, the ZP seems to have an important influence on this process, thereby affecting the pre- and post-implantation survival rates of fetuses. Therefore, I asked why embryos without ZP still have the ability to divide and develop into blastocysts. In addition to the protective effect of ZP, one of its main functions is to maintain the three-dimensional (3D) structure of each blastomere in a form that is most likely to provide the highest developmental potential for the blastocyst [35]. For example, encapsulating the ZF embryos in alginate may have a positive effect on blastocyst development [183]. Once the physical restrictions of the close packing of blastomeres in the ZP are lost, the cleavage plane, and hence lineage allocations, may become less predictable. Although ZF embryos have a similar developmental ability at the start of culture, loss of the protection of the ZP, resulting in a 2D structure of blastomeres, may irreversibly lose their developmental competence to the blastocyst stage. Therefore, the viability of the fetuses may vary depending on the ratio of ICM and TE on blastocysts in ZF embryos [78, 184].

In humans, although *in vitro* culture of embryos is an important step in assisted reproduction, only 1.2% of studies published in five major journals in the field of human reproduction since 2019 focused on *in vitro* culture conditions, this led to the optimization process approaching the limit level [54]. In this thesis, I report on a new cWOW culture system designed for the size of mouse ZF embryos. Because of the 2D

structure of ZF embryos, although I think this cWOW culture system does not change the cleavage process from the 2-cell stage to the 4-cell stage, it exerts a greater beneficial influence on the compaction process after the 4-cell stage, such as morula stage, blastocyst stage. Therefore, I think that it is still necessary to continue to seek and develop a system that can maximum possibly replace the zona pellucida *in vitro* culture, thus providing a new opportunity for human reproduction and the IVP procedure in the livestock.

Chapter VIII

General Conclusion

Overall, the present study suggests that ZPR at the 2-cell stage not only decreases the developmental ability and disturbs the expression pattern of ICM/TE-related genes and epigenetic modification during the preimplantation development, but affects the post-implantation development of mouse embryos.

In Chapter II, I first isolated 2-cell embryos using acid Tyrode's solution and then cultured these ZF embryos under flat microdroplets, commercially available WOW or cWOW, respectively. The rate of blastocyst was significantly increased by the use of cWOW when compared with other culture systems.

In Chapter III, under the cWOW system, I investigated the effects of the ZP on the development and ICM/TE differentiation-related gene expression during the preimplantation process. Compaction occurred earlier after the ZPR at the 2-cell stage. In addition, the expression of differentiation-related genes in the ICM (*Oct4, Sox21*) and TE (*Cdx2, Eomes,* and *Tfap2c*) was significantly altered in both ZF morula and blastocyst compared with ZI embryos. The results in this Chapter III suggest that ZPR at the 2-cell stage disrupts the expression pattern of ICM/TE-related genes.

In Chapter IV, after ET, the implantation rate and the number of live fetuses were lower in ZF embryos than in control embryos, whereas the fetal weight at E17.5 was not different. However, placental weight was significantly increased in ZF embryos.

RNA-seq analysis of the placenta showed a total of 473 DEGs that significantly influenced the biological process.

In Chapter V, I investigated the developmental ability and heterogeneity of ZF embryos influenced at the 4-cell stage as well as epigenetic modification patterns. ZF embryos have four different types of morphological changes at the 4-cell stage and there is no difference in their *in vitro* developmental capacity. However, the TCN of blastocysts in the 3P type of 4-cell is significantly lower than the other 4-cell types as well as the ZI embryos. Moreover, at the 4-cell stage, ZF embryos are also heterogeneous and have higher mRNA and protein expression levels of CARM1 than ZI embryos. Expression of DNA methylation-related genes (*Dnmt1, Uhrf1, Dnmt3a,* and *Dnmt3b*) was significantly decreased in the ZF blastocyst compared with ZI embryos, which indicated that ZPR disturbs the regulation of epigenetic modification. Overall, these results in this Chapter V suggest that ZPR affects the blastomere allocation at the early stage and subsequent development, and epigenetic modification patterns.

In Chapter VI, I evaluated the use of a two-step ZPR protocol, relying on acid Tyrode's solution and proteinase K, and subsequent culture in the cWOW system. Although acid Tyrode's solution treatment alone reduced ZPR time, blastomere morphology became wrinkled, and a significant decrease in blastocyst rate associated with an increased apoptotic cell number and expression of apoptosis-related genes was observed. Using proteinase K alone increased ZPR time and significantly decreased the blastocyst rate, but did not induce an increase in apoptotic cell number or apoptosis-

related gene expression. In contrast, the two-step method significantly reduced ZPR time and improved blastocyst rate by increasing the TCN in these microwells and reducing the apoptotic cell number. These results suggest that the two-step ZPR protocol is beneficial for reducing the toxic effects of ZPR on ZF embryo development and quality when combined with the cWOW culture system.

In conclusion, the absence of the ZP not only affects blastocyst formation [36], but also affects the developmental potential associated with gene expression. ZF embryos may enhance cell-to-cell communication, thereby accelerating the compaction process during the 8-cell stage. Subsequently, changes in the expression patterns of ICM- and TE-related genes and proteins were observed in ZF embryos. During post-implantation development, the rate of fetuses at E17.5 and the implantation rate in ZF embryos are relatively low. However, there is still a potential effect of the ZPR methods for development and differentiation as well as ZPR itself. So, it is necessary to investigate the chemical effect of the ZPR process on embryonic development to improve the success of ART. Besides, for a better understanding of the function of the ZP during preimplantation, it would be meaningful to discuss these findings in mammals and might be important for future research related to the production of ZF embryos or clone embryos. These findings may provide deeper insights into the role of the ZP during early embryonic development for the production of multiple gene-modified animals and cloned embryos.

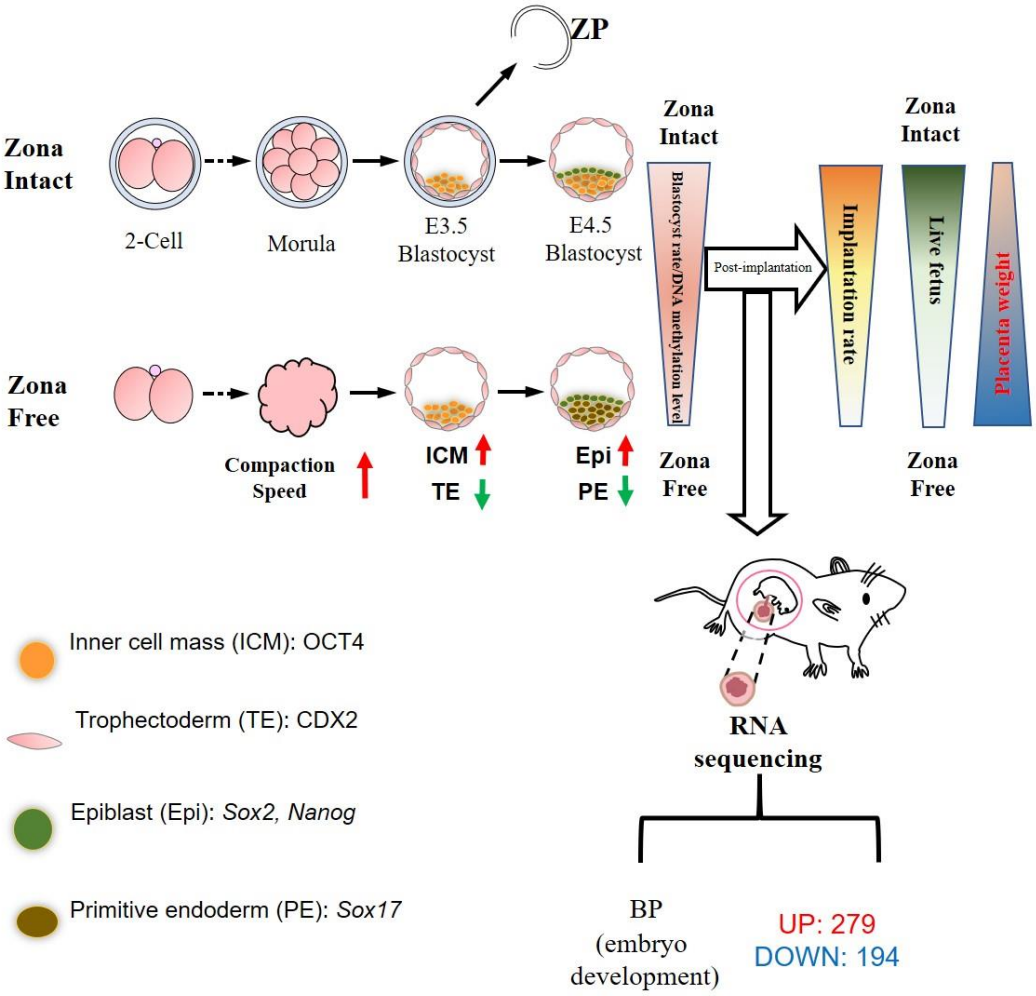

Figure 27. Schematic hypothesis of the effects of ZPR on the pre- and post-implantation development of mouse embryos.

Acknowledgement

I would like to express my deepest appreciation to Professor Masashi Takahashi, Laboratory of Animal Genetics and Reproduction, Graduate School of Global Food Resources and Research Faculty of Agriculture, Hokkaido University, for his continuous mentoring, guidance, assistance, and encouragement throughout this work.

I deeply appreciate Professor Satoshi Koike, Laboratory of Animal Function and Nutrition, and Professor Takanori Nishimura, Laboratory of Cell and Tissue Biology, Graduate School of Agriculture, for their assistance and comments throughout this work.

I would like to express my sincere gratitude to Associate Professor Manabu Kawahara, Laboratory of Animal Genetics and Reproduction, Graduate School of Agriculture, Hokkaido University, for his assistance throughout this work.

I appreciate Associate Professor Toshikazu Kawaguchi, Faculty of Environmental Earth Science, Hokkaido University, for his assistance throughout this work.

I am deeply grateful to Assistant Professor Hanako Bai, Laboratory of Animal Genetics and Reproduction, Graduate School of Agriculture, Hokkaido University, for her assistance and encouragement while this work.

I greatly thank all students help from the Laboratory of Animal Genetics and Reproduction, for their helpful discussion, and valuable advice. I would like to express my deep appreciation to my family, for their encouragement and support. I would like to thank all people who helped me through this thesis study.

Finally, I gratefully acknowledge the financial support by a Grant-in-Aid for Scientific Research from the Tojuro Iijima Foundation for Food Science and JST SPRING in Japan.

Reference

1. Wassarman PM. Zona pellucida glycoproteins. Annu Rev Biochem 1988; 57:415-42.
2. Spargo SC, Hope RM. Evolution and nomenclature of the zona pellucida gene family. Biol Reprod 2003; 68:358-62.
3. Conner SJ, Lefièvre L, Hughes DC, Barratt CL. Cracking the egg: increased complexity in the zona pellucida. Hum Reprod 2005; 20:1148-52.
4. Nawroth F, Müller P, Wolf C, Sudik R. Is the Zona pellucida thickness of metaphase-II oocytes in an IVF/ICSI program influenced by the patient's age? Gynecol Obstet Invest 2001; 52:55-9.
5. Sun YP, Xu Y, Cao T, Su YC, Guo YH. Zona pellucida thickness and clinical pregnancy outcome following in vitro fertilization. Int J Gynaecol Obstet 2005; 89:258-62.
6. Herrler A, Beier HM. Early embryonic coats: morphology, function, practical applications. An overview. Cells Tissues Organs 2000; 166:233-46.
7. Rossant J, Tam PP. Blastocyst lineage formation, early embryonic asymmetries and axis patterning in the mouse. Development 2009; 136:701-13.
8. Bedzhov I, Graham SJ, Leung CY, Zernicka-Goetz M. Developmental plasticity, cell fate specification and morphogenesis in the early mouse embryo. Philos Trans R Soc Lond B Biol Sci 2014; 369:20130538.
9. Chávez DJ, Enders AC, Schlafke S. Trophectoderm cell subpopulations in the

periimplantation mouse blastocyst. J Exp Zool 1984; 231:267-71.

10. Rassoulzadegan M, Rosen BS, Gillot I, Cuzin F. Phagocytosis reveals a reversible differentiated state early in the development of the mouse embryo. EMBO J 2000; 19:3295-303.

11. Liu DY, Baker HW. Defective sperm-zona pellucida interaction: a major cause of failure of fertilization in clinical in-vitro fertilization. Hum Reprod 2000; 15:702-8.

12. Bielinska M, Narita N, Wilson DB. Distinct roles for visceral endoderm during embryonic mouse development. Int J Dev Biol 1999; 43:183-205.

13. Tam PP, Loebel DA. Gene function in mouse embryogenesis: get set for gastrulation. Nat Rev Genet 2007; 8:368-81.

14. Brennan J, Lu CC, Norris DP, Rodriguez TA, Beddington RS, Robertson EJ. Nodal signalling in the epiblast patterns the early mouse embryo. Nature 2001; 411:965-9.

15. Cohen J, Alikani M, Trowbridge J, Rosenwaks Z. Implantation enhancement by selective assisted hatching using zona drilling of human embryos with poor prognosis. Hum Reprod 1992; 7:685-91.

16. Urman B, Balaban B, Alatas C, Aksoy S, Mumcu A, Isiklar A. Zona-intact versus zona-free blastocyst transfer: a prospective, randomized study. Fertil Steril 2002; 78:392-6.

17. Fong CY, Bongso A, Sathananthan H, Ho J, Ng SC. Ultrastructural observations of enzymatically treated human blastocysts: zona-free blastocyst transfer and

rescue of blastocysts with hatching difficulties. Hum Reprod 2001; 16:540-6.

18. Cohen J, Elsner C, Kort H, Malter H, Massey J, Mayer MP, Wiemer K. Impairment of the hatching process following IVF in the human and improvement of implantation by assisting hatching using micromanipulation. Hum Reprod 1990; 5:7-13.

19. Fong CY, Bongso A, Ng SC, Kumar J, Trounson A, Ratnam S. Blastocyst transfer after enzymatic treatment of the zona pellucida: improving in-vitro fertilization and understanding implantation. Hum Reprod 1998; 13:2926-32.

20. Jelinkova L, Pavelkova J, Strehler E, Paulus W, Zivny J, Sterzik K. Improved implantation rate after chemical removal of the zona pellucida. Fertil Steril 2003; 79:1299-303.

21. Ritchie WA, Taylor JE, Gardner JO, Wilmut I, Carlisle A, Neil C, King T, Whitelaw CB. Live lambs born from zona-pellucida denuded embryos. Cloning Stem Cells 2005; 7:178-82.

22. Lagutina I, Lazzari G, Duchi R, Turini P, Tessaro I, Brunetti D, Colleoni S, Crotti G, Galli C. Comparative aspects of somatic cell nuclear transfer with conventional and zona-free method in cattle, horse, pig and sheep. Theriogenology 2007; 67:90-8.

23. Rodríguez L, Navarrete FI, Tovar H, Cox JF, Castro FO. High developmental potential in vitro and in vivo of cattle embryos cloned without micromanipulators. J Assist Reprod Genet 2008; 25:13-6.

24. Palermo G, Joris H, Devroey P, Van Steirteghem AC. Pregnancies after

intracytoplasmic injection of single spermatozoon into an oocyte. Lancet 1992; 340:17-8.

25. Van Steirteghem AC, Nagy Z, Joris H, Liu J, Staessen C, Smitz J, Wisanto A, Devroey P. High fertilization and implantation rates after intracytoplasmic sperm injection. Hum Reprod 1993; 8:1061-6.

26. Nagy ZP, Liu J, Joris H, Verheyen G, Tournaye H, Camus M, Derde MC, Devroey P, Van Steirteghem AC. The result of intracytoplasmic sperm injection is not related to any of the three basic sperm parameters. Hum Reprod 1995; 10:1123-9.

27. Devroey P, Nagy P, Tournaye H, Liu J, Silber S, Van Steirteghem A. Outcome of intracytoplasmic sperm injection with testicular spermatozoa in obstructive and non-obstructive azoospermia. Hum Reprod 1996; 11:1015-8.

28. Stanger JD, Stevenson K, Lakmaker A, Woolcott R. Pregnancy following fertilization of zona-free, coronal cell intact human ova: Case Report. Hum Reprod 2001; 16:164-167.

29. Sjunnesson Y. In vitro fertilisation in domestic mammals-a brief overview. Ups J Med Sci 2020; 125:68-76.

30. Tarkowski AK. Mouse chimaeras developed from fused eggs. Nature 1961; 190:857-60.

31. Nagy A, Rossant J, Nagy R, Abramow-Newerly W, Roder JC. Derivation of completely cell culture-derived mice from early-passage embryonic stem cells. Proc Natl Acad Sci U S A 1993; 90:8424-8.

32. Maemura M, Taketsuru H, Nakajima Y, Shao R, Kakihara A, Nogami J, Ohkawa Y, Tsukada YI. Totipotency of mouse zygotes extends to single blastomeres of embryos at the four-cell stage. Sci Rep 2021; 11:11167.

33. Li R, Miao J, Wang Z. Production of genetically engineered porcine embryos by handmade cloning. Methods Mol Biol 2019: 347-360.

34. Ikeda S, Sugimoto M, Kume S. Lipofection of siRNA into bovine 8-16-cell stage embryos using zona removal and the well-of-the-well culture system. J Reprod Dev 2018; 64:199-202.

35. Suzuki H, Togashi M, Adachi J, Toyoda Y. Developmental ability of zona-free mouse embryos is influenced by cell association at the 4-cell stage. Biol Reprod 1995; 53:78-83.

36. Fan W, Homma M, Xu R, Kunii H, Bai H, Kawahara M, Kawaguchi T, Takahashi M. The use of a two-step removal protocol and optimized culture conditions improve development and quality of zona free mouse embryos. Biochem Biophys Res Commun 2021; 577:116-123.

37. Velásquez A, Manríquez J, Castro F, Rodríguez-Alvarez L. Effect of zona pellucida removal on early development of in vitro produced bovine embryos. Arch Med Vet 2013; 45:7-15.

38. Park CH, Jeong YH, Lee DK, Hwang JY, Uh KJ, Yeom SC, Ahn C, Lee CK. Availability of empty zona pellucida for generating embryonic chimeras. PLoS One 2014; 10:e0123178.

39. Thouas GA, Jones GM, Trounson AO. The 'GO' system--a novel method of

microculture for in vitro development of mouse zygotes to the blastocyst stage. Reproduction 2003; 126:161-9.

40. Vajta G, Peura TT, Holm P, Páldi A, Greve T, Trounson AO, Callesen H. New method for culture of zona-included or zona-free embryos: the Well of the Well (WOW) system. Mol Reprod Dev 2000; 55:256-64.

41. Wassarman PM, Litscher ES. Mammalian fertilization: the egg's multifunctional zona pellucida. Int J Dev Biol 2008; 52:665-76.

42. Florman HM, Ducibella T. Fertilization in mammals. Knobil and Neill's physiology of reproduction 2006; 3:55-112.

43. Gupta SK. The human egg's zona pellucida. Curr Top Dev Biol 2018; 130:379-411.

44. Liang L-F, Dean J. Oocyte development: Molecular biology of the zona pellucida. Vitam Horm 1993; 47:115-59.

45. Wassarman PM, Litscher ES. The mouse egg's zona pellucida. Curr Top Dev Biol 2018; 130:331-356.

46. Hamm DC, Harrison MM. Regulatory principles governing the maternal-to-zygotic transition: insights from drosophila melanogaster. Open Biol 2018; 8:180183.

47. Gurdon JB. The developmental capacity of nuclei taken from intestinal epithelium cells of feeding tadpoles. J Embryol Exp Morphol 1962; 10:622-40.

48. Tadros W, Lipshitz HD. The maternal-to-zygotic transition: a play in two acts. Development 2009; 136:3033-42.

49. Hamatani T, Carter MG, Sharov AA, Ko MS. Dynamics of global gene expression changes during mouse preimplantation development. Dev Cell 2004; 6:117-31.

50. Yartseva V, Giraldez AJ. The Maternal-to-Zygotic Transition During Vertebrate Development: A Model for Reprogramming. Curr Top Dev Biol 2015; 113:191-232.

51. Schulz KN, Harrison MM. Mechanisms regulating zygotic genome activation. Nat Rev Genet 2019; 20:221-234.

52. Eckersley-Maslin MA, Alda-Catalinas C, Reik W. Dynamics of the epigenetic landscape during the maternal-to-zygotic transition. Nat Rev Mol Cell Biol 2018; 19:436-450.

53. Yumoto K, Shimura T, Mio Y. Removing the zona pellucida can decrease cytoplasmic fragmentations in human embryos: a pilot study using 3PN embryos and time-lapse cinematography. J Assist Reprod Genet 2020; 37:1349-1354.

54. Vajta G, Parmegiani L, Machaty Z, Chen WB, Yakovenko S. Back to the future: optimised microwell culture of individual human preimplantation stage embryos. J Assist Reprod Genet 2021; 38:2563-2574.

55. Matoba S, Fair T, Lonergan P. Maturation, fertilisation and culture of bovine oocytes and embryos in an individually identifiable manner: a tool for studying oocyte developmental competence. Reprod Fertil Dev 2010; 22:839-51.

56. Sugimura S, Akai T, Somfai T, Hirayama M, Aikawa Y, Ohtake M, Hattori H,

Kobayashi S, Hashiyada Y, Konishi K. Time-lapse cinematography-compatible polystyrene-based microwell culture system: a novel tool for tracking the development of individual bovine embryos. Biol Reprod 2010; 83:970-8.

57. Sugimura S, Akai T, Hashiyada Y, Aikawa Y, Ohtake M, Matsuda H, Kobayashi S, Kobayashi E, Konishi K, Imai K. Effect of embryo density on in vitro development and gene expression in bovine in vitro-fertilized embryos cultured in a microwell system. J Reprod Dev 2013; 59:115-22.

58. Hasegawa A, Tanaka H, Shibahara H. Infertility and Immunocontraception based on zona pellucida. Reprod Med Biol 2013; 13:1-9.

59. Piotrowska-Nitsche K, Perea-Gomez A, Haraguchi S, Zernicka-Goetz M. Four-cell stage mouse blastomeres have different developmental properties. Development 2005; 132:479-90.

60. Sasaki H. Mechanisms of trophectoderm fate specification in preimplantation mouse development. Dev Growth Differ 2010; 52:263-73.

61. Kohri N, Akizawa H, Iisaka S, Bai H, Yanagawa Y, Takahashi M, Komatsu M, Kawai M, Nagano M, Kawahara M. Trophectoderm regeneration to support full-term development in the inner cell mass isolated from bovine blastocyst. J Biol Chem 2019; 294:19209-19223.

62. Fleming TP. A quantitative analysis of cell allocation to trophectoderm and inner cell mass in the mouse blastocyst. Dev Biol 1987; 119:520-31.

63. Chazaud C, Yamanaka Y, Pawson T, Rossant J. Early lineage segregation between epiblast and primitive endoderm in mouse blastocysts through the

Grb2-MAPK pathway. Dev Cell 2006; 10:615-24.

64. Pedersen RA, Wu K, Bałakier H. Origin of the inner cell mass in mouse embryos: cell lineage analysis by microinjection. Dev Biol 1986; 117:581-95.

65. Nichols J, Zevnik B, Anastassiadis K, Niwa H, Klewe-Nebenius D, Chambers I, Schöler H, Smith A. Formation of pluripotent stem cells in the mammalian embryo depends on the POU transcription factor Oct4. Cell 1998; 95:379-91.

66. Avilion AA, Nicolis SK, Pevny LH, Perez L, Vivian N, Lovell-Badge R. Multipotent cell lineages in early mouse development depend on SOX2 function. Genes Dev 2003; 17:126-40.

67. Mitsui K, Tokuzawa Y, Itoh H, Segawa K, Murakami M, Takahashi K, Maruyama M, Maeda M, Yamanaka S. The homeoprotein Nanog is required for maintenance of pluripotency in mouse epiblast and ES cells. Cell 2003; 113:631-42.

68. Artus J, Piliszek A, Hadjantonakis AK. The primitive endoderm lineage of the mouse blastocyst: sequential transcription factor activation and regulation of differentiation by Sox17. Dev Biol 2011; 350:393-404.

69. Mallanna SK, Ormsbee BD, Iacovino M, Gilmore JM, Cox JL, Kyba M, Washburn MP, Rizzino A. Proteomic analysis of Sox2-associated proteins during early stages of mouse embryonic stem cell differentiation identifies Sox21 as a novel regulator of stem cell fate. Stem Cells 2010; 28:1715-27.

70. Kuzmichev AN, Kim SK, D'Alessio AC, Chenoweth JG, Wittko IM, Campanati L, McKay RD. Sox2 acts through Sox21 to regulate transcription in pluripotent

and differentiated cells. Curr Biol 2012; 22:1705-10.

71. Chakravarthy H, Ormsbee BD, Mallanna SK, Rizzino A. Rapid activation of the bivalent gene Sox21 requires displacement of multiple layers of gene-silencing machinery. FASEB J 2011; 25:206-18.

72. Niwa H, Toyooka Y, Shimosato D, Strumpf D, Takahashi K, Yagi R, Rossant J. Interaction between Oct3/4 and Cdx2 determines trophectoderm differentiation. Cell 2005; 123:917-29.

73. Livak KJ, Schmittgen TD. Analysis of relative gene expression data using real-time quantitative PCR and the 2(-Delta Delta C(T)) Method. Methods 2001; 25:402-8.

74. Kang Y, Wu Z, Cai D, Lu B. Evaluation of reference genes for gene expression studies in mouse and N2a cell ischemic stroke models using quantitative real-time PCR. BMC Neurosci 2018; 19:3.

75. Schneider CA, Rasband WS, Eliceiri KW. NIH Image to ImageJ: 25 years of image analysis. Nat Methods 2012; 9:671-5.

76. Hasegawa A, Fukui A, Shibahara H. The current perspectives on the mammalian zona pellucida. Journal of Mammalian Ova Research 2017; 34:57-64.

77. Rankin TL, O'Brien M, Lee E, Wigglesworth K, Eppig J, Dean J. Defective zonae pellucidae in Zp2-null mice disrupt folliculogenesis, fertility and development. Development 2001; 128:1119-26.

78. Casser E, Israel S, Witten A, Schulte K, Schlatt S, Nordhoff V, Boiani M. Totipotency segregates between the sister blastomeres of two-cell stage mouse

embryos. Sci Rep 2017; 7:8299.

79. Papaioannou VE, Ebert KM. Mouse half embryos: viability and allocation of cells in the blastocyst. Dev Dyn 1995; 203:393-8.

80. Katayama M, Ellersieck MR, Roberts RM. Development of monozygotic twin mouse embryos from the time of blastomere separation at the two-cell stage to blastocyst. Biol Reprod 2010; 82:1237-47.

81. Chambers I, Colby D, Robertson M, Nichols J, Lee S, Tweedie S, Smith A. Functional expression cloning of Nanog, a pluripotency sustaining factor in embryonic stem cells. Cell 2003; 113:643-55.

82. Silva J, Nichols J, Theunissen TW, Guo G, van Oosten AL, Barrandon O, Wray J, Yamanaka S, Chambers I, Smith A. Nanog is the gateway to the pluripotent ground state. Cell 2009; 138:722-37.

83. Guo G, Huss M, Tong GQ, Wang C, Li Sun L, Clarke ND, Robson P. Resolution of cell fate decisions revealed by single-cell gene expression analysis from zygote to blastocyst. Dev Cell 2010; 18:675-85.

84. Ao A, Erickson RP. Injection of Antisense RNA specific for E-cadherin demonstrates that E-cadherin facilitates compaction, the first differentiative step of the mammalian embryo. Antisense Res Dev 1992; 2:153-63.

85. Larue L, Ohsugi M, Hirchenhain J, Kemler R. E-cadherin null mutant embryos fail to form a trophectoderm epithelium. Proc Natl Acad Sci U S A 1994; 91:8263-7.

86. Stephenson RO, Yamanaka Y, Rossant J. Disorganized epithelial polarity and

excess trophectoderm cell fate in preimplantation embryos lacking E-cadherin. Development 2010; 137:3383-91.

87. Veraguas-Davila D, Cordero MF, Saez S, Saez-Ruiz D, Gonzalez A, Saravia F, Castro FO, Rodriguez-Alvarez L. Domestic cat embryos generated without zona pellucida are capable of developing in vitro but exhibit abnormal gene expression and a decreased implantation rate. Theriogenology 2021; 174:36-46.

88. Dean J. Biology of mammalian fertilization: role of the zona pellucida. J Clin Invest 1992; 89:1055-9.

89. Bertrand E, Van den Bergh M, Englert Y. Does zona pellucida thickness influence the fertilization rate? Hum Reprod 1995; 10:1189-93.

90. Tanaka S, Kunath T, Hadjantonakis AK, Nagy A, Rossant J. Promotion of trophoblast stem cell proliferation by FGF4. Science 1998; 282:2072-5.

91. Strumpf D, Mao C-A, Yamanaka Y, Ralston A, Chawengsaksophak K, Beck F, Rossant J. Cdx2 is required for correct cell fate specification and differentiation of trophectoderm in the mouse blastocyst. Development 2005; 132:2093-102.

92. Rossant J, Cross JC. Placental development: lessons from mouse mutants. Nat Rev Genet 2001; 2:538-48.

93. Uy GD, Downs KM, Gardner RL. Inhibition of trophoblast stem cell potential in chorionic ectoderm coincides with occlusion of the ectoplacental cavity in the mouse. Development 2002; 129:3913-24.

94. Carney EW, Prideaux V, Lye SJ, Rossant J. Progressive expression of trophoblast-specific genes during formation of mouse trophoblast giant cells in

vitro. Mol Reprod Dev 1993; 34:357-68.

95. Rossant J, Tamura-Lis W. Effect of culture conditions on diploid to giant-cell transformation in postimplantation mouse trophoblast. J Embryol Exp Morphol 1981; 62:217-27.

96. Cohen J, Inge KL, Suzman M, Wiker SR, Wright G. Videocinematography of fresh and cryopreserved embryos: a retrospective analysis of embryonic morphology and implantation. Fertil Steril 1989; 51:820-7.

97. Palmstierna M, Murkes D, Csemiczky G, Andersson O, Wramsby H. Zona pellucida thickness variation and occurrence of visible mononucleated blastomers in preembryos are associated with a high pregnancy rate in IVF treatment. J Assist Reprod Genet 1998; 15:70-5.

98. Kawahara M, Wu Q, Takahashi N, Morita S, Yamada K, Ito M, Ferguson-Smith AC, Kono T. High-frequency generation of viable mice from engineered bi-maternal embryos. Nat Biotechnol 2007; 25:1045-50.

99. Wang F, Tian X, Zhang L, Tan D, Reiter RJ, Liu G. Melatonin promotes the in vitro development of pronuclear embryos and increases the efficiency of blastocyst implantation in murine. J Pineal Res 2013; 55:267-74.

100. Love MI, Huber W, Anders S. Moderated estimation of fold change and dispersion for RNA-seq data with DESeq2. Genome Biol 2014; 15:550.

101. Alexa A, Rahnenführer J, Lengauer T. Improved scoring of functional groups from gene expression data by decorrelating GO graph structure. Bioinformatics 2006; 22:1600-7.

102. Hiraoka K, Hiraoka K, Horiuchi T, Kusuda T, Okano S, Kinutani M, Kinutani K. Impact of the size of zona pellucida thinning area on vitrified-warmed cleavage-stage embryo transfers: a prospective, randomized study. J Assist Reprod Genet 2009; 26:515-21.

103. Carroll J, Depypere H, Matthews CD. Freeze-thaw-induced changes of the zona pellucida explains decreased rates of fertilization in frozen-thawed mouse oocytes. J Reprod Fertil 1990; 90:547-53.

104. Coan PM, Angiolini E, Sandovici I, Burton GJ, Constância M, Fowden AL. Adaptations in placental nutrient transfer capacity to meet fetal growth demands depend on placental size in mice. J Physiol 2008; 586:4567-76.

105. Roberts H, Woodman AG, Baines KJ, Jeyarajah MJ, Bourque SL, Renaud SJ. Maternal Iron Deficiency Alters Trophoblast Differentiation and Placental Development in Rat Pregnancy. Endocrinology 2021; 162:bqab215.

106. Bronson RA, McLaren A. Transfer to the mouse oviduct of eggs with and without the zona pellucida. J Reprod Fertil 1970; 22:129-37.

107. Modliński JA. The role of the zona pellucida in the development of mouse eggs in vivo. J Embryol Exp Morphol 1970; 23:539-47.

108. Mintz B. Experimental study of the developing mammalian egg: removal of the zona pellucida. Science 1962; 138:594-5.

109. Singh EL. The disease control potential of embryos. Theriogenology 1987; 27:9-20.

110. Takaoka K, Hamada H. Cell fate decisions and axis determination in the early

mouse embryo. Development 2012; 139:3-14.

111. Zernicka-Goetz M, Morris SA, Bruce AW. Making a firm decision: multifaceted regulation of cell fate in the early mouse embryo. Nat Rev Genet 2009; 10:467-77.

112. Hillman N, Sherman MI, Graham C. The effect of spatial arrangement on cell determination during mouse development. J Embryol Exp Morphol 1972; 28:263-78.

113. Tarkowski AK. Experiments on the development of isolated blastomers of mouse eggs. Nature 1959; 184:1286-7.

114. Bischoff M, Parfitt DE, Zernicka-Goetz M. Formation of the embryonic-abembryonic axis of the mouse blastocyst: relationships between orientation of early cleavage divisions and pattern of symmetric/asymmetric divisions. Development 2008; 135:953-62.

115. Tabansky I, Lenarcic A, Draft RW, Loulier K, Keskin DB, Rosains J, Rivera-Feliciano J, Lichtman JW, Livet J, Stern JN, Sanes JR, Eggan K. Developmental bias in cleavage-stage mouse blastomeres. Curr Biol 2013; 23:21-31.

116. Burton A, Muller J, Tu S, Padilla-Longoria P, Guccione E, Torres-Padilla ME. Single-cell profiling of epigenetic modifiers identifies PRDM14 as an inducer of cell fate in the mammalian embryo. Cell Rep 2013; 5:687-701.

117. Plachta N, Bollenbach T, Pease S, Fraser SE, Pantazis P. Oct4 kinetics predict cell lineage patterning in the early mammalian embryo. Nat Cell Biol 2011; 13:117-23.

118. Torres-Padilla ME, Parfitt DE, Kouzarides T, Zernicka-Goetz M. Histone arginine methylation regulates pluripotency in the early mouse embryo. Nature 2007; 445:214-8.

119. Young LE, Beaujean N. DNA methylation in the preimplantation embryo: the differing stories of the mouse and sheep. Anim Reprod Sci 2004; 82-83:61-78.

120. Bestor TH. The DNA methyltransferases of mammals. Hum Mol Genet 2000; 9:2395-402.

121. Robertson KD, Wolffe AP. DNA methylation in health and disease. Nat Rev Genet 2000; 1:11-9.

122. Li E, Beard C, Jaenisch R. Role for DNA methylation in genomic imprinting. Nature 1993; 366:362-5.

123. Moore LD, Le T, Fan G. DNA methylation and its basic function. Neuropsychopharmacology 2013; 38:23-38.

124. Jaenisch R, Bird A. Epigenetic regulation of gene expression: how the genome integrates intrinsic and environmental signals. Nat Genet 2003; 33 Suppl:245-54.

125. Robertson KD, Jones PA. DNA methylation: past, present and future directions. Carcinogenesis 2000; 21:461-7.

126. Issa JP. CpG island methylator phenotype in cancer. Nat Rev Cancer 2004; 4:988-93.

127. Saitou M, Kagiwada S, Kurimoto K. Epigenetic reprogramming in mouse pre-implantation development and primordial germ cells. Development 2012;

139:15-31.

128. Lucifero D, Mann MR, Bartolomei MS, Trasler JM. Gene-specific timing and epigenetic memory in oocyte imprinting. Hum Mol Genet 2004; 13:839-49.

129. Swales AK, Spears N. Genomic imprinting and reproduction. Reproduction 2005; 130:389-99.

130. Hiura H, Obata Y, Komiyama J, Shirai M, Kono T. Oocyte growth-dependent progression of maternal imprinting in mice. Genes Cells 2006; 11:353-61.

131. Li E, Bestor TH, Jaenisch R. Targeted mutation of the DNA methyltransferase gene results in embryonic lethality. Cell 1992; 69:915-26.

132. Lister R, Pelizzola M, Dowen RH, Hawkins RD, Hon G, Tonti-Filippini J, Nery JR, Lee L, Ye Z, Ngo QM, Edsall L, Antosiewicz-Bourget J, et al. Human DNA methylomes at base resolution show widespread epigenomic differences. Nature 2009; 462:315-22.

133. Maenohara S, Unoki M, Toh H, Ohishi H, Sharif J, Koseki H, Sasaki H. Role of UHRF1 in de novo DNA methylation in oocytes and maintenance methylation in preimplantation embryos. PLoS Genet 2017; 13: e1007042.

134. Bostick M, Kim JK, Estève PO, Clark A, Pradhan S, Jacobsen SE. UHRF1 plays a role in maintaining DNA methylation in mammalian cells. Science 2007; 317:1760-4.

135. Meilinger D, Fellinger K, Bultmann S, Rothbauer U, Bonapace IM, Klinkert WE, Spada F, Leonhardt H. Np95 interacts with de novo DNA methyltransferases, Dnmt3a and Dnmt3b, and mediates epigenetic silencing of

the viral CMV promoter in embryonic stem cells. EMBO Rep 2009; 10:1259-64.

136. Beaujean N, Taylor J, Gardner J, Wilmut I, Meehan R, Young L. Effect of limited DNA methylation reprogramming in the normal sheep embryo on somatic cell nuclear transfer. Biol Reprod 2004; 71:185-93.

137. Bird A. DNA methylation patterns and epigenetic memory. Genes Dev 2002; 16:6-21.

138. Li E. Chromatin modification and epigenetic reprogramming in mammalian development. Nat Rev Genet 2002; 3:662-73.

139. Jedrusik A. Making the first decision: lessons from the mouse. Reprod Med Biol 2015; 14:135-150.

140. Goolam M, Scialdone A, Graham SJL, Macaulay IC, Jedrusik A, Hupalowska A, Voet T, Marioni JC, Zernicka-Goetz M. Heterogeneity in Oct4 and Sox2 Targets Biases Cell Fate in 4-Cell Mouse Embryos. Cell 2016; 165:61-74.

141. White MD, Angiolini JF, Alvarez YD, Kaur G, Zhao ZW, Mocskos E, Bruno L, Bissiere S, Levi V, Plachta N. Long-lived binding of Sox2 to DNA predicts cell fate in the four-cell mouse embryo. Cell 2016; 165:75-87.

142. Parfitt DE, Zernicka-Goetz M. Epigenetic modification affecting expression of cell polarity and cell fate genes to regulate lineage specification in the early mouse embryo. Mol Biol Cell 2010; 21:2649-60.

143. Shi J, Chen Q, Li X, Zheng X, Zhang Y, Qiao J, Tang F, Tao Y, Zhou Q, Duan E. Dynamic transcriptional symmetry-breaking in pre-implantation mammalian

embryo development revealed by single-cell RNA-seq. Development 2015; 142:3468-77.

144. Ma H, Baumann CT, Li H, Strahl BD, Rice R, Jelinek MA, Aswad DW, Allis CD, Hager GL, Stallcup MR. Hormone-dependent, CARM1-directed, arginine-specific methylation of histone H3 on a steroid-regulated promoter. Curr Biol 2001; 11:1981-5.

145. Bedford MT, Richard S. Arginine methylation: an emerging regulatorof protein function. Mol Cell 2005; 18:263-72.

146. Cook JR, Lee J-H, Yang Z-H, Krause CD, Herth N, Hoffmann R, Pestka S. FBXO11/PRMT9, a new protein arginine methyltransferase, symmetrically dimethylates arginine residues. Biochem Biophys Res Commun 2006; 342:472-81.

147. Wu Q, Bruce AW, Jedrusik A, Ellis PD, Andrews RM, Langford CF, Glover DM, Zernicka-Goetz M. CARM1 is required in embryonic stem cells to maintain pluripotency and resist differentiation. Stem cells 2009; 27:2637-2645.

148. Xu Z, Jiang J, Xu C, Wang Y, Sun L, Guo X, Liu H. MicroRNA-181 regulates CARM1 and histone aginine methylation to promote differentiation of human embryonic stem cells. PLoS One 2013; 8:e53146.

149. O'Neill LP, VerMilyea MD, Turner BM. Epigenetic characterization of the early embryo with a chromatin immunoprecipitation protocol applicable to small cell populations. Nat Genet 2006; 38:835-41.

150. Parfitt D-E, Zernicka-Goetz M. Epigenetic modification affecting expression of

cell polarity and cell fate genes to regulate lineage specification in the early mouse embryo. Mol Biol Cell 2010; 21:2649-60.

151. Gardner RL. Experimental analysis of second cleavage in the mouse. Hum Reprod 2002; 17:3178-89.

152. Piotrowska-Nitsche K, Zernicka-Goetz M. Spatial arrangement of individual 4-cell stage blastomeres and the order in which they are generated correlate with blastocyst pattern in the mouse embryo. Mech Dev 2005; 122:487-500.

153. Kim J, Lee J, Choi YJ, Kwon O, Lee TB, Jun JH. Evaluation of morphokinetic characteristics of zona pellucida free mouse pre-implantation embryos using time-lapse monitoring system. Int J Dev Biol 2020; 64:415-422.

154. Morris SA, Guo Y, Zernicka-Goetz M. Developmental plasticity is bound by pluripotency and the Fgf and Wnt signaling pathways. Cell Rep 2012; 2:756-65.

155. Tsunoda Y, McLaren A. Effect of various procedures on the viability of mouse embryos containing half the normal number of blastomeres. J Reprod Fertil 1983; 69:315-22.

156. Fujimori T, Kurotaki Y, Miyazaki J, Nabeshima Y. Analysis of cell lineage in two- and four-cell mouse embryos. Development 2003; 130:5113-22.

157. Graham CF, Deussen ZA. Features of cell lineage in preimplantation mouse development. J Embryol Exp Morphol 1978; 48:53-72.

158. Torres-Padilla M-E, Parfitt D-E, Kouzarides T, Zernicka-Goetz M. Histone arginine methylation regulates pluripotency in the early mouse embryo. Nature 2007; 445:214-8.

159. Hupalowska A, Jedrusik A, Zhu M, Bedford MT, Glover DM, Zernicka-Goetz M. CARM1 and paraspeckles regulate pre-implantation mouse embryo development. Cell 2018; 175:1902-1916. e13.

160. Wang J, Wang L, Feng G, Wang Y, Li Y, Li X, Liu C, Jiao G, Huang C, Shi J. Asymmetric expression of LincGET biases cell fate in two-cell mouse embryos. Cell 2018; 175:1887-1901. e18.

161. Piotrowska K, Wianny F, Pedersen RA, Zernicka-Goetz M. Blastomeres arising from the first cleavage division have distinguishable fates in normal mouse development. Development 2001; 128:3739-48.

162. Chróścicka A, Komorowski S, Maleszewski M. Both blastomeres of the mouse 2-cell embryo contribute to the embryonic portion of the blastocyst. Mol Reprod Dev 2004; 68:308-12.

163. Motosugi N, Bauer T, Polanski Z, Solter D, Hiiragi T. Polarity of the mouse embryo is established at blastocyst and is not prepatterned. Genes Dev 2005; 19:1081-92.

164. Dean W, Santos F, Stojkovic M, Zakhartchenko V, Walter J, Wolf E, Reik W. Conservation of methylation reprogramming in mammalian development: aberrant reprogramming in cloned embryos. Proc Natl Acad Sci U S A 2001; 98:13734-8.

165. Oswald J, Engemann S, Lane N, Mayer W, Olek A, Fundele R, Dean W, Reik W, Walter J. Active demethylation of the paternal genome in the mouse zygote. Curr Biol 2000; 10:475-8.

166. Mayer W, Niveleau A, Walter J, Fundele R, Haaf T. Demethylation of the zygotic paternal genome. Nature 2000; 403:501-2.

167. Rougier N, Bourc'his D, Gomes DM, Niveleau A, Plachot M, Pàldi A, Viegas-Péquignot E. Chromosome methylation patterns during mammalian preimplantation development. Genes Dev 1998; 12:2108-13.

168. Fernández-Gonzalez R, Moreira P, Bilbao A, Jiménez A, Pérez-Crespo M, Ramírez MA, Rodríguez De Fonseca F, Pintado B, Gutiérrez-Adán A. Long-term effect of in vitro culture of mouse embryos with serum on mRNA expression of imprinting genes, development, and behavior. Proc Natl Acad Sci U S A 2004; 101:5880-5.

169. Wrenzycki C, Niemann H. Epigenetic reprogramming in early embryonic development: effects of in-vitro production and somatic nuclear transfer. Reprod Biomed Online 2003; 7:649-56.

170. Young LE, Fernandes K, McEvoy TG, Butterwith SC, Gutierrez CG, Carolan C, Broadbent PJ, Robinson JJ, Wilmut I, Sinclair KD. Epigenetic change in IGF2R is associated with fetal overgrowth after sheep embryo culture. Nat Genet 2001; 27:153-4.

171. Li R, Miao J, Wang Z. Production of Genetically Engineered Porcine Embryos by Handmade Cloning. Methods Mol Biol 2019; 1874:347-360.

172. Yano K, Yano C, Kubo T, Ohashi I, Maeda N, Fukaya T. Chemical zona pellucida thinning with acidified Tyrode's solution: comparison between partial and circumferential techniques. J Assist Reprod Genet 2007; 24:471-5.

173. Menino AR, Jr., Wright RW, Jr. Effect of pronase treatment, microdissection, and zona pellucida removal on the development of porcine embryos and blastomeres in vitro. Biol Reprod 1983; 28:433-46.

174. Vajta G, Lewis IM, Hyttel P, Thouas GA, Trounson AO. Somatic cell cloning without micromanipulators. Cloning 2001; 3:89-95.

175. Booth PJ, Tan SJ, Holm P, Callesen H. Application of the zona-free manipulation technique to porcine somatic nuclear transfer. Cloning Stem Cells 2001; 3:191-7.

176. Nichols J, Gardner RL. Effect of damage to the zona pellucida on development of preimplantation embryos in the mouse. Hum Reprod 1989; 4:180-7.

177. Mansour RT, Rhodes CA, Aboulghar MA, Serour GI, Kamal A. Transfer of zona-free embryos improves outcome in poor prognosis patients: a prospective randomized controlled study. Hum Reprod 2000; 15:1061-4.

178. Gordon JW, Dapunt U. Restoration of normal implantation rates in mouse embryos with a hatching impairment by use of a new method of assisted hatching. Fertil Steril 1993; 59:1302-7.

179. Porter AG, Jänicke RU. Emerging roles of caspase-3 in apoptosis. Cell Death Differ 1999; 6:99-104.

180. Gómez E, Caamaño JN, Bermejo-Alvarez P, Díez C, Muñoz M, Martín D, Carrocera S, Gutiérrez-Adán A. Gene expression in early expanded parthenogenetic and in vitro fertilized bovine blastocysts. J Reprod Dev 2009; 55:607-14.

181. Yamatoya K, Ito C, Araki M, Furuse R, Toshimori K. One-step collagenase method for zona pellucida removal in unfertilized eggs: easy and gentle method for large-scale preparation. Reprod Med Biol 2011; 10:97-103.

182. Graham CF, Lehtonen E. Formation and consequences of cell patterns in preimplantation mouse development. J Embryol Exp Morphol 1979; 49:277-94.

183. Elsheikh AS, Takahashi Y, Hishinuma M, Nour MS, Kanagawa H. Effect of encapsulation on development of mouse pronuclear stage embryos in vitro. Anim Reprod Sci 1997; 48:317-24.

184. Illmensee K, Levanduski M, Vidali A, Husami N, Goudas VT. Human embryo twinning with applications in reproductive medicine. Fertil Steril 2010; 93:423-7.

Supplementary list

Supplementary Table 1. Primers used for qPCR analysis

Gene	Accession No.	Sequence	Product length (bp)
Sox2	NM_011443.4	F: 5’- CACAGATGCAACCGATGCA -3’ R: 5’- GGTGCCCTGCTGCGAGTA -3’	122
Nanog	NM_001289828	F: 5’- AAGCAGAAGATGCGGACTGT -3’ R: 5’- ATCTGCTGGAGGCTGAGGTA -3’	92
Cdx2	NM_007673.3	F: 5’- AGGCTGAGCCATGAGGAGTA -3’ R: 5’- GAGGTCCATAATTCCACTCA -3’	123
Sox17	NM_001289464.1	F: 5’- GTTTTCCCCAAGGCTAGCTTCC -3’ R: 5’- TGGTCGTCACTGGCGTATC -3’	134
Eomes	NM_001164789.1	F: 5’- CCACTGGATGAGGCAGGAGATTTCC -3’ R: 5’- AGTCTTGGAAGGTTCATTCAAGTCC -3’	178
Tfap2c	NM_001159696.1	F: 5’- AGGAGGGTTGTTGAACGAGG -3’ R: 5’- GAGTCGTGGCGATCCTGAG -3’	174
Oct4	NM_001252452.1	F: 5’- AAGAACATGTGTAAGCTGCGGCCC -3’ R: 5’- GGAGGGCTTCGGGCACTTCAGAAA -3	186
Sox21	NM_177753.3	F: 5’- GCCGGTGACTCGTGTCTTTA -3’ R: 5’- GAACGGCGGTCATCTCTCAT -3’	168

Gene	Accession No.	Sequence	Product length (bp)
Bax	NM_007527.3	F: 5'- CATCTTTGTGGCTGGAGTCCTC -3' R: 5'- AAGTGGACCTGAGGTTTATTGGC -3'	216
Caspase3	NM_ 001284409.1	F: 5'- GTTCATCCAGTCCCTTTGCAG -3' R: 5'- GTACAGTTCTTTCGTGAGCATGG -3'	181
Gapdh	NM_008084	F: 5'- GTCGTGGAGTCTACTGGTGTC -3' R: 5'- GAGCCCTTCCACAATGCCAAA -3'	240
Dnmt1	NM_001199431.2	F: 5'- AGTGTGTACCTTCCTCCCGA -3' R: 5'- AGGGTACAGGGTCTCGTTCA -3'	99
Uhrf1	NM_001111078.1	F: 5'- TGTCAAGTATGATGACTATCCAGAG -3' R: 5'- CTACAGATCTCAACATCATACCAGA -3'	180
Dnmt3a	NM_001271753.1	F: 5'- AGGCCGAATTGTGTCTTGGT -3' R: 5'- CTTGTTGTAGGTGGCCTGGT -3'	163
Dnmt3b	NM_001003960.4	F: 5'- GCCAGACCTTGGAAACCTCA -3' R: 5'- GCTGGCACCCTCTTCTTCAT -3'	150
Carm1	NM_021531.6	F: 5'- GCTGTGCAGTACTTCCAGTTC -3' R: 5'- TGTCCTTGAAGTCCGTGTGG -3'	121

1 × PBS	**(g/500mL)**
NaCl (Wako)	4 g
KCl (Wako)	0.1 g
$Na_2HPO_4 \cdot 12H_2O$ (Wako)	1.4405 g
KH_2PO_4 (Wako)	0.1 g

After sterilization and store at room temperature.

4% PFA	**10 mL**
Paraformaldehyde	0.4 g
1x PBS (-)	10 mL

Heat in a beaker at approximately 60˚C, after dissolving, store at 4˚C

0.2% TritonX-100	**10 mL**
TritonX-100	20 µl
1x PBS (-)	10 mL

Store at 4 ˚C

Blocking solution	**5 mL**
TritonX-100 (Wako)	5 µl
FBS (Wako)	50 µl
PBS (-)	5 mL

Store at 4 ˚C

Washing solution	**50 mL**
TritonX-100 (Wako)	50 µl
BSA (Sigma-Aldrich, A9418)	150 mg
PBS (-)	50 mL

Store at 4 ˚C

0.5% Proteinase	**(g/5mL)**
Proteinase (Wako)	20 µl
PB1	10 mL

Centrifugation at 1800 rpm for 5 min, remove the supernatant, divided 50 µl/tube, store at -20 ˚C.

PB1	**100 mL**
10 x PBS	10 mL
Glucose (Wako)	0.1 g
Sodium Pyruvate (Wako)	0.0036 g
x 1000 $CaCl_2$・ $2H_2O$	40 µl
x 1000 $MgCl_2$・ $6H_2O$	94.6 µl
Antibiotic	50 µl
BSA (Sigma-Aldrich, A9418)	0.4 g

Sterile filtered, store at 4 ˚C.

PBS + 0.2% PVA	**50 mL**
10% PVA	100 µl
PBS (-)	50 mL

Store at 4 ˚C

Stock A	**(g/50mL)**
NaCl (Wako)	2.767 g
KCl (Wako)	0.178 g
KH_2PO_4 (Wako)	0.081 g
$MgSO_4 \cdot 7H_2O$ (Wako)	0.1465 g
Sodium DL-lactase solution (60%) (Sigma)	2.1745 mL
D (+) – Glucose (Wako)	0.5 g
Penicillin G Potassium Salt (Nacalai tesque, INC)	0.03 g
Streptomycin Sulfate (Nacalai tesque, INC)	0.025 g

Sterile filtered, store at 4 ˚C for 3 months

Stock A'	**(g/50mL)**
NaCl (Wako)	2.96875 g
KCl (Wako)	0.1748 g
KH_2PO_4 (Wako)	0.0252 g
MgSO4 $\cdot 7H_2O$ (Wako)	0.0246 g
Sodium DL-lactase solution (60%) (Sigma)	1.71 mL
D (+) – Glucose (Wako)	0.25 g
Penicillin G Potassium Salt (Nacalai tesque, INC)	0.0375 g
Streptomycin Sulfate (Nacalai tesque, INC)	0.025 g

Sterile filtered, store at 4 ˚C for 3 months

Stock B	**(g/50mL)**
$NaHCO_3$ (Wako)	1.0505 g
Phenol red solution (0.5%) (Sigma)	1 mL

Store at 4 ˚C for 1 week

Stock C	**(g/10mL)**
Sodium Pyruvate (Wako)	0.036 g

Store at 4 ˚C for 1 week

Stock D	**(g/10mL)**
$Cacl_2 \cdot 2H_2O$ (Wako)	0.252 g

Sterile filtered, store at 4 ˚C for 3 months

Stock E	**(g/50mL)**
HEPES (Sigma)	2.979 g
Phenol red solution (0.5%) (Sigma)	1 mL
10N NaOH	0.875 mL

Sterile filtered, store at 4 ˚C for 3 months

Stock EDTA	**(g/10mL)**
EDTA (DOJINDO)	0.03722 g

Store at 4 ˚C for 1 week

M2 culture medium	**100 mL**
A	10 mL
B	1.6 mL
C	1 mL
D	1 mL
E	8.4 mL
BSA	0.4 g

Sterile filtered, store at 4 ˚C for 3 months

M16 culture medium	**50 mL**
A	5 mL
B	5 mL
C	0.5 mL
D	0.5 mL
EDTA	0.5 mL
BSA	0.2 g

Sterile filtered, store at 4 ˚C for 3 months

HTF culture medium	**50 mL**
A’	5 mL
B	5 mL
C	0.5 mL
D	0.595 mL
BSA	0.2 g

Sterile filtered, store at 4 ˚C for 3 months